Keystone Review

Future Molecular Science

Piezocatalysis for Small-molecule Conversion: From Mechanistic Fundamentals to Emerging Applications

Haiyan Xie[1#], Jing Zhang[1#], Yifan Pan[1], Pengwei Jia[1], Xiaowen Ruan[1,2], Sai Kishore Ravi[1,2], Hongwei Huang[1*]

[1] Engineering Research Center of Ministry of Education for Geological Carbon Storage and Low Carbon Utilization of Resources, Beijing Key Laboratory of Materials Utilization of Nonmetallic Minerals and Solid Wastes, National Laboratory of Mineral Materials, School of Materials Science and Technology, China University of Geosciences (Beijing), Beijing 100083, China
[2] School of Energy and Environment, City University of Hong Kong, Tat Chee Avenue, Kowloon, Hong Kong SAR, 999077, China

Abstract

Piezocatalysis harnesses the electromechanical coupling of non-centrosymmetric materials to convert mechanical energy into dynamic interfacial polarization and redox driving forces, thus offering a distinctive route for small-molecule activation under mild conditions. This review first examines the fundamental mechanisms underlying piezocatalytic charge generation, charge separation, charge transport, and interfacial reaction The rapidly expanding family of piezocatalytic materials—including perovskite and related oxides, layered bismuth-based compounds, ferroelectric polymers, wurtzite-type semiconductors, two-dimensional van der Waals materials, and other inorganic piezoresponsive materials—is then discussed along with framework, molecular, and organic–inorganic hybrid systems. Strategies for tuning the piezocatalytic activity are further organized within a four-dimensional regulation framework encompassing lattice polarization and microstructure, interfacial, and surface properties, highlighting the relationships among the material structure, electromechanical response, and catalytic performance. The emerging application landscape, spanning water splitting, CO_2 reduction, N_2 fixation, nitrate reduction, O_2 reduction for H_2O_2 production, reactive oxygen species -mediated degradation of small organic pollutants, and oxidative conversion of methane is discussed. Particular attention is focused on the mechanistic complexity of piezocatalytic reactions and the challenges associated with comparing the piezocatalytic performance across different materials and operating conditions. Finally, the key barriers to practical deployment, including mechanistic decoupling, performance standardization, stability, and reactor engineering, are discussed. By connecting fundamental electromechanical phenomena with materials design and small-molecule reactivity, this review outlines the opportunities and principles for advancing piezocatalysis from proof-of-concept demonstrations toward robust and scalable chemical conversion technologies.

1 Introduction

The global shift toward low-carbon energy systems and the strict enforcement of environmental governance standards have highlighted prominent challenges in ensuring energy security, mitigating greenhouse gas emissions, and addressing environmental degradation (Figure 1a). Most of the molecules that are crucial to energy and the environment have stable structural configurations and feature high reaction barriers; hence, activation of these molecules is considerably difficult. Transformation of such molecules requires the coordinated regulation of multiple reaction steps, including adsorption, charge transfer, bond breaking, stabilization of intermediates, and product desorption.[1-4] The development of catalytic routes toward the conversion of abundant or low-value raw materials into high-value chemicals such as hydrogen, ammonia, and carbon-based fuels enables the realization of carbon cycling, clean energy storage, and sustainable industrial production.[5-7] Meanwhile, the conversion of such small molecules offers a valuable research paradigm for understanding the mechanism underlying the transfer of external energy to the reaction interface. Therefore, achieving efficient and high-selectivity conversion under mild conditions is of fundamental scientific importance and holds substantial engineering application potential.

Thermocatalysis, photocatalysis, and electrocatalysis offer distinct advantages in terms of process maturity, solar energy utilization efficiency, and precise process control. Nevertheless, these three technologies face inherent practical bottlenecks, including restrictions imposed by the need for high temperatures and high pressures, inadequate spectral utilization, high carrier recombination loss, reliance on external power supply,

Received: September 11, 2026; Revised: September 27, 2026;
Accepted: October 14, 2026; Published Online: October 22, 2026
*Corresponding author: Hongwei Huang (hhw@cugb.edu.cn)
#These authors contributed equally to this work.

Check for updates

DOI: 10.68642/ftms.202600008

and challenges in reactor design.[8-10] In this context, piezocatalysis, which is based on force-electric coupling in noncentrosymmetric materials, is an innovative supplementary catalytic strategy that has attracted widespread research attention. Mechanical vibration, fluid flow, acoustic excitation, and periodic deformation can induce strain in piezocatalysts.[11-14] The resulting polarized charges and piezoelectric potential can modulate the degree of band bending, carrier migration behavior, interfacial charge compensation processes, and surface redox energy states. Although piezocatalysis requires external energy input, it can convert ambient mechanical energy, which would otherwise be dissipated, into a localized electrochemical driving force. This unique mechanism facilitates the implementation of catalytic reactions under conditions where continuous illumination is infeasible, application of a direct bias is inconvenient, or high-temperature heating is impractical (Figure 1b).[15,16] Hence, piezocatalysis shows broad application potential across multiple domains. A literature search in the Web of Science database using "piezocatalysis" as the keyword revealed a massive number of publications, indicating sustained academic interest in this field (Figure 1c). Bibliometric network analysis further corroborated the prominent status and extensive influence of piezocatalysis -based research across various scientific disciplines (Figure 1d).

Despite the rapid development and expanding scale of research into piezocatalysis in recent years, current investigations are still hindered by considerable limitations. Most existing studies are confined to specific material systems and single-application scenarios, and few reviews have systematically summarized piezocatalysis from the dimensions of fundamental mechanism, material design, modification strategy, and practical application. To fill this gap, the present review first examines the crystallographic origin of piezoelectricity, spontaneous polarization, piezoelectric tensors, stress-induced charge generation, carrier migration, interfacial screening, and redox potential matching to clarify the intrinsic physicochemical essence of pure piezocatalysis and multifield coupling in catalytic processes. Subsequently, the design principles for inorganic, organic, and porous piezocatalysts are summarized, with a discussion on morphology regulation, dimensional construction, exposed crystal facet engineering, ferroelectric domain modulation, elemental doping, defect dipole design, heterojunction fabrication, cocatalyst modification, and creation of atomically dispersed active sites, all of which are aimed at catalytic performance optimization. Typical applications encompassing water splitting, CO_2 reduction (CO_2RR), nitrogen fixation, O_2 reduction for H_2O_2 production, reactive oxygen species (ROS)-mediated degradation of small organic pollutants, and oxidative conversion of methane are comprehensively reviewed. Finally, the remaining challenges in multifield coupling decoupling, energy conversion efficiency enhancement, performance standardization, long-term stability improvement, selectivity modulation in multielectron reactions, and reactor scale-up are outlined. Correspondingly, the study provides forward-looking outlooks for next-generation research avenues directed at mechanism quantification, intelligent-material discovery, unified evaluation systems, domain engineering, and continuous-flow industrial systems driven by ambient mechanical energy, thereby establishing a closed-loop framework that bridges fundamental research, material innovation, and practical implementation.

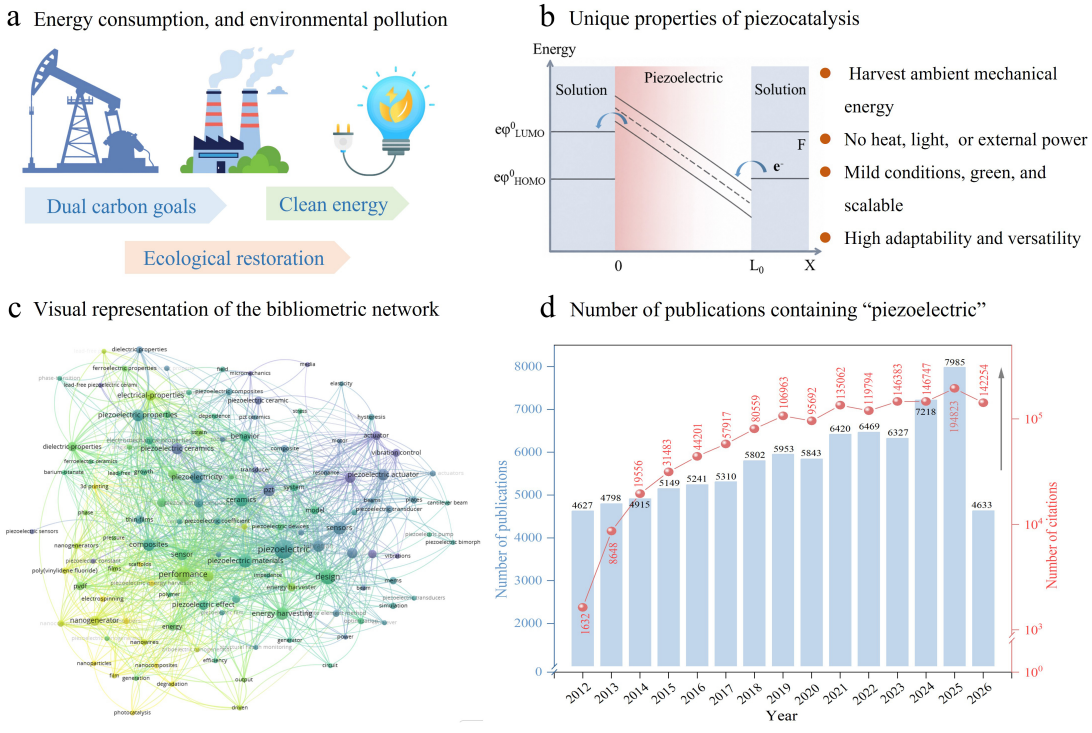


Figure 1 a, Imperative demand and feasibility for transition to clean energy. b, Unique properties of piezocatalysis. c, Visual representation of the bibliometric network related to piezocatalysis. d, Number of publications including "piezoelectric" as a topic published using the Web of Science database, the period 2012–2026, date of search: August 2026.

DOI: 10.68642/ftms.202600008

2 Physicochemical Fundamentals and Mechanisms of Piezocatalysis

Piezocatalysis is a force-electric-chemical coupled technology that converts mechanical energy into the driving force for chemical reactions via the piezoelectric effect. Thus, piezocatalysis is distinct from thermocatalysis, photocatalysis, and electrocatalysis, which are driven by a single energy source. In a piezocatalytic process, mechanical stress induces lattice distortion and polarization reorganization, generating a dynamic built-in electric field and a surface piezoelectric potential. These, in turn drive carrier separation and directed migration, ultimately triggering redox reactions at the solid–liquid interface. This multiscale process encompasses microscopic lattice polarization, mesoscopic carrier transport, and macroscopic interfacial reactions. The present chapter systematically elucidates the stepwise reaction mechanisms underlying piezocatalysis, analyzes the core regulatory principles and multifield synergistic effects, and thereby establishes a comprehensive theoretical foundation for the rational design and practical application of piezocatalysts.

2.1 Crystallographic and physical fundamentals of piezocatalysis

The generation of piezoelectric responses requires noncentrosymmetric crystals, intrinsic spontaneous polarization, and ferroelectric domains. Structural effects and mechanical properties at the nanoscale can further amplify these piezoelectric responses (Figure 2a). Consequently, the abovementioned factors together lay the physical foundation for the highly efficient energy conversion in piezocatalysis.

2.1.1 Symmetry and spontaneous polarization

The crystallographic origin of the piezoelectric effect lies in the absence of inversion symmetry in a crystal. In an ideal crystal with a center of inversion, the positive and negative ion displacements caused by an external force cancel out each other in space, and the macroscopic dipole moment typically remains zero. In contrast, in most crystals lacking center symmetry, mechanical stress can alter the unit cell dipole moment, thus generating measurable polarized charges.[17] However, non-centrosymmetry alone cannot ensure an excellent macroscopic piezoelectric response, because crystal orientation and practical testing conditions also critically regulate the actual piezoelectric performance. More precisely, the piezoelectric tensor is a third-order tensor that enables linear coupling between stress and polarization, and electric displacement is derived from this linear coupling through a contracted product rather than through a tensor product. Consequently, the overall piezoelectric performance depends not only on the crystal symmetry but also on the refined atomic arrangement and orientation of the applied stress.[18] Spontaneous polarization is an inherent steady-state characteristic of polar piezocatalysts, and it originates from the permanent relative displacement between the cation and anion sublattices in the crystal lattice under thermodynamic equilibrium.[19] This displacement occurs in the absence of an external electric field or mechanical stress, further generating stable intrinsic electric dipole moments and macroscopic polarization vectors in polar piezoelectric systems. The magnitude of the polarization vector is jointly determined by the lattice distortion degree, atomic coordination structure, and crystal symmetry.

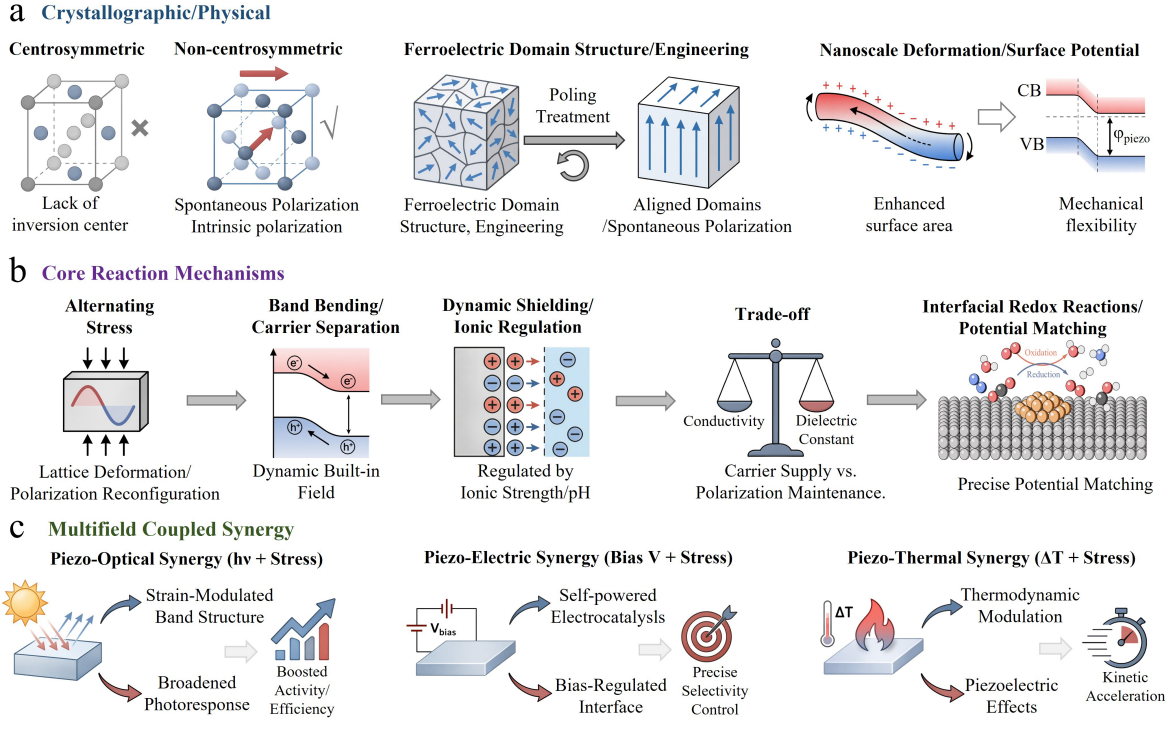


Figure 2 Physical foundation and reaction mechanisms of piezocatalysis. a, Piezocatalytic crystallography and physical foundations. b, Core reaction mechanisms of piezocatalysis. c, Multifield coupled catalytic systems.

DOI: 10.68642/ftms.202600008

Furthermore, the polarization vector of ferroelectric materials can be reversed under an external field; however, not all polar piezocatalysts exhibit such reversible behavior. On the basis of polarization tunability, piezocatalysts can be categorized into two major types: ferroelectric and non-ferroelectric. Ferroelectrics show reversible spontaneous polarization, and their comprehensive functional performance can be optimized via poling treatment, domain engineering, and defect modification.[20] In non-ferroelectric piezocatalysts, however, the piezoelectric tensor parameters are determined by intrinsic crystal configuration, and no polarization reversal occurs.[21] This structural feature endows them with a stable piezoelectric response but restricts the feasibility of artificial performance modulation. This categorization offers valuable guidance for fundamental material research as well as targeted material selection and design in piezocatalysis.

2.1.2 Piezoelectric effect and ferroelectric domain structure

A positive piezoelectric effect governs energy conversion since the mechanical load induces a reversible lattice strain that alters the unit cell dipole moment and generates bound polarization charges on the material surface.[22] These charges create a dynamic internal electric field within the piezocatalyst. When the external force is removed, the lattice returns to its unstrained state, and the induced charges disappear. Nevertheless, alternating mechanical stress enables the cyclic generation and dissipation of polarized charges; this cyclic behavior sustains continuous catalytic reactions throughout the process. Non-ferroelectric piezoelectric semiconductors do not show intrinsic spontaneous polarization. Hence, the piezoelectric response of these materials originates from the asymmetric lattice deformation triggered by external mechanical stimuli.[23] Polarization of such materials appears/disappears in synchrony with the applied stress, without kinetic hysteresis during the stress cycle. Because of this property, non-ferroelectric piezoelectrics feature reversible interfacial charge exchange and thus adapt well to high-frequency dynamic mechanical excitation conditions. The response intensity of non-ferroelectric piezoelectric semiconductors depends on the intrinsic piezoelectric coefficient and stress transfer efficiency. In contrast, ferroelectric materials possess stable spontaneous polarization characteristics and feature abundant multidomain structures below the Curie temperature.[24] Each domain shows uniform polarization, while randomly oriented domains in polycrystalline samples nullify the overall macroscopic polarization. Appropriate electrical poling treatment can effectively regulate the domain orientations and thereby strengthen the macroscopic piezoelectric response. Ferroelectric materials possess higher polarization intensity and show a more stable piezoelectric potential output compared with their non-ferroelectric counterparts. However, domain wall migration causes dynamic hysteresis, which degrades the catalytic performance under high-frequency mechanical stress.[25] Meanwhile, the domain walls create localized electric fields and induce band bending, providing abundant active sites and efficient transport channels for charge carriers.[26] Furthermore, oxygen vacancies exert a pinning effect on the domain walls and prevent domain flipping.[27] The pinning effect leads to a typical trade-off between the defect-derived active sites and polarization shielding, and this trade-off in turn acts as the key parameter for the performance optimization of piezoelectric catalysts.

2.1.3 Nanoscale deformation and surface piezoelectric potential

Nanoscale piezocatalysts possess a large specific surface area, excellent mechanical flexibility, a low deformation threshold, and a short charge migration distance, all of which enable them to respond efficiently even to weak mechanical stimuli such as water waves, acoustic vibrations, and microfluidic shear.[28] Consequently, under non-uniform strain, these materials show prominent size effects and strain-gradient effects Elastic deformation can produce a continuous polarization gradient; such gradients further promote directional charge accumulation on the material surface.[29] The accumulated surface charges generate a surface piezoelectric potential. Two-dimensional piezocatalysts such as monolayer MoS_2 and WS_2 show layer-dependent piezoelectric activity, which originates from the broken in-plane inversion symmetry in odd-layer configurations.[30] By contrast, in even-layer structures, the central symmetry is recovered and the piezoelectric performance is significantly degraded; hence, the piezoelectric coefficients increase with a decrease in the number of layers.[31] Surface defects, dangling bonds, and interfacial stress relaxation can tune the charge distribution and suppress carrier recombination;[32,33] moreover, the flexoelectric effect originating from strain gradients contributes to the overall polarization.[34] The tunable polarization and charge behavior lay physical foundation for subsequent piezocatalytic conversions.

2.2 Mechanisms underlying piezocatalysis

Piezocatalysis relies on three hierarchical, closely interrelated physicochemical steps: 1) force-induced generation of polarization charges; 2) bulk carrier separation and migration; 3) interfacial redox potential matching (Figure 2b). These cascaded processes mutually constrain and synergistically coordinate with one another, thus determining the overall catalytic efficiency and small-molecule conversion selectivity.

2.2.1 Polarization and interfacial screening

Mechanical stress induces surface polarization and lattice-bound charges, which attract solution counterions, polar molecules, and free carriers for interfacial charge compensation. Under static conditions, electrolyte ions accumulate on polarized surfaces to form compact and diffuse electric double layers, which shield the intrinsic piezoelectric potential and suppress continuous interfacial charge exchange and long-term catalytic turnover.[35] In contrast, periodic mechanical stress dynamically modulates the magnitude and direction of polarization, enabling cyclic polarization, screening, depolarization, and rescreening to sustain stable redox reactions.[36] During mechanical compression, the rapid accumulation of surface-bound charges outpaces the slow ionic rearrangement in electrolytes, generating a transient unscreened piezopotential to drive spontaneous interfacial electron transfer and subsequent redox reactions. Stress release or reverse deformation reorganizes the electric double layer and revives interfacial charge states for successive catalytic cycles. From an electrochemical perspective, piezoelectric nanoparticles act as mechanically regulated micro-electrochemical capaci-

DOI: 10.68642/ftms.202600008

tors, inducing cyclic charge–discharge processes under periodic deformation and converting mechanical energy into chemical energy via interfacial catalytic reactions.[37] Moderate interfacial charge screening prevents excessive surface charge accumulation and carrier recombination to prolong carrier lifetime; periodic descreening continuously renews the material surface active sites, ensuring stable adsorption, activation, and conversion of small molecules.[38]

2.2.2 Band bending and carrier migration

Strain-triggered dynamic band bending is the core characteristic that distinguishes piezocatalysts from conventional catalytic systems. Stress-free semiconductors maintain flat band structures, accompanied by spontaneous carrier recombination that limits the intrinsic catalytic activity. Mechanical polarization creates internal built-in electric fields and modulates electronic band bending, thus providing a stable and efficient driving force for spatial carrier separation and directional interfacial migration.[39] The direction and intensity of band bending are jointly determined by the polarization orientation, strain magnitude, semiconductor type, and Fermi level. Positively polarized surfaces induce upward band bending with hole enrichment to boost oxidation reactions, while negative polarization charges trigger downward band bending with electron accumulation to facilitate reduction reactions. A larger strain intensity amplifies the degree of band bending, improves the efficiency of carrier separation and inhibits carrier recombination loss.[40] Unlike photocatalysis, which relies on band-to-band photoexcitation, piezocatalysis utilizes strain fields to regulate the transport of intrinsic carriers, defect-state charges, and interfacial compensation charges without external optical excitation. The carrier transport behavior differs notably among various piezocatalysts. Semiconducting piezoelectric materials can effectively suppress bulk carrier recombination and promote directional charge migration. Insulating ferroelectrics show negligible carrier recombination but suffer from sluggish charge migration kinetics. Conductive composite piezoelectrics feature high-speed charge transport channels to optimize the mechano-electric conversion efficiency; however, excessive conductive components shield the polarization electric field and weaken the band-bending effect. Therefore, the optimal compositional ratio that balances the abovementioned effects must be identified.[15] Consequently, a delicate trade-off between the electrical conductivity and the dielectric constant is required: moderate conductivity and high electromechanical coupling synergistically balance carrier supply and piezopotential retention, optimizing the overall catalytic kinetics via dynamic space-charge layer modulation.[41]

2.2.3 Surface redox reactions

The thermodynamic feasibility and product selectivity of piezocatalytic reactions are governed by precise interfacial potential matching. Effective interfacial redox reactions can proceed spontaneously when the surface hole potential is sufficiently positive to drive molecular oxidation, and the surface electron potential is sufficiently negative to support reactant reduction.[42] Periodic polarization reversal alternately switches the oxidative and reductive capacities of the catalyst surface; thus, a single piezocatalyst can sequentially drive multistep coupled redox reactions and show unique advantages for complex small-molecule conversion processes.[43] Polarization modulation effectively tunes the surface work function, electronic band structure, and interfacial dipoles, imparting distinct redox activities to different particle domains. Reverse polarization swaps the dominant reactive regions of the catalyst and facilitates spatial separation of oxidation and reduction reactions, thereby precisely regulating the product selectivity of the catalytic.[38] Nevertheless, randomly oriented grains in conventional powder catalysts lead to mutual polarization cancellation and hinder macroscopic directional charge flow. Fabrication of oriented nanoarrays, membrane polarization, and rectification of interface composite structures can help overcome this limitation.[44] In real electrolyte environments, a reliable piezocatalytic mechanism must be implemented so that the interfacial potential can be duly modulated by adjusting the pH, ionic strength, and dielectric properties of the electrolyte. Strict control experiments are indispensable to eliminate non-piezoelectric interferences, including ultrasonic cavitation and thermal effects, thereby verifying the authenticity of the mechanical-energy-driven piezocatalytic behavior.

2.3 Piezo-photocatalytic systems

Piezocatalysis is inherently hampered by the poor mechanical-to-chemical energy conversion efficiency, which severely restricts the kinetic accessibility to small molecules with high activation energy barriers. External physical fields such as light fields can be introduced to construct multifield coupled systems (Figure 2c). These systems can achieve synergy among multiple energy-source, thus overcoming the limitations of single-energy-input modes while expanding the applicable scope of catalytic reactions. Piezo-photo-coupled catalysis is the most widely investigated multi-field synergy system that helps achieve remarkable performance improvement. The core advantage of this catalytic system lies in the bidirectional complementary promotion of carrier generation and spatial separation. Light irradiation excites the semiconductor to produce electron–hole pairs, and the piezoelectric field originating from mechanical deformation drives these carriers to migrate toward different spatial positions.[45] This process reduces the probability of bulk recombination and prolongs the lifetime of available carriers. Additionally, band bending induced by the piezoelectric potential modulates interfacial potential barriers; hence, electrons can be injected into the reduction sites more easily, while holes can smoothly migrate toward the oxidation sites.[46] In heterojunction systems with type-II, Z-scheme, or S-scheme configurations, piezo-polarization can strengthen or weaken the built-in electric field, thereby regulating charge-transfer pathways This synergy mechanism involves three major coupling effects: 1) strain engineering modulates the band structures; 2) polarization electric fields drive the spatial separation of charges 3) alternating electric fields suppress the accumulation and recombination of interfacial carriers.[47] Notably, the piezo-photo synergy spans multiple mechanisms such as electrostatic-field modulation, strain engineering, mass-transfer enhancement, and cavitation-based effects. Therefore, a rigorous quantitative compari-

DOI: 10.68642/ftms.202600008

son is required to verify the validity of this synergy. Reaction rates under single-field conditions should be compared with those under dual-field coupling conditions, and *in situ* potential measurements, transient spectroscopy, and carrier-lifetime characterization should be combined to establish complete mechanistic evidence chains. Furthermore, the apparent performance improvement caused by rapid mass transfer should be excluded.

In summary, piezocatalysis originates from the dynamic coupling among stress, polarization, charge transport, and interfacial chemistry. From a structural perspective, non-centrosymmetric crystal structures are the fundamental prerequisite for piezoelectric responses, and piezoelectric tensors quantitatively characterize the magnitude of the electromechanical coupling capacity. Ferroelectric domain structures and artificial polarization treatments are critical approaches to maximize the macroscopic piezoelectric response. Nanoscale effects optimize the deformation capacity and specific surface area, thereby providing the structural foundation for high-efficiency piezocatalysis. From a mechanistic perspective, piezocatalysis involves key processes such as stress-induced polarization reconstruction, dynamic interfacial screening and descreening, band bending, carrier transport, and interfacial potential matching. Multifield coupled catalysis achieves complementary synergy between external light fields and piezoelectric effects, thus effectively circumventing performance bottlenecks originating from mechanical-only energy input. Such improvements are reflected in the higher carrier generation efficiency, enhanced charge-separation capability, improved interfacial kinetics, and optimized reaction selectivity. Overall, the theoretical mechanisms illustrated in this chapter clarify the core merits and regulatory keys that distinguish piezocatalysis from conventional catalysis. These mechanisms also provide solid theoretical support for subsequent structural design, modification-strategy optimization, and targeted small-molecule conversion applications of piezocatalytic materials.

3 Classification, Characteristics, and Design Strategies of Piezocatalysts

Single-component piezocatalysts suffer from critical bottlenecks, including a mismatch between the piezoelectric response and the electrical conductivity, rapid carrier recombination, scarcity of active sites, poor selectivity for multielectron reactions, and insufficient structural stability. To address these issues, the field has developed a comprehensive design paradigm centered on the expansion of material systems and the application of multiscale structural modification. This chapter systematically classifies and summarizes the structural characteristics as well as the performance advantages and limitations of mainstream piezocatalysts. Furthermore, it provides an in-depth analysis of the intrinsic mechanisms and structure–property relationships for three core modification strategies, namely microscopic morphology control, electronic band structure control, and heterointerface control. The ultimate aim is to provide a theoretical foundation for the precise design and performance optimization of efficient, selective, and stable piezocatalysts.

3.1 Classification and characteristics of piezocatalysts

To enable a systematic comparison of the crystal chemistry, polarization behavior, charge-transport properties, mechanical characteristics, structural stability, and modification strategies, piezocatalysts are classified herein according to their material families and structural motifs. Accordingly, mainstream piezocatalytic materials are divided into seven major groups: perovskite and related oxides, layered bismuth-based materials, ferroelectric polymers, wurtzite-type semiconductors, two-dimensional van der Waals materials, other inorganic piezoresponsive materials, and framework/molecular/organic-inorganic hybrid materials. This classification is based on the dominant structural framework and is not intended to define strictly mutually exclusive material categories.

3.1.1 Perovskite and related oxides

Three-dimensional perovskite and the structurally related non-layered oxides represent one of the most extensively investigated piezocatalyst families (Figure 3a). Typical representatives include $BaTiO_3$,[48] $BiFeO_3$,[49] and $PbTiO_3$,[50] as well as lead-free perovskite derivatives.[51] In polar ABO_3 perovskites, spontaneous polarization originates from the collective relative displacements of the cationic and anionic sublattices. Depending on the specific composition and crystalline phase, polar distortion arises from B-site cation off-centering, lone-pair-driven A-site displacement, octahedral tilting, or coupling among multiple symmetry-adapted lattice modes. Such lattice polarization can be modulated by A-site ionic-size mismatch, tolerance-factor-induced lattice instability, epitaxial or intrinsic strain, and the electronic configurations of the constituent ions.[52] Notably, octahedral tilting does not universally enhance macroscopic polarization, as it can either compete with or reinforce polar distortion depending on the specific crystal chemistry. In the case of ferroelectric perovskites, external mechanical loading induces elastic unit-cell deformation and may additionally promote polarization rotation and reversible or hysteretic domain-wall motion. These structural responses dynamically modulate the magnitude and direction of macroscopic polarization, leading to time-dependent changes in the bound-charge density at strained surfaces and interfaces.[53] Perovskite oxides offer several advantages, including robust spontaneous polarization in ferroelectric phases, chemically stable oxide frameworks, diverse polymorphs, and highly tunable domain architectures. Their polarization output can be precisely regulated via aliovalent doping, isovalent substitution, electrical pre-poling, strain engineering, particle-size modulation, phase-boundary design, and domain engineering.[54,55] These structural and polarizable features make perovskite oxides valuable model systems for elucidating the relationships among lattice distortion, polarization-charge generation, interfacial redox kinetics, and catalytic selectivity. Perovskite oxides also serve as versatile mechanically active building blocks for multifunctional semiconductor heterojunction catalysts. Nevertheless, many perovskite oxides suffer from wide bandgaps, high electrical resistivity, and low mobile-carrier densities. Mechanically generated polarization charges are readily trapped and electrostatically screened by surface states, adsorbed intermediates, and lattice defects as well as by interfacial charge accumulation, thus severely restricting

DOI: 10.68642/ftms.202600008

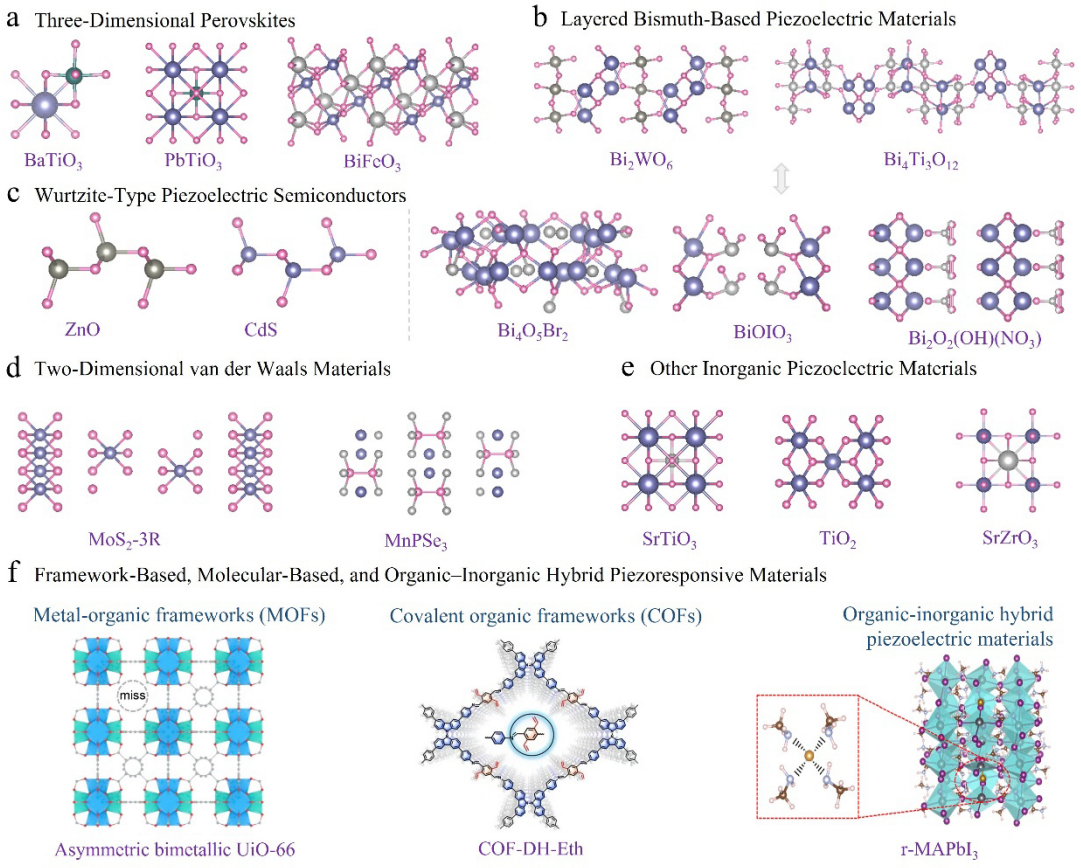


Figure 3 **Classification of piezocatalysts.** a, Three-dimensional perovskites. b, Layered bismuth-based piezoelectric materials. c, Wurtzite-type piezoelectric semiconductors. d, Two-dimensional van der Waals materials. e, Other inorganic piezoelectric materials. f, Framework-based, molecular-based, and organic–inorganic hybrid piezoresponsive materials: MOFs, Reproduced with permission.[93] Copyright 2026, Wiley-VCH GmbH; COFs, Reproduced with permission.[97] Copyright 2025, Wiley-VCH GmbH; organic–inorganic hybrid piezoelectric materials. Reproduced with permission.[100] Copyright 2025, Wiley-VCH GmbH.

charge delivery to catalytic active sites. Moreover, at a given polarization-charge density and under specific electrical boundary conditions, high dielectric permittivity can reduce the resulting open-circuit piezopotential. Moderate defect engineering can optimize the carrier concentration, surface adsorption behavior, and interfacial electronic structure. On the other hand, excessive oxygen vacancies or aliovalent doping can induce leakage currents and domain-wall pinning, suppress the ferroelectric long-range order, and create deep charge-recombination centers. Accordingly, optimization of perovskite piezocatalysts requires a coordinated balance among polarization strength, electrical conductivity, dielectric screening, domain-wall mobility, carrier lifetime, interfacial charge-transfer kinetics, mechanical durability, and structural stability, rather than the unilateral maximization of any single parameter.

3.1.2 Layered bismuth-based materials

Layered bismuth-based materials adopt distinctive structural geometries and show charge-transport behaviors that fundamentally differ from those of conventional three-dimensional perovskite oxides (Figure 3b). Representative systems include Aurivillius-phase oxides such as Bi_2WO_6, $Bi_4Ti_3O_{12}$, and Bi_3TiNbO_9;[56-58] Sillén-type bismuth oxyhalides (BiOX, X = Cl, Br, I);[59-61] and bismuth-rich derivative phases such as $BiOIO_3$, $Bi_2O_2CO_3$, and bismuth-rich halide oxides.[62-65] The stereochemically active $6s^2$ lone pair of Bi^{3+} promotes asymmetric coordination in many bismuth compounds, while the Aurivillius phases comprise alternating $(Bi_2O_2)^{2+}$ layers and perovskite-like slabs that generate pronounced structural and charge-transport anisotropy.[66] By virtue of the layered architecture, ultrathin nanosheets fabricated using these materials feature tunable in-plane and out-of-plane charge-transport pathways, abundant exposed crystal facets, and short carrier-migration distances. Unsaturated surface coordination and facet-dependent atomic arrangements provide plentiful active sites for the adsorption and activation of small molecules. Layered ultrathin materials can accommodate bending deformation and large strain gradients more efficiently than do their rigid bulk counterparts, enabling effective piezoelectric and flexoelectric coupling under vibration, fluid fluctuation, and ultrasonic excitation. Because some layered bismuth compounds, particularly BiOX phases, are centrosymmetric in their ideal bulk structures, the intrinsic piezoelectricity should be distinguished from flexoelectric, defect-induced, surface-induced, and interface-induced responses. However, the macroscopic electromechanical output is highly sensitive to the phase purity, layer thickness, defect distribution, crystal orientation, and interlayer stacking configuration. Undesired interlayer slippage dissipates the mechanical energy without generating the net effective polarization, while halogen depletion, bismuth-rich surface reconstruction, and

DOI: 10.68642/ftms.202600008

excessive vacancy defects in bismuth oxyhalides can trigger structural degradation and progressive catalytic fatigue. Consequently, the development of high-efficiency layered bismuth-based piezocatalysts requires simultaneous regulation of the phase-specific symmetry, polarization or flexoelectric response, anisotropic charge transport, facet chemistry, defect concentration, interlayer mechanical coupling, and long-term chemical stability.

3.1.3 Ferroelectric polymers

Ferroelectric polymers are predominantly represented by Polyvinylidene fluoride (PVDF) and its copolymers, including poly(vinylidene fluoride-co-hexafluoropropylene) [P(VDF–HFP)] and Poly (vinylidene fluoride-trifluoroethylene) [P(VDF-TrFE)].[67,68] Unlike the case of inorganic piezoelectrics, which rely on lattice ionic displacement, the piezoresponse of ferroelectric polymers originates from the ordered alignment and deformation of molecular dipoles within polar crystalline domains. In PVDF, the all-trans β-phase typically provides the dominant piezoelectric response, although the polar γ- and δ-phases and copolymer-specific crystalline states can also contribute to macroscopic polarization.[69] Therefore, an effective piezoelectric response depends not only on the nominal polymer composition but also on the crystalline-phase fraction, chain conformation, crystallite orientation, domain texture, residual stress, and poling history. Benefiting from the low elastic modulus, superior mechanical flexibility, low density, and excellent solution processability, ferroelectric polymers facilitate efficient energy coupling with weak, low-frequency mechanical stimuli. The remarkable deformability of these polymers under water-flow fluctuations, acoustic vibrations, mechanical bending, stretching, and pressure variations makes them suitable for use in flexible catalytic membranes, porous films, functional fibers, and continuous-flow catalytic reaction interfaces.[70] In addition, the intrinsic mechanical compatibility of these polymers facilitates their integration with inorganic semiconductors, conductive fillers, and multifunctional cocatalysts toward the construction of composite catalysts. The piezoelectric performance of ferroelectric polymers can be enhanced through polar-phase regulation, chain and crystallite orientation, electrical poling, interfacial hydrogen-bond engineering, and textured microstructures formation. Conductive or redox-active cocatalysts can improve the charge extraction efficiency, whereas excessive conductive-filler loading can increase leakage, mechanically stiffen the polymer matrix, and screen the piezopotential. Long-term optimization must also address thermal depolarization, viscoelastic creep, cyclic fatigue, interfacial aging, and performance stability under aqueous or chemically reactive conditions.

3.1.4 Wurtzite-type semiconductors

Wurtzite-type piezoelectric semiconductors include ZnO,[71] wurtzite-phase CdS,[72] and compositionally tunable $Cd_xZn_{1-x}S$ solid solutions (Figure 3c).[73] Since CdS, ZnS, and their alloys can crystallize in multiple polymorphs, accurate phase identification is a prerequisite for confirming the intrinsic piezoelectric activity. In standard wurtzite lattices, the cationic and anionic sublattices are stacked alternately along the crystallographic c-axis. The inherent lack of inversion symmetry and the non-ideal tetrahedral coordination geometry endow these materials with intrinsic linear piezoelectricity. Mechanical deformation alters the relative displacement the of cation–anion sublattices and generates a piezopotential independent of ferroelectric domain switching or structural phase transition.[74] Compared with the highly insulating ferroelectric oxides, wurtzite semiconductors possess lower resistivity and more favorable electronic transport properties. However, this conductivity advantage must be balanced against the piezopotential screening by mobile carriers. The strain -induced piezopotential effectively redistributes the mobile carriers, modulates interfacial band bending and the Schottky-barrier height, and promotes the separation and interfacial migration of photogenerated, chemically generated, or externally injected charge carriers. Notably, the strain-induced piezopotential primarily redistributes or separates the available charge carriers and should not be considered to continuous generate long-lived electron–hole pairs across the bandgap in the absence of a known carrier source. One-dimensional nanowires, nanorods, nanobelts, and vertically aligned arrays possess unique structural advantages: the anisotropic geometry amplifies axial strain, maintains consistent polar-axis orientation, and suppresses polarization cancellation among randomly oriented grains.[75] These features enable wurtzite semiconductors to function efficiently in ultrasonic-driven, fluid-flow-driven, and piezo-photocoupled catalytic systems.

3.1.5 Two-dimensional van der Waals materials

Two-dimensional van der Waals piezoelectric and ferroelectric materials include non-centrosymmetric or thickness-dependent transition-metal dichalcogenides such as MoS_2,[76] WS_2,[77] $MoSe_2$,[78] reported strain- or distortion-activated layered systems such as $MnPSe_3$,[79] and emerging two-dimensional ferroelectric materials (Figure 3d).[80,81] As opposed to the case of bulk materials, the electromechanical properties of 2D systems are determined by the actual crystal phase, layer-number parity, stacking sequence, lattice orientation, substrate interaction, and defect states, and not solely by the chemical composition. The piezoelectric behavior of layered transition-metal dichalcogenides is strongly governed by the layer number and stacking configuration. In ideal 2H-phase lattices, odd-layer structures break the inversion symmetry to induce in-plane piezoelectricity, whereas even-layer structures show complete interlayer polarization cancellation. Nevertheless, the substrate asymmetry, lattice twisting, stacking faults, unequal surface termination, and intrinsic defects can induce a residual extrinsic piezoresponse in nominally centrosymmetric even-layer samples. In contrast, non-centrosymmetric 3R stacking retains stable piezoelectric activity in multilayer structures.[82] Two-dimensional van der Waals materials feature high surface-to-volume ratios, ultrashort carrier-transport distances, mechanically flexible lattices, and abundant edge and defect sites. Notably, geometrically accessible basal planes are not always catalytically dominant, and the edge defects often serve as major reactive centers. The band structures and interfacial electronic states can be tuned via strain modulation, layer-number engineering, stacking-angle regulation, phase transition, elemental substitution, and heterostructure construction.[83] Monolayers provide a small total polarization charge, whereas layer restacking can simultaneously reduce

DOI: 10.68642/ftms.202600008

the effective surface area and macroscopic piezoelectric output. In addition, some ultrathin structures are susceptible to oxidation, surface reconstruction, and fragmentation under cavitation impact. Thus, the catalytic performance may vary non-monotonically with the layer number rather than following a universal principle of "thinner is better". The atomic thinness enables intimate interfacial contact with cocatalysts and photosensitive semiconductors, thus facilitating the coupling of strain-induced polarization, photoexcitation, and interfacial redox catalysis.

3.1.6 Other inorganic piezoresponsive materials

Symmetry engineering in nominally centrosymmetric materials can substantially broaden the range of mechanically responsive catalytic materials. Materials such as $SrTiO_3$, TiO_2, and $SrZrO_3$ can develop localized polar regions via ordered or graded oxygen-vacancy distributions, ionic doping, surface or interfacial asymmetry, strain gradients, and structural confinement in ultrathin layers (Figure 3e).[84-86] Reported low-dimensional systems include nitrogen-doped graphene and HfO_2-based ultrathin structures, in which local coordination asymmetry, stabilization of a polar phase, and size or interface effects may contribute to electromechanical coupling.[87] The responses of these materials are often highly localized and strongly dependent on the defect concentration, defect distribution, actual crystal phase, sample dimensions, and mode of mechanical loading. Consequently, the apparent piezoelectric output may have limited reproducibility and cycling stability. Experimental investigations of these systems must distinguish the proposed electromechanical contribution from ultrasonic-cavitation-induced radical chemistry, triboelectric charging, and localized thermal effects. By contrast, intrinsically non-centrosymmetric crystals such as $Ca_2B_3O_6Cl$ and natural tourmaline possess genuine bulk piezoelectricity, although their wide bandgaps, high resistivity, and mechanical rigidity can restrict free-carrier migration and mechanical energy transfer.[88,89] Therefore, these materials are often employed as mechanically active phases in composite catalytic systems.

3.1.7 Framework/molecular/organic-inorganic hybrid materials

Framework-based, molecular-based, and organic–inorganic hybrid piezoresponsive materials include metal–organic frameworks (MOFs), covalent organic frameworks (COFs), coordination polymers, metal-organic cages, molecular crystals, conjugated organic materials, natural molecular assemblies, and organic-inorganic hybrid crystals (Figure 3f). The electromechanical responses of these materials stem from multiple synergistic mechanisms such as metal–ligand relative displacement, polar functional group orientation, molecular dipole rotation, donor–acceptor charge transfer, guest molecule ordering, interfacial polarization, and defect/mixed-linker-induced local symmetry breaking. Not all framework and molecular materials possess intrinsic bulk piezoelectricity. A nonzero macroscopic piezoelectric tensor requires a piezoelectrically active non-centrosymmetric crystal class together with a non-canceling arrangement of polar structural units. The local dipole moments of individual molecules, clusters, or pores can be completely offset by antiparallel packing or random particle orientation, resulting in zero macroscopic piezoresponse. The principal advantage of this material family lies in its molecular-scale programmability, which enables the coordinated design of polarization generation, reactant adsorption, molecular recognition, mass transfer, electronic structures, and catalytic active sites.

Reported piezoresponsive MOFs include NH_2-UiO-66, MIL-125, and MIL-101(Al).[90-92] The high specific surface area, tunable pore microenvironment, and coordinatively unsaturated metal nodes of these MOFs facilitate the enrichment and activation of CO_2, O_2, and nitrogen-containing small molecules.[93] Flexible coordination bonds can enable local structural deformation under mild mechanical loading, while ligand functionalization, mixed-metal nodes, linker vacancies, modulator incorporation, and guest encapsulation precisely regulate the local dipole moments, electronic structures, adsorption energetics, and charge-transfer pathways.[94] The ideal parent structures of many widely studied MOFs are centrosymmetric, and their measurable electromechanical responses predominantly originate from missing-linker defects, defect gradients, oriented growth, asymmetric surface termination, guest-molecule ordering, finite-size effects, flexoelectricity, or interfacial symmetry breaking rather than from the intrinsic bulk piezoelectric tensor of the ideal framework. This limitation does not apply to deliberately designed polar or chiral MOFs with confirmed piezoelectrically active crystal symmetry. MOFs also suffer from several inherent drawbacks, including low electrical conductivity, randomly oriented polycrystalline particles, inefficient stress transfer through porous architectures, solvent-induced framework softening, and coordination-bond fatigue. Therefore, a high specific surface area does not guarantee high mechanical-to-chemical energy-conversion efficiency.

Typical piezoresponsive COFs are TP-BT-0F-COF,[95] COF-TpDb,[96] and COF-DH-Eth.[97] The molecular dipole moments and macroscopic polarization of these COFs can be modulated by appropriate choice of polar linkage, asymmetric/twisted monomer design, structural engineering of the donor–acceptor interface, and non-centrosymmetric stacking configuration. Both building-block symmetry and long-range stacking order determine the constructive superposition or mutual cancellation of local molecular dipoles. Extended π-conjugated channels allow for improved light absorption and better charge transport, endowing COFs with considerable potential for application to piezo-photocatalysis.[98] Nevertheless, a small degree of extended conjugation does not guarantee high macroscopic mobility because stacking disorder, grain boundaries, incomplete polymerization, structural defects, and poor interdomain connectivity may disrupt charge-transport pathways. The design of high-performance COF piezocatalysts therefore requires careful consideration of the trade-offs among multiple competing factors. Increasing the molecular dipole moments and breaking the inversion symmetry can strengthen polarization, whereas excessive structural torsion can disrupt π-conjugation and suppress carrier mobility. Enlarged pore channels accelerate mass transfer but may weaken the framework rigidity and reduce the stress-transfer efficiency. Improved conductivity promotes charge extraction but can accelerate piezopotential screening. Therefore, coherently aligned and non-canceling

DOI: 10.68642/ftms.202600008

dipoles, mechanically coupled crystalline domains, controlled flexibility, stable stacking, accessible reactive sites, and continuous charge-transport pathways are central to efficient COF-based piezocatalysis.[99]

Within this broad material family, representative organic, molecular, and organic–inorganic systems include hybrid halide perovskites,[100] $ZnS(en)_{0.5}$,[101] HETP-Ni-GY conjugated frameworks,[102] donor-acceptor-type conjugated polymers,[103] and microcrystalline cellulose.[104] The piezoresponses of this family stem from cooperative molecular dipole orientations, asymmetric coordination, hydrogen-bond networks, interfacial strain polarization, and relative displacement between the organic and inorganic sublattices. The coupling of molecular and lattice polarization can enhance the net electromechanical output, but the magnitude and stability of this enhancement strongly depend on the structural phase order, dipole alignment, and interfacial coupling strength.

Overall, the seven piezocatalyst families differ substantially in the polarization mechanism, charge transport, mechanical response, surface chemistry, and structural stability. Three-dimensional perovskite oxides show strong spontaneous polarization but often suffer from limited carrier density, dielectric screening, and inefficient interfacial charge extraction. Layered bismuth-based materials allow for anisotropic transport and effective strain-gradient coupling, but their performance is strongly dependent on the phase symmetry, thickness, defect chemistry, and chemical stability. Ferroelectric polymers are advantageous for harvesting weak and low-frequency mechanical energy, although their polar-phase content, orientation, conductivity, and long-term mechanical reliability require careful control. Wurtzite semiconductors combine intrinsic piezoelectricity with favorable electronic transport, but their piezopotentials are readily screened by mobile carriers, and sulfide-based systems may suffer from corrosion and elemental-release risks. Two-dimensional van der Waals materials provide short carrier-transport paths and highly tunable symmetry; however, polarization cancellation, restacking, limited total polarization charge, and structural degradation remain important limitations. Other inorganic non-centrosymmetric crystals can provide intrinsic electromechanical coupling, whereas nominally centrosymmetric systems require clear identification of the defect-, interface-, flexoelectric-, or phase-induced origin of their piezoelectric responses. Framework-based and molecular materials offer the advantages of high structural programmability but suffer from dipole cancellation, poor conductivity, inefficient stress transfer, and framework instability. High-performance piezocatalysts therefore require a coordinated balance among mechanical energy transfer, polarization generation, dielectric screening, carrier lifetime, surface reaction kinetics, and structural durability; in other words, performance evaluation cannot rely on the piezoelectric coefficients alone. Rational heterostructure construction, together with domain, defect, interface, and multi-field engineering, can mitigate the limitations of individual material families and provide a systematic basis for catalyst design, mechanistic analysis, and reliable performance assessment.

3.2 Material design and modification strategies

A clear understanding of the material system through multiscale control of the microstructure, electronic band, and heterojunction would aid the systematic optimization of the activity and selectivity of piezocatalysts. This section comprehensively constructs a four-dimensional progressive modification system covering atomic-scale lattice polarization modulation, mesoscopic microstructure regulation, interfacial optimization, and surface functionalization toward hierarchical and precise regulation of the piezocatalytic performance, from intrinsic lattice properties to external surface reaction behavior.

3.2.1 Lattice polarization modulation

Atomic-scale lattice polarization modulation is the core intrinsic regulation strategy for piezocatalysts. Such modulation, fundamentally changes the lattice symmetry, local dipole moment distribution, and electronic structure of materials, thereby optimizing the intrinsic piezoelectric response and charge generation capacity (Figure 4a). This strategy includes ion doping and substitution, defect engineering, as well as phase structure and phase boundary engineering. Ion doping is an efficient and controllable method to tune the lattice distortion, band structure, electrical conductivity, and carrier density. Metal dopants such as Ca, Sr, La and Nb regulate the lattice parameters, phase composition, and Curie temperature of perovskite oxides, thereby improving the piezoelectric output and charge migration efficiency.[105-108] Non-metal dopants such as N, S, and P modify the valence band composition and introduce hybridized states, which optimize the surface acid–base properties and enhance the adsorption capacity for reactant molecules.[109-111] Nevertheless, strict control of the dopant concentration and occupation sites is essential, because excessive doping can destroy the long-range ordered crystal structure, weaken the intrinsic polarization, and introduce deep recombination centers. Defect engineering allows for the effective coupling of electronic state regulation and surface reaction activation. Commonly engineered defects in piezoelectric materials include oxygen, sulfur, and metal vacancies.[112-114] These defects induce local lattice distortion, alter the carrier concentration, and create unique adsorption and activation sites for small molecules. Moderate oxygen vacancies form shallow donor states in multiple piezoelectric systems, accelerating electron migration and strengthening chemisorption on the catalyst surfaces.[115] On the one hand, appropriate defect levels promote charge separation and reactant activation; on the other hand, excessive defects act as recombination centers and degrade structural stability. Precise regulation of the defect concentration, spatial distribution, and valence states is therefore a core prerequisite for efficient defect engineering. Dipole modulation focuses on optimizing the intrinsic polarization properties of piezoelectric materials. This strategy controls lattice distortion as well as the magnitude and orientation of intrinsic dipole moments, thereby optimizing the polarization response of ferroelectric domains and polar lattices.[116] Consequently, this process modulates band offset and the space-charge layer thickness, while the enhanced piezopotential provides a stronger driving force for directional carrier migration. Phase structure and phase boundary engineering is a unique atomic-scale regulation strat-

DOI: 10.68642/ftms.202600008

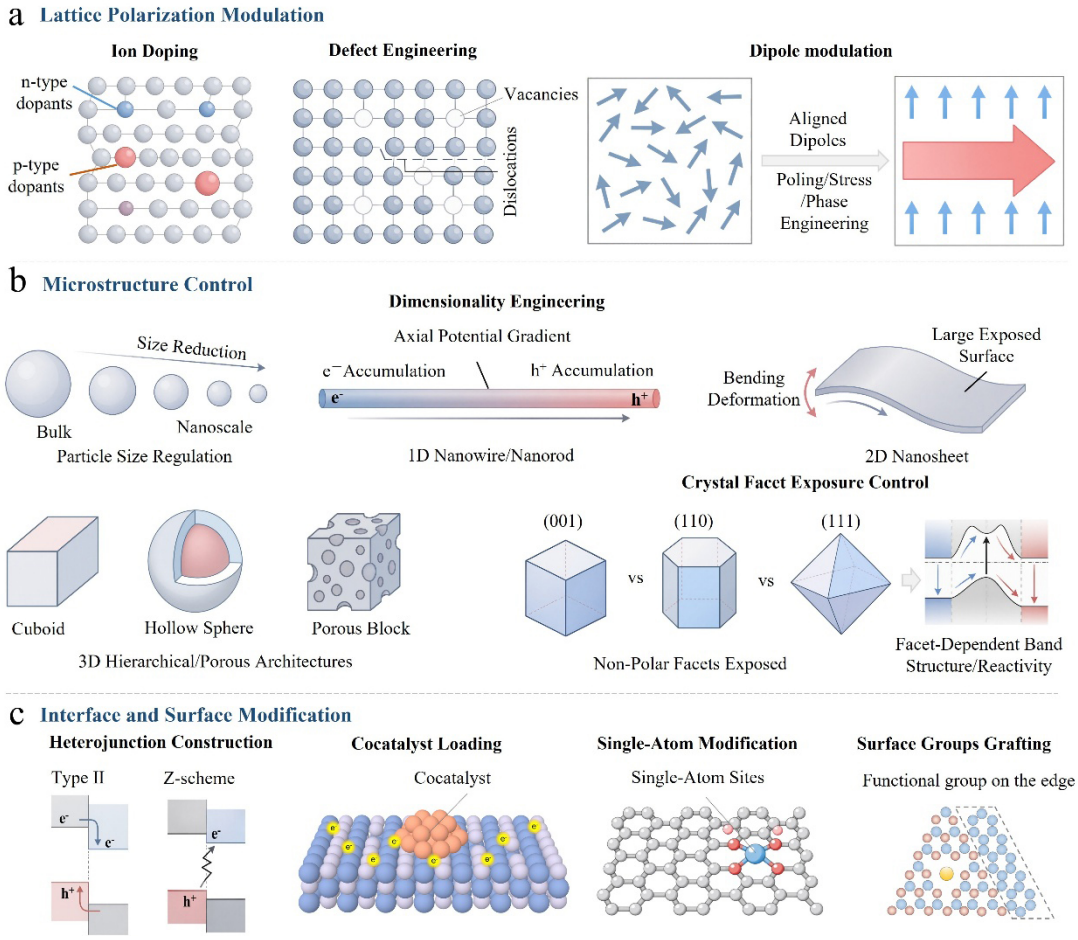


Figure 4 **Modification and regulation strategies for piezoelectric materials.** a, Lattice polarization modulation (including ion doping, defect engineering and dipole modulation). b, Microstructure regulation (including size/dimensionality/hierarchical structures and crystal facet regulation). c, Interface and surface regulation (including heterostructure construction, cocatalyst modification, single-atom/dual-atom site construction and surface functional group modification).

egy to optimize the piezoelectric polarization. The morphotropic phase boundary with coexisting multi-phase structures can effectively reduce the domain flipping barrier, induce enhanced lattice distortion, and significantly amplify the macroscopic piezoelectric response of the material.[117] A reasonable degree of phase regulation can stabilize the polarized lattice structure, prevent polarization attenuation under cyclic mechanical excitation, and sustain stable charge-generation performance for long-term catalytic reactions.

3.2.2 Microstructure control

Microstructure control is a fundamental modification strategy to improve the mechanical response, carrier migration behavior, and interfacial reaction performance of piezocatalysts. This effective regulation method optimizes a series of key structural parameters, including the particle size, dimensionality, morphology, porosity, and exposed crystal facets (Figure 4b). Consequently, the optimized structural characteristics further enhance the internal stress transfer efficiency, increase the exposure density of active sites, shorten the diffusion distance of charge carriers, and promote interfacial mass transport. Nanoscale structural engineering significantly improves the overall piezocatalytic performance of the material. Nanosized particles induce larger local deformation under external mechanical excitation. This structural advantage not only strengthens the intrinsic piezoelectric response but also shortens the migration path of internal carriers, thereby reducing the probability of electron–hole recombination.[118] Dimensional engineering achieves directional and precise regulation of the stress response and charge migration behavior. One-dimensional nanowires and nanorods show high structural anisotropy and large stress concentration effects, which facilitate the formation of stable axial piezopotential gradients and facilitate the spatial separation of oxidation and reduction sites.[119,120] By contrast, two-dimensional nanosheets are more susceptible to bending deformation under low-frequency mechanical excitation; this property imparts the material with excellent low-frequency responses and large exposed surfaces.[121] Three-dimensional porous, hollow, and hierarchical structures help optimize the distribution of acoustic cavitation stress and construct interconnected channels for electrolyte penetration, reactant adsorption, and product desorption.[122-124] Hierarchical structural design therefore offers prominent advantages for catalytic systems with poor interfacial mass transfer. Besides the particle size and dimensionality, precise morphology control also exerts an extremely significant impact on the piezocatalytic activity. For instance, a supramolecular-driven hydrothermal strategy using self-assembled natural

DOI: 10.68642/ftms.202600008

betulinic acid as a dynamic soft template has enabled the precise synthesis of ZnO/CuO heterojunctions with progressively tuned morphologies, including rod-like, airship-like, star-like, and urchin-like particles.[125] The large number of sharp protrusions and highly bendable features of these structures increase the strain probability and strain gradients, leading to improved piezoelectric performance under low-frequency mechanical excitation. Crystal facet regulation is indispensable for improving reaction selectivity. Different exposed facets result in distinct atomic arrangements, surface polarities, molecular adsorption configurations, and local electronic band structures, which effectively adjust the activation barriers and redox pathways of small molecules. For example, selective exposure of the polar facets in typical piezoelectric materials such as $BaTiO_3$, ZnO, and $BiVO_4$ strengthens localized polarization fields and promotes interfacial charge redistribution.[126-128] This precise structural regulation guides multielectron pathways and prevents undesirable side reactions, ultimately improving the selectivity and yield of the target products.

3.2.3 Interfacial regulation

The interfacial and surface properties of piezocatalysts decide interfacial carrier transport, molecular adsorption configuration, and final reaction selectivity (Figure 4c). These surface characteristics connect the intrinsic piezoelectric performance of a given material with the macroscopic catalytic behavior. Interfacial regulation includes heterostructure fabrication, interfacial bonding modulation, and piezopotential synergistic coupling, thereby fundamentally solving the issues of slow charge transfer and rapid carrier recombination in single piezoelectric materials. Heterostructure fabrication is the mainstream and most effective approach to enhance interfacial charge separation. Combining piezocatalysts with semiconductors or conductive materials that possess different band structures and polarization characteristics can aid the construction of diverse high-efficiency heterojunctions such as Z-scheme, II-type, and Schottky junctions.[4,129,130] Depending on interfacial band matching, these heterojunctions enable the rapid separation and directional migration of piezoelectric-induced electron–hole pairs, thus mitigating recombination losses. In addition, the heterojunction interface exposes abundant unsaturated active sites and optimizes the adsorption and activation of small molecules. Interfacial bonding regulation focuses on optimizing the interfacial contact state between different components. Strong interfacial chemical bonding can reduce the interfacial contact resistance, facilitate rapid cross-interface charge transmission, and prevent charge accumulation at the heterojunction interface. In contrast, loose physical contact leads to the formation of interfacial defects and hinder carrier migration, limiting the synergistic catalytic effect of heterostructures.[131-133] Synergistic piezopotential coupling aids the superposition of multiple electric fields to amplify the catalytic performance.[134] The built-in electric field of heterojunctions can couple with the strain-induced piezopotential, leading to further interfacial band bending, enhancing the driving force for directional carrier migration, and effectively suppressing interfacial charge recombination.[135] This multifield synergistic effect significantly improves the thermodynamic and kinetic conditions of interfacial redox reactions.

3.2.4 Surface modification

Surface modification is the terminal regulation strategy for piezocatalytic reactions, which optimizes the surface active sites, reactant adsorption behavior, and reaction kinetics without changing the intrinsic lattice and microstructure of piezoelectric substrates. The main technical routes for surface modification include cocatalyst decoration, monoatomic/diatomic site construction, and surface functional group/molecular skeleton modification. Cocatalyst loading and single-atom modification further optimize the kinetic characteristics of interfacial reactions. Noble metals such as Pt, Au, and Ag, as well as transition-metal oxides and MXene, can serve as efficient electron- or hole-trapping sites.[136-140] Selective deposition of cocatalysts on positive and negative polarization surfaces promotes the spatial separation of charges and suppresses side reactions.[141] At the atomic scale, single-atom sites provide nearly full atomic utilization and highly tunable coordination environments.[142] These sites can regulate the adsorption configurations and activation barriers of key intermediates with high precision, which is especially valuable for multielectron reactions with complex selectivity requirements. Furthermore, grafting polar functional groups or constructing donor–acceptor (D–A) molecular skeletons on the surface of piezocatalysts can modify the surface electron density distribution, optimize the adsorption affinity and the configuration of target small molecules and key intermediates, and precisely regulate the reaction pathway to inhibit side reactions.[143]

This chapter systematically establishes a comprehensive classification system for piezocatalysts, and it has clarified the structural characteristics, performance advantages, and application limitations of inorganic, organic, and composite piezocatalysts. Furthermore, it identifies the suitable reaction scenarios for different material systems. Building on this foundation, the chapter delves into the action mechanisms and structure–property relationships for the four major modification strategies–lattice polarization modulation, microstructure control, interface engineering, and surface modification–from four core dimensions spanning atomic-scale to surface-level regulation. This chapter also elucidates the synergistic mechanisms and applicability limits of each strategy. Overall, inorganic piezoelectric semiconductors, with their advantages of polarization stability and structural controllability, constitute the core material system for piezocatalysis, while organic and porous composite framework materials expand the flexibility and precision of catalytic system design. Notably, lattice polarization, microstructure modification, interface modification, and surface modification are not independent but operate in a unified manner. For example, two-dimensional ultrathin structures can provide fully exposed anchoring sites for single-atom sites; defect engineering can modulate the band structure and heterojunction coupling as well as the nucleation behavior of the cocatalyst; superposition of the ferroelectric polarization field and built-in electric field within the heterojunction can significantly enhance carrier separation. However, highly conductive networks may screen the piezopotentials if their structure is not carefully designed. Therefore, the design of high-performance piezocatalysts should move beyond single-parame-

DOI: 10.68642/ftms.202600008

ter optimization and toward multiscale synergistic regulation. Future studies should focus on reaction-oriented reverse design, wherein the catalyst composition, morphology, defects, interfaces, and active sites are optimized according to the adsorption configuration, activation barrier, redox potential, stability of intermediates, and product selectivity in the target small-molecule reaction.

4 Piezocatalysis for Efficient Conversion of Core Small Molecules

Piezocatalysis can harvest the ubiquitous mechanical energy from various environmental sources such as vibrations, impact, fluid shear, acoustic waves, and human motion. Noncentrosymmetric crystal structures can generate internal polarization electric fields under mechanical excitation, which in turn drive bulk charge separation and trigger surface redox reactions. By replacing the externally supplied electricity with the locally available mechanical energy, piezocatalysis offers complementary advantages for distributed and sustainable small-molecule conversion. This chapter systematically reviews the mechanisms, material advances, modification strategies, and major bottlenecks related to piezocatalysis in water splitting, CO_2RR, nitrogen fixation, nitrate reduction, O_2 reduction for H_2O_2 production, ROS-mediated degradation of small organic pollutants, and oxidative conversion of methane (Figure 5).

4.1 Water splitting for hydrogen and oxygen production

Water splitting is the most extensively studied reaction in piezocatalysis. The entire reaction process includes three core steps: mechanical strain-induced polarization, charge separation and migration, and interfacial redox reactions. The corresponding standard Gibbs free energy change is approximately 237 kJ mol^{-1}, and the theoretical thermodynamic decomposition voltage is 1.23 V.[61] Application of periodic mechanical strain materials with effective piezoelectric or strain-polarization responses triggers relative displacement between the positive and negative charge centers inside crystals and further generates dynamic polarized charges.[144] This process is accompanied by band bending, changes in the work function, and reconstruction of the interfacial potential. At the reduction sites, electrons or negative shielding charges drive H^+ or the adsorbed H_2O to generate H* intermediates through the Volmer pathway, and subsequent H_2 formation follows on the Tafel or Heyrovsky mechanism.[145] At the oxidation sites, holes or positive shielding charges promote the sequential transformation of H_2O and OH^- into *OH, *O, and *OOH intermediates, ultimately forming O–O bonds and releasing O_2.[55] The oxygen evolution reaction proceeds via a four-electron transfer process and involves multiple oxygen-containing intermediates, thereby leading to drastically slower kinetics compared with the case of the hydrogen evolution reaction. Consequently, bulk carrier recombination, screening of polarization charges, and deficiency of efficient oxidation sites jointly limit the overall water-splitting efficiency. Some catalytic systems instead couple H_2 evolution with H_2O_2 formation through a two-electron water-oxidation pathway; therefore, evolution of intermediates evolution and the product stoichiometry are fundamentally different from those in conventional H_2/O_2 overall water splitting.[146]

Ferroelectric perovskites and layered polar oxides are the core material systems for the fabrication of high-efficiency piezoelectric water-splitting catalysts. Precise exposure of a high proportion of (001) polar crystal planes effectively guides the oriented migration of $BaTiO_3$ charge carriers along the out-of-plane polarization direction and substantially increases the number of effective surface reaction sites. Accordingly, oriented $BaTiO_3$ nanosheets deliver better piezocatalytic H_2 evolution performance than randomly oriented nanoparticles.[147] Under the combined effects of size confinement and nonuniform tensile strain (001)-oriented $PbTiO_3$ nanosheets with a thickness of approximately 3.5 nm undergo reconstruction from a predominantly c-axis-oriented polarization state to a multidirectional

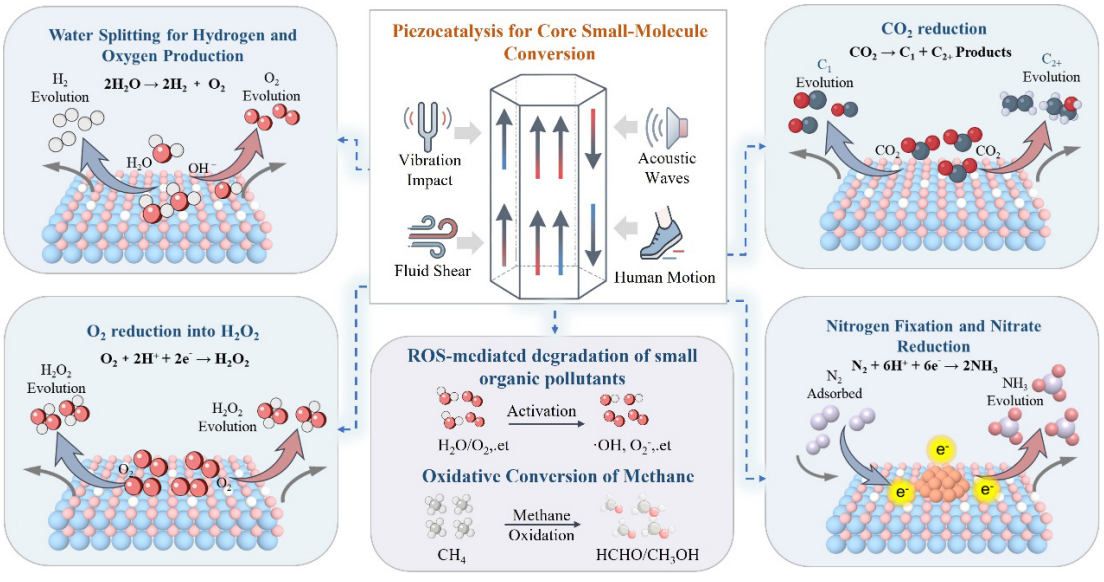


Figure 5 **Schematic illustration of piezocatalysis driven by diverse mechanical stimuli and its representative small-molecule conversion reactions.**

DOI: 10.68642/ftms.202600008

polarization configuration (Figure 6a).[148] This structural regulation substantially enhances the nanoscale piezoelectric response and enables overall pure-water splitting without sacrificial agents. Bismuth-based materials feature intrinsic asymmetric crystal structures and facilitate synchronous optimization of the local polarization field and surface reaction kinetics. Ultrafine hollow Bi_5O_7Br nanotubes constructed from axially asymmetric $[Bi_5O_7]$ polar units exhibit a large local electrostatic potential difference. External mechanical stress further enhances the polarization intensity and precisely modulates the interaction between the Bi active sites and H* intermediates to optimize the kinetic process of pure-water hydrogen evolution.[149] Single-unit-cell-thick $Bi_2O_2(OH)(NO_3)$ layers bear fully exposed polar hydroxyl groups, which weaken the interlayer electric field shielding effect and initiate strain-induced self-polarization toward the controllable synchronous generation of hydrogen and hydrogen peroxide.[150] These examples show that polar-facet regulation, thickness reduction, and polarization-orientation reconstruction not only improve the mechanical-to-electrical energy conversion efficiency but also modify the water adsorp-

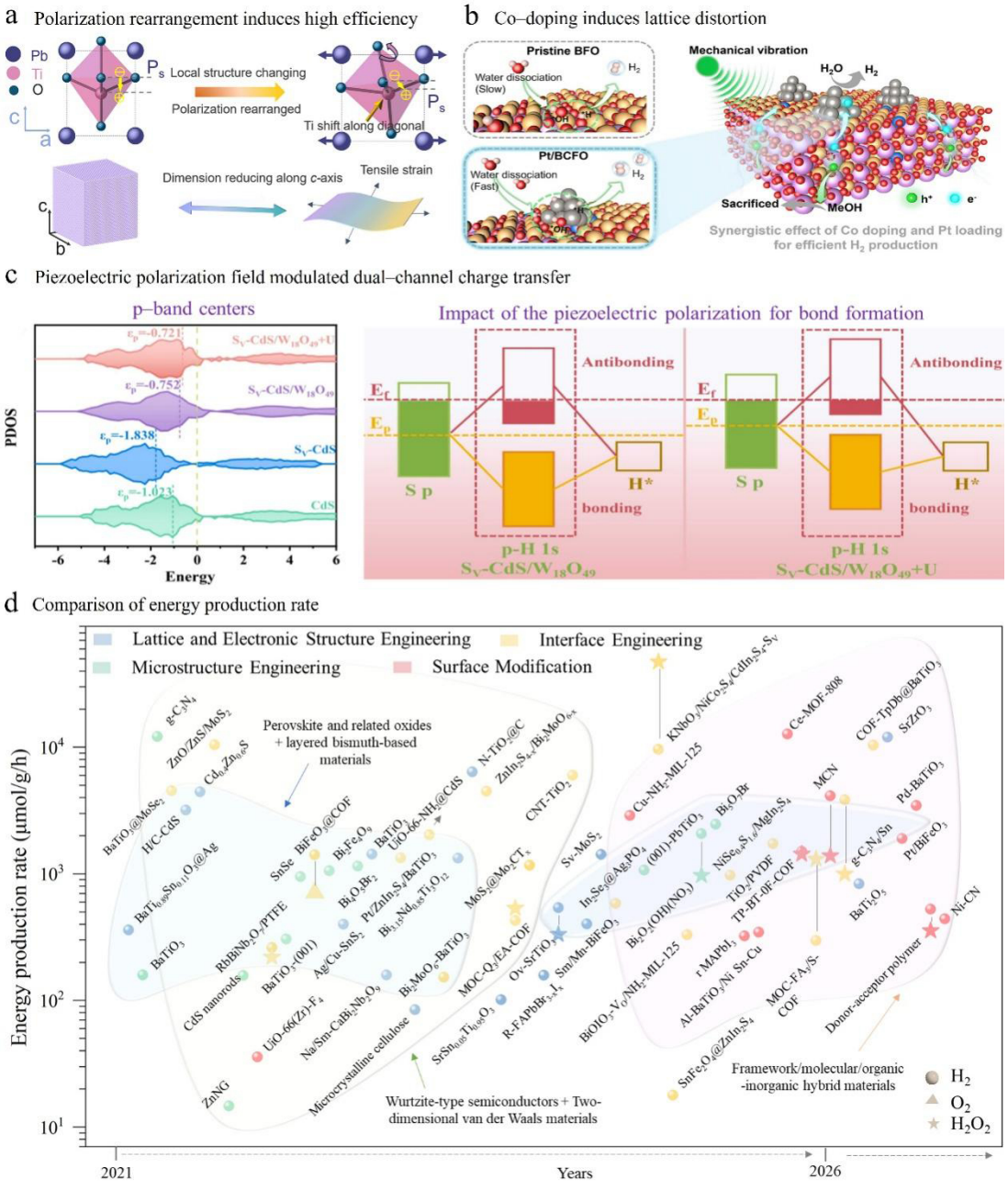


Figure 6 a, Schematic of local structural modifications in $PbTiO_3$. Reproduced with permission.[148] Copyright 2025, American Chemical Society. b, Piezo-induced carrier motion and H_2O dissociation site preference visualized on Pt/$BiFeO_3$. Reproduced with permission.[154] Copyright 2026, Wiley-VCH GmbH. c, Piezo-field-driven dual-channel carrier transfer in S_V-$CdS/W_{18}O_{49}$. Reproduced with permission.[156] Copyright 2025, Elsevier. d, Comparison of H_2 production rates over representative piezocatalysts. Detailed data are provided in Table S1 of the Supporting Information.

DOI: 10.68642/ftms.202600008

tion configurations and the energy barriers of key intermediates. Defect engineering and near-surface structural modulation break the local lattice symmetry and thus trigger the catalytic activity of inert materials that show a weak intrinsic piezoelectric response or feature centrosymmetric materials crystal structures. Oxygen-vacancy-modified $SrTiO_3$ nanorods integrate the high stress collection capability of one-dimensional structures with defect-induced surface asymmetry for the synchronous production of hydrogen and hydrogen peroxide in pure water systems without using sacrificial agents.[84] Mild acid etching modification induces near-surface lattice distortion and surface potential restructuring while fully preserving the $SrZrO_3$ perovskite bulk framework. This strategy, successfully activates localized electromechanical responses in centrally symmetric materials and significantly enhances piezoelectric catalytic hydrogen production performance.[86] An oxygen-vacancy-rich amorphous TiO_x shell constructed on the surface of $BaTi_2O_5$ nanorods forms an ordered–disordered composite core–shell interface, effectively amplifying the interfacial polarization field and optimizing the efficiency of charge separation and migration.[120] Sulfur-vacancy modification can regulate the local charge distribution and hydrogen adsorption properties of MoS_2, further enhancing the strain polarization capability and hydrogen evolution catalytic activity.[151]

Atomic-site modification and interface engineering enable the multidimensional synergistic optimization of polarization enhancement, charge capture, and surface reaction kinetics. The Ni–N_6 planar coordination structure formed by single-atom-anchored Ni species improves the in-plane dipole moment of carbon nitride frameworks and induces radial local polarization fields around the active sites. External strain simultaneously modulates the polarization field intensity and Ni atom spin state. This dual response spatially matches the electron-rich regions with the hydrogen-evolution sites and alleviates both piezopotential screening and the spatiotemporal mismatch between charge generation and interfacial reactions.[152] Atomic-level Fe active sites in Fe-N_4/r-$MAPbI_3$ composites derived from lead-zinc slag synchronously enhance the lattice polarization intensity and interfacial proton transfer efficiency, demonstrating the advantages of multifunctional regulation at single-atom sites.[100] Pd quantum dot-modified $BaTiO_3$ promotes interfacial charge migration through the electron pooling effect. Modulation of the d-band center optimizes the adsorption and desorption behavior of H* intermediates to continuously accelerate the hydrogen evolution reaction.[153] Pt-modified Co-doped $BiFeO_3$ enhances the piezoelectric polarization effect via lattice distortion and accelerates water molecule dissociation and the Volmer elementary reaction at the Pt active sites (Figure 6b).[154] The MoS_2@Mo_2CT_x heterojunction integrates piezoelectric polarization with high-conductivity MXene networks to enable sustainable hydrogen evolution using the mechanical energy from natural sources such as water flow and gravity.[155]

In the $CaBi_2Nb_2O_9$/BiOX system, the shared $(Bi_2O_2)^{2+}$ units act as atomic-scale charge-transfer bridges, and the additional polarization field induced by structural distortion significantly reduces the interfacial charge migration barrier, thereby ensuring efficient charge transport.[117] Collectively, these studies indicate that an effective catalytic interface must combine rapid electron transport with spatial alignment across the piezoelectric polarization field, built-in electric field, and catalytic active sites. Coupling piezocatalysis with photocatalysis is an important strategy for increasing the charge-generation rate in single-mode piezocatalysis. Light irradiation continuously generates electron–hole pairs, whereas the piezoelectric field promotes directional charge separation and dynamically regulates the heterojunction band structures and surface adsorption states. A Z-scheme COF-TpDb/$BaTiO_3$ heterojunction couples ferroelectric polarization with an intrinsic interfacial electric field, thus suppressing charge recombination and reducing the calculated hydrogen-evolution barrier from 0.14 to 0.04 eV.[96] A sulfur-vacancy-modified CdS/$W_{18}O_{49}$ system integrates dual-vacancy regulation, surface-plasmon effects, and piezoelectric polarization to establish separate transfer channels for photogenerated and thermally generated electrons, thereby improving charge utilization (Figure 6c).[156] Organic and framework materials can enhance the piezoelectric performance through rational molecular structural design. Pyridine-nitrogen-modified donor–acceptor polymers, hydroxy-cyano co-modified carbon nitride, Sn-modified g-C_3N_4 composites, and high-dipole-moment polar COFs increase the intrinsic dipole moment and improve the carrier separation capability by breaking the molecular framework symmetry.[95,103,157,158] Composite systems such as MOC/COF heterojunctions, Ce-MOF-808 pore donor–acceptor composites, and amino-copper dual-modified MIL-125 further demonstrate that the polarity of molecular-scale frameworks, active sites, and charge channels can be integrated and synergistically designed, thus providing a novel approach for constructing highly efficient piezoelectric catalytic systems.[159-161] In summary, piezocatalytic water splitting is a multistep energy-conversion process governed by strain-induced polarization, directional charge separation and transport, and interfacial hydrogen- and oxygen-evolution kinetics. The performance of this reaction depends not only on the nominal piezoelectric coefficient but also on the magnitude, persistence, and spatial distribution of the polarization field; the lifetime and mobility of the charge carriers; and the adsorption and conversion of the reaction intermediates. To systematically compare the effects of different modification strategies, the relevant studies were reviewed and classified by publication year. The results are summarized in Figure 6d and Table S1.

High-performance piezocatalysts can be developed by hierarchical structural regulation across the crystal, defect, atomic-site, and interface levels. Preferential exposure of polar facets, reduction of material thickness, and reconstruction of polarization orientation enhance the efficiency of mechanical-to-electrical energy conversion and promote directional carrier migration. Defect engineering and near-surface lattice distortion can break the local symmetry, activate the electromechanical responses in weakly piezoelectric or centrosymmetric materials, and optimize the adsorption energetics of intermediates. At the atomic scale, single-atom sites, quantum dots, and cocatalysts simultaneously provide charge-trapping centers and kinetically favorable reaction sites. Meanwhile, heterojunctions and ordered–disordered interfaces establish efficient charge-transfer pathways and

DOI: 10.68642/ftms.202600008

strengthen the coupling between piezoelectric polarization fields, built-in electric fields, and catalytic active sites. The piezocatalytic efficiency can be enhanced by optimizing the polar crystal facets, defect engineering, atomic-site modulation, and interface design. Meanwhile, polar polymers, carbon nitride derivatives, COFs, MOFs, and other framework materials expand the design space from inorganic crystal engineering to molecular-level control of dipole moments, framework symmetry, pore environments, active sites, and charge-transfer channels. Future catalyst design should integrate polar-facet and dimensional control, local symmetry breaking, atomic-site engineering, and interface construction so that mechanical-energy harvesting, charge transport, and surface kinetics are optimized within a single architecture.

4.2 CO_2 reduction

Piezocatalytic CO_2 is a mechanically driven interfacial proton-coupled electron-transfer process. Periodic stress induces alternating polarization within the piezoelectric material and causes the catalyst surface to undergo continuous cycles of polarization, shielding, and deshielding, accompanied by dynamic band bending and transient charge migration.[102] The incompletely shielded piezoelectric potential drives the directed enrichment of electrons at the reduction sites while disrupting the electron cloud distribution of linear CO_2 molecules and weakening their molecular structural symmetry.[162] These effects facilitate CO_2 adsorption and activation and lower the interfacial reaction barrier. The adsorbed substrate typically undergoes stepwise electron and proton transfer processes via intermediates such as $*CO_2^-$, *COOH, or *OCHO. The binding strength of the active sites to intermediates such as *COOH, *CO, and *CHO directly determines the formation of C_1 products, including CO, formic acid, methanol, and CH_4.[76,163,164] However, the transient and periodic piezoelectric response makes sustained multi-electron delivery difficult. Together with the high mass-transfer resistance of CO_2 in aqueous media, this limitation explains why existing piezocatalytic CO_2RR systems predominantly yield C_1 products. Achieving high yields and selective formation of multicarbon products therefore remains a central challenge.

Ferroelectric perovskites, two-dimensional layered semiconductors, bismuth halide oxides, and inorganic–organic hybrid materials constitute the primary material platforms for current piezoelectric CO_2RR systems. $BaTiO_3$, $K_{0.5}Na_{0.5}NbO_3$, and $BiFeO_3$ exhibit excellent intrinsic polarization responses and rely on piezoelectric or ferroelectric fields to accelerate carrier separation, thereby efficiently driving the continuous interfacial reduction reaction. The $ZnIn_2S_4/BaTiO_3$ direct Z-scheme heterojunction, constructed using $BaTiO_3$ as the piezoelectric substrate, shows enhanced interfacial carrier mobility while retaining the strong electron reduction capability.[165] The sulfur-vacancy-modified $BaTiO_3/SnS_2$ heterojunction integrates the multiple synergistic effects of defect site regulation, Z-scheme charge pathways, and piezoelectric polarization fields to precisely enrich high-energy electrons on the SnS_2 surface, ultimately achieving the multielectron deep conversion of the substrate to C_2H_4.[166] The $BaTiO_3$-TiO_2-CuO-Cu_2O system relies on the Cu^+/Cu^{2+} redox pair to construct a dynamic proton relay system, and the lattice distortion induced by the piezoelectric field weakens the C–C coupling energy barrier, thereby providing favorable conditions for the formation of multicarbon products.[167] The KNN/PVDF-HFP dual-piezoelectric composite film combines the high polarization characteristics of inorganic materials with the flexible deformation advantages of polymers, and the conductive network formed by acetylene black optimizes the collection and long-distance transport efficiency of polarized charges.[168] Lattice tuning, defect engineering, and size control are effective methods for enhancing the piezoelectric catalytic activity of weakly piezoelectric and even centrosymmetric materials. SnS_2 nanosheets with (001) preferential orientation deliver superior piezoelectric photocatalytic performance compared to randomly oriented nanoflower structures. This finding clearly demonstrates that crystal orientation control and efficient stress transfer are key to enhancing the macroscopic piezoelectric catalytic output of materials.[169]

Oxygen vacancies within the BiOBr system induce localized structural distortions and strengthen the dipole effect of the Bi–Br bond. This significantly enhances the stress-induced polarization effect while simultaneously improving the catalytic selectivity for CO production.[60] Er-doped BiOCl simultaneously induces oxygen vacancy defects, broadens the light absorption response range, and improves the piezoelectric properties. When combined with the photocatalytic memory effect, this material comprehensively promotes substrate adsorption, activation, and interfacial charge separation processes.[170] HfO_2–phosphomolybdic acid hybrid subnanobands enhance strain responsiveness through size-dependent effects and the formation of flexible microstructures. The asymmetric Hf–O–Mo coordination structure induces spontaneous interfacial electron transfer and establishes a stable built-in electric field, while the reversible redox properties of PMA clusters effectively increase the interfacial electron density and significantly lower the formation energy barrier for the COOH intermediate.[87] Metal-free F-C_3N_4 reconfigures the electronic state distribution near the Fermi level through hybridization of the F-2p and C-2p orbitals and constructs an interfacial hydrogen-bond network tailored for substrate adsorption and COOH generation, ultimately achieving highly selective catalytic conversion of CO.[171] UV-activated $ZnS(en)_{0.5}$, $CsPbBr_3$(which exhibits isostructural-phase-transition-induced piezoelectricity), and high-entropy oxides (GaFeCoAlNi)O_x with lattice-distortion-enhanced piezoelectric properties continue to enrich the system of piezoelectric catalytic materials and further expand the boundaries of research in this field (Figure 7a).[101,172,173] The common objective of heterostructure construction, interfacial-bond regulation, and spatial cocatalyst arrangement is to direct polarization charges toward the active sites while maintaining the appropriate binding energies for key intermediates. ZnO/$Cs_3Bi_2Br_9$, Cu/Zr-MOF@CdS, and Co-NC/$BiFeO_3$ exploit band alignment, interfacial electric fields, and displacement currents to regulate electron transport, enabling processes such as coupled CO_2RR–organic oxidation, efficient methanation, and simultaneous CO and CH_4 production.[174-176] The yolk-in-shell structure of Au@$BaTiO_3$ integrates multiple advantages, including enhanced ferroelectric polarization, stress gain from the hollow

DOI: 10.68642/ftms.202600008

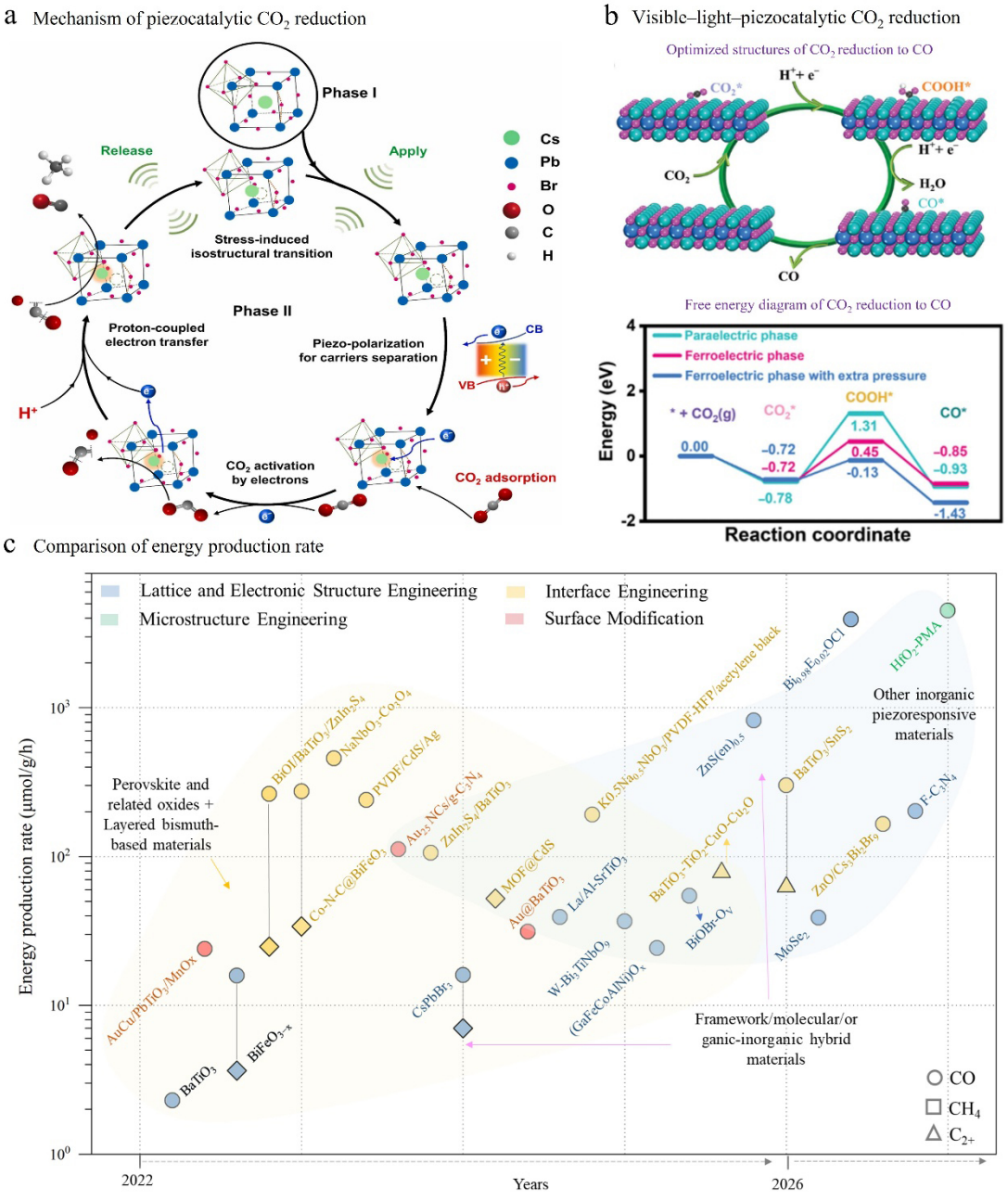


Figure 7 a, Isostructural phase-transition-driven piezoelectric generation in $CsPbBr_3$ all-inorganic perovskite for CO_2RR catalysis. Reproduced with permission.[173] Copyright 2024, Elsevier. b, Visible-light-piezocatalytic CO_2RR synergistically boosted by enhanced ferroelectric polarization in Au@$BaTiO_3$ yolk-in-shell structures. Reproduced with permission.[177] Copyright 2024, Wiley-VCH GmbH. c, Comparison of CO_2RR product formation rates over representative piezocatalysts. Detailed data are provided in Table S2 of the Supporting Information.

structure, and plasmonic interfacial charge transfer, thus effectively promoting substrate adsorption and the transformation of key intermediates (Figure 7b).[177] Au_{25} nanoclusters modified on red g-C_3N_4 and the PVDF/CdS/Ag composite system suppress carrier recombination losses through short-range electron transport, ordered interfacial electric fields, and surface plasmon resonance effects.[178,179] Embedding nanoscale piezoelectric materials at the S-scheme heterojunction interface triggers the preferential recombination of carriers with weak redox capabilities, thereby effectively retaining high-energy reducing electrons for continuous participation in this interfacial reaction.[180] AuCu and MnO_x, when loaded onto the oppositely polarized surface of $PbTiO_3$, enable precise spatial separation of the reduction and oxidation sites while simultaneously lowering the kinetic barriers for CO_2RR and water oxidation reactions.[181]

In summary, current piezoelectrically catalyzed CO_2RR systems predominantly yield C_1 products, although phased breakthroughs have been achieved in the controlled synthesis of high-value-added C_{2+} products such as C_2H_4. To systematically compare the effects of different modification strategies, the relevant studies were reviewed and classified by publication year. The results are summarized in Figure 7c and Table S2. The construction of Z-scheme heterostructures, exposure of C–C coupling sites mediated by the introduction of sulfur vacancies,

DOI: 10.68642/ftms.202600008

and optimization of proton-coupled electron transfer pathways by Cu-based redox pairs together effectively lower the C–C coupling energy barrier and promote the deep multi-electron reduction of the substrate. The transient pulsed nature of piezoelectric potentials leads to insufficient capacity for sustained multielectron supply to the system, while the C–C coupling reaction imposes stringent requirements on the spatial configuration and electronic structure of dual active sites. Because of these dual constraints, the current yields and selectivity of C_{2+} products significantly lag behind those of traditional thermocatalytic and electrocatalytic systems. Future research should rely on a combination of in situ spectroscopic characterization and theoretical calculations to precisely elucidate the microscopic reaction mechanisms of C–O bond cleavage and C–C coupling under dynamic alternating piezoelectric fields. A combination of controlled lattice strain modulation, precise defect engineering, bifunctional interfacial design, and optimization of the hydrophobic microenvironment should be pursued to overcome the kinetic bottlenecks in multielectron reduction reactions. This integrated approach will ultimately enable the directed and efficient conversion of CO_2 into high-value-added multicarbon fuels and steadily advance the practical application of piezoelectric catalysis in the field of carbon resource utilization.

4.3 Nitrogen fixation and nitrate reduction

Piezocatalytic ammonia production can proceed through two distinct routes: direct N_2 fixation and nitrate reduction. Direct N_2 fixation is constrained by the high N≡N bond energy (945 kJ mol^{-1}), as well as the nonpolar nature and low aqueous solubility of N_2.[182] Although nitrate reduction exhibits more favorable initial thermodynamics, it still requires successive deoxygenation, protonation, and multielectron transfer processes, with continuous competition from side reactions such as hydrogen evolution and NO_2^- accumulation.[183] Periodic mechanical stress induces alternating polarization, dynamic band bending, and interface shielding–unshielding cycles, thereby driving the directional migration of charge carriers. Local strain, defect dipoles, and interfacial bonding effects simultaneously regulate the adsorption configuration of the reactants, binding strength of the intermediates, and dissociation behavior of water. Therefore, the piezoelectric field does not simply provide an additional reduction potential but reshapes the reaction kinetics of nitrogen-containing species through a synergistic "charge transport–adsorption activation–proton-coupled electron transfer" mechanism. Periodic modulation of the electronic structure of active sites by time-varying piezoelectric polarization enables dynamic catalytic optimization, which distinguishes this approach from traditional photocatalytic and electrocatalytic systems involving steady-state interfacial regulation.

Under mild conditions, N_2 reduction predominantly proceeds through an associative hydrogenation mechanism. After N_2 adsorption onto vacancies, low-coordination metal sites, or single-atom active centers, piezoelectric electrons are continuously injected into its π^* antibonding orbital and stretch the N≡N bond, thereby gradually hydrogenating it via key intermediates such as $*N_2H$, $*NNH_2$, *NHNH, and $*NH_2$ to form NH_3. Defect engineering effectively enhances the nitrogen fixation performance. Oxygen vacancies extend the carrier lifetime within the ZnO system and improve the N_2 adsorption capacity, enabling ZnO nanoflowers to show an approximately 220% enhancement in the nitrogen fixation activity under piezoelectric–photonic synergy (Figure 8a).[184] MoS_2 modified with disulfide vacancies weakens the N≡N bond through electron feedback from the uncoordinated Mo d-orbitals, thereby enabling sacrificial-agent-free nitrogen fixation in an air–pure water system.[185] The synergistic effect of the sulfur vacancies and the pyramid-shaped morphology of CdS enhances the stress concentration capability and electron supply efficiency while stabilizing the hydrogenation intermediate; consequently, the ammonia production performance is quadrupled as compared with that of the pristine material.[113] Symmetry breaking and micro/nanostructure design effectively improve the efficiency of mechanical energy utilization. Oxygen vacancy-induced lattice distortion and localized Coulomb repulsion break the central symmetry of $BaZrO_3$, endowing the material with a piezoelectric response and N_2 reduction activity, thus providing new insights for the functionalization design of non-piezocatalysts.[186] Nanopits with polarized orientations within $PbTiO_3$ nanosheets enhance localized dipoles and form "electron reservoirs," thereby shortening the migration distance of photogenerated electrons to low-coordination Ti active sites and consequently improving the nitrogen fixation efficiency in pure water.[187] TiO_2@magnesite, MOF-derived $BiFeO_3$, and donor–acceptor polyheptazine imide broaden the piezoelectric potential distribution, couple visible-light responsiveness, and reconfigure the charge centers, respectively, while creating stress concentration sites, toward efficient photo–piezo synergistic nitrogen fixation.[188-190] Defective $BaTiO_3$ loaded with single Fe atoms shows dynamic switching of the spin state of the Fe site under an alternating polarization field. The differently polarized faces are suited for the N_2 reduction and oxidation reactions, thereby enabling the synergistic co-synthesis of NH_3 and NO_3^-.[191] This result indicates that alternating polarization can dynamically regulate orbital occupancy of the active sites and adsorption energies in addition to controlling charge transport.

The initial thermodynamic conditions for the reduction of NO_3^- to NH_3 are more favorable than those for direct N_2 fixation, although the selectivity of this process depends critically on the effective coordination between the deoxygenation and hydrogenation steps. This conversion pathway typically involves NO_3^-, NO_2^-, *NO, and a series of hydrogen- and nitrogen-containing intermediates, with the active hydrogen generated by water dissociation and proton-coupled electron transfer playing critical roles in the overall reaction. Mn-doped CaZnOS simultaneously generates piezoelectric and mechanoluminescent effects under mechanical stimulation, thereby establishing a force–electric–optical cascade catalytic system. Isotope labeling and electron spin resonance characterizations reveal hydrogenation as the rate-determining step, while the piezoelectric potential promotes interfacial NO_3^- enrichment and proton-coupled charge transfer.[192] The SnS_2/TiC heterojunction exploits interfacial electric field restructuring to enhance the adsorption and

DOI: 10.68642/ftms.202600008

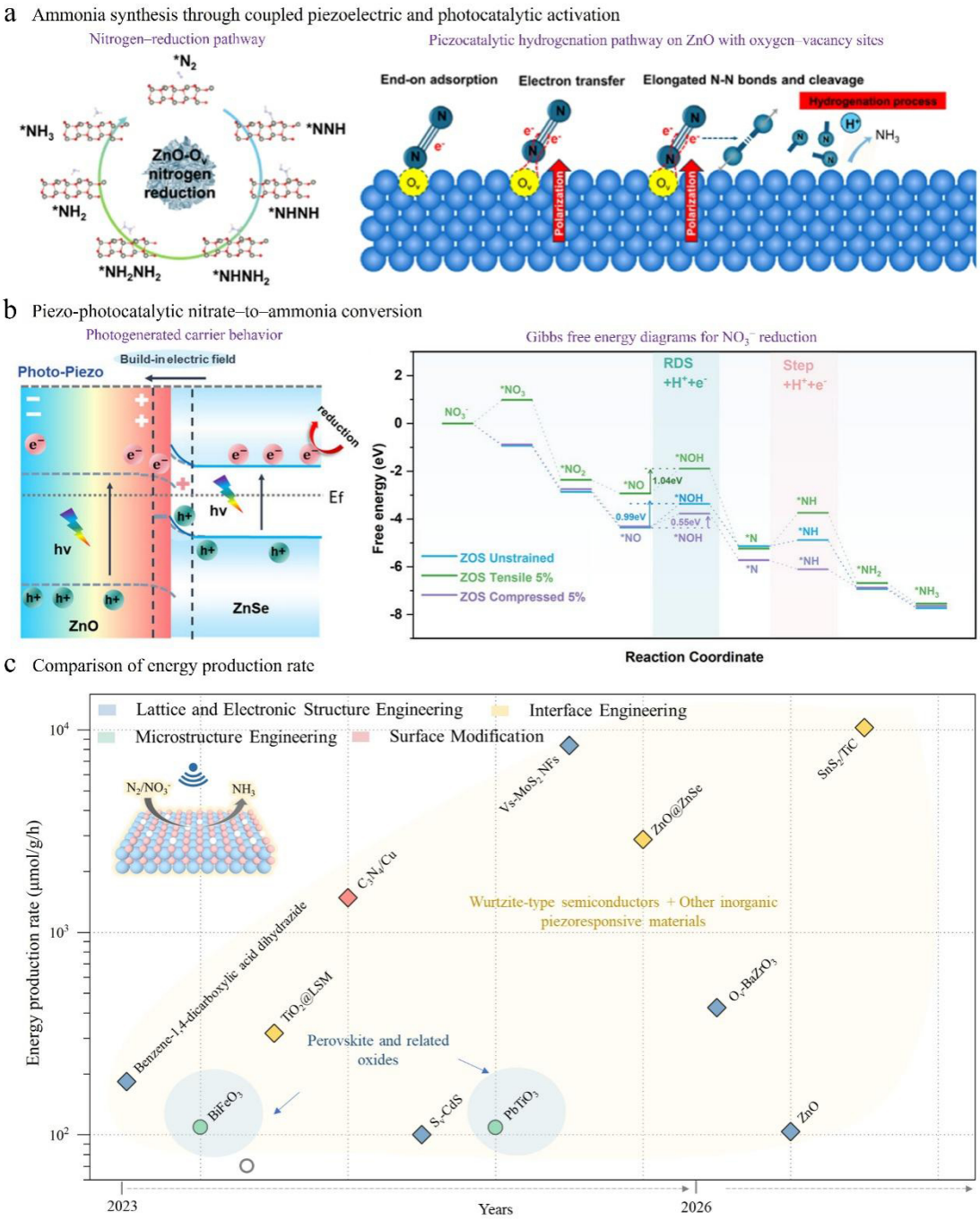


Figure 8 a, Defect-controlled ZnO nanoflowers promote metal-free ammonia synthesis via piezo-photocatalytic coupled processes. Reproduced with permission.[184] Copyright 2026, Royal Society of Chemistry. b, Lattice strain and piezo-field co-modulate nitrate-to-NH_3 conversion in chemically bonded S-scheme heterojunctions. Reproduced with permission.[194] Copyright 2025, Wiley-VCH GmbH. c, Comparison of NH_3 production rates over representative piezocatalysts. Detailed data are provided in Table S3 of the Supporting Information.

activation of NO_3^- and reactive hydrogen species, sustaining high electron utilization efficiency even in low-concentration nitrate systems.[193] The ZnO@ZnSe S-scheme heterojunction employs the O-Zn-Se interfacial bond to dissipate the coherent lattice strain, thereby promoting the dissociation of water molecules and optimizing the adsorption of intermediates, and the piezoelectric field generated by ZnO continuously facilitates carrier separation (Figure 8b).[194] Upon modification with single Cu atoms, g-C_3N_4 exhibits a non-centrosymmetric pore structure and shows enhanced macroscopic polarization. Combined with the water activation effect resulting from nitrogen vacancies, the modified catalyst maintains stable catalytic activity over a wide range of pH levels and substrate concentrations.[195] M/$BaTiO_3$ (M = Ru, Pd, Pt) composites modulate the interfacial potential barrier under mechanical polarization, thereby accelerating the transport of electrons and active hydrogen species and suppressing the competing hydrogen evolution reaction; correspondingly, the selectivity for ammonia production via nitrate reduction is also enhanced.[142]

In summary, both direct N_2 fixation and nitrate-to-ammonia

DOI: 10.68642/ftms.202600008

conversion are dependent on polarization-driven charge delivery but are limited by different elementary steps. Direct fixation requires efficient N_2 adsorption, π orbital population, stabilization of hydrogenated intermediates, and suppression of proton reduction. Nitrate reduction instead requires coordinated nitrate enrichment, sequential deoxygenation, water activation, and selective hydrogenation without NO_2^- accumulation or excessive H_2 evolution. To systematically compare the effects of different modification strategies, the relevant studies were reviewed and classified by publication year. The results are summarized in Figure 8c and Table S3 (Supporting Information). Defects, low-coordination sites, interfacial bonds, controlled morphology, and single-atom centers determine the manner in which piezo-generated charges are converted into chemically productive electrons and active hydrogen. Future work should establish quantitative relationships among the mechanical input, local polarization, electronic structure of the active sites, NH_3 yield, selectivity, and electron-utilization efficiency. Standardized energy reporting, isotope-labeling experiments, and operando characterization are particularly important for distinguishing genuine piezocatalytic contributions from the effects of cavitation, mechanoluminescence, and mechanically enhanced mass transfer.

4.4 O_2 reduction into H_2O_2

Piezocatalysis converts mechanical energy from ultrasound, vibration, or water flow into redox driving forces via stress-induced polarization charges, dynamic band bending, and transient interfacial potentials. Therefore, piezocatalysis offers a facile route to H_2O_2 synthesis under ambient conditions without an external electrical bias. The reduction pathway follows a two-electron oxygen reduction reaction expressed as $O_2 + 2H^+ + 2e^- \rightarrow H_2O_2$, while the oxidation pathway proceeds via a two-electron water oxidation reaction expressed as $2H_2O \rightarrow H_2O_2 + 2H^+ + 2e^-$.[105,196,197] These two pathways can operate independently or collaboratively to realize parallel H_2O_2 generation. The catalytic selectivity and product yield in these pathways are predominantly determined by the O_2 adsorption configuration, binding strength of the *OOH intermediate, proton-coupled electron transfer efficiency, and coupling characteristics of the interfacial intermediates.[67,90,198] Weak adsorption of *OOH on the catalyst surface severely restricts O_2 activation, whereas excessively strong adsorption readily induces O–O bond cleavage and promotes the four-electron reduction side reaction to generate H_2O as the final product.[77,199,200] In the oxidation pathway, the competing four-hole oxygen-evolution reaction must also be suppressed. Efficient H_2O_2 production therefore requires the coordinated optimization of mechanical-energy harvesting, polarization-potential generation, charge transport, stabilization of intermediates, and product desorption rather than merely maximizing the piezoelectric coefficient.

Current mainstream material systems for piezocatalytic H_2O_2 production cover perovskites, layered bismuth-based oxides, two-dimensional chalcogenides, carbon nitride-based materials, and MOF/COF framework materials. Atomic-scale modification is a critical strategy to simultaneously enhance the intrinsic polarization capability and catalytic activity of materials. Such modification is primarily achieved through ion substitution, defect engineering, and reconstruction of the local coordination environment to realize synergistic performance enhancement. For instance, selenium substitution for the sulfur atoms in $MnPS_3$ induces a prominent lattice strain and distorts the coordination geometry.[79] The resulting $MnPSe_3$ delivers an improved piezoelectric response and reconstructs the surface phosphorus sites into highly active centers for two-electron oxygen reduction. This modified catalyst enables simultaneous piezo-photocatalytic H_2O_2 generation and aquatic uranium recovery, thus showing dual application prospects in green chemical synthesis and environmental remediation. The Sillén-Aurivillius-phase $Bi_5Ti_2O_{11}Cl$ induces a strong ferroelectric polarization field through an asymmetric perovskite framework to facilitate the high-efficiency piezocatalytic synthesis of the target product in the absence of a sacrificial agent.[201] Al-anchored, defect-rich crystalline carbon nitride stabilizes metastable vacancies, amplifies localized piezoelectric fields, and creates Al-N-coordinated redox centers, thus enabling the coupled production of H_2O_2 and acetaldehyde.[202] Iron-doped Bi_3TiNbO_9 produces octahedral lattice eccentricity to strengthen the piezoelectric effect. The spin polarization effect of the optimized material modulates the thermodynamics and kinetics of the oxygen reduction reaction and improves carrier mobility and the yield of the desired two-electron product.[203]

Mesoscale structure regulation governs the efficiency of mechanical energy conversion to interfacial chemical potential, serving as the core factor for improving the mechanical energy utilization and boosting the piezocatalytic performance. For example, $BaTiO_3$ single-crystal microplates with highly exposed (111) polar crystal planes efficiently accumulate polarization charges and enhance intrinsic piezoelectric responses. Decoration of $BaTiO_3$ with silver quantum dots further optimizes the interfacial electron transport pathways and accelerates the kinetics of O_2 adsorption, activation, and two-electron reduction.[126] Few-layer, oxygen-vacancy-modified $Bi_2O_2(OH)NO_3$ adopts an ultrathin two-dimensional structure to amplify the mechanical deformation effects and defect dipole polarization, thereby activating dual reaction pathways (two-electron oxygen reduction and two-electron water oxidation) and improving the peroxide production capacity.[204] Carbon-quantum-dot-modified $Ca_2B_3O_6Cl$ generates localized intense piezoelectric fields at the material tips, which promote the formation of ordered interfacial hydrogen-bond networks around water molecules and accelerate proton-coupled electron transfer. Consequently, the modified material is well suited for high efficient H_2O_2 production in pure water systems (Figure 9a).[205] The proposed "piezoelectric performance matching window" for ZnO-based systems indicates that the intrinsic piezoelectric properties must be matched to the mechanical-deformation and energy-harvesting behavior of the material. Increasing the piezoelectric coefficient alone does not necessarily maximize the catalytic output.[206]

Interface engineering and surface modification are efficient strategies to suppress carrier recombination and precisely modulate the catalytic reaction pathways. Notably, the HfO_2/CdS piezo-photo-coupled heterojunction utilizes external-field-induced dynamic polarization effects to weaken interfacial

DOI: 10.68642/ftms.202600008

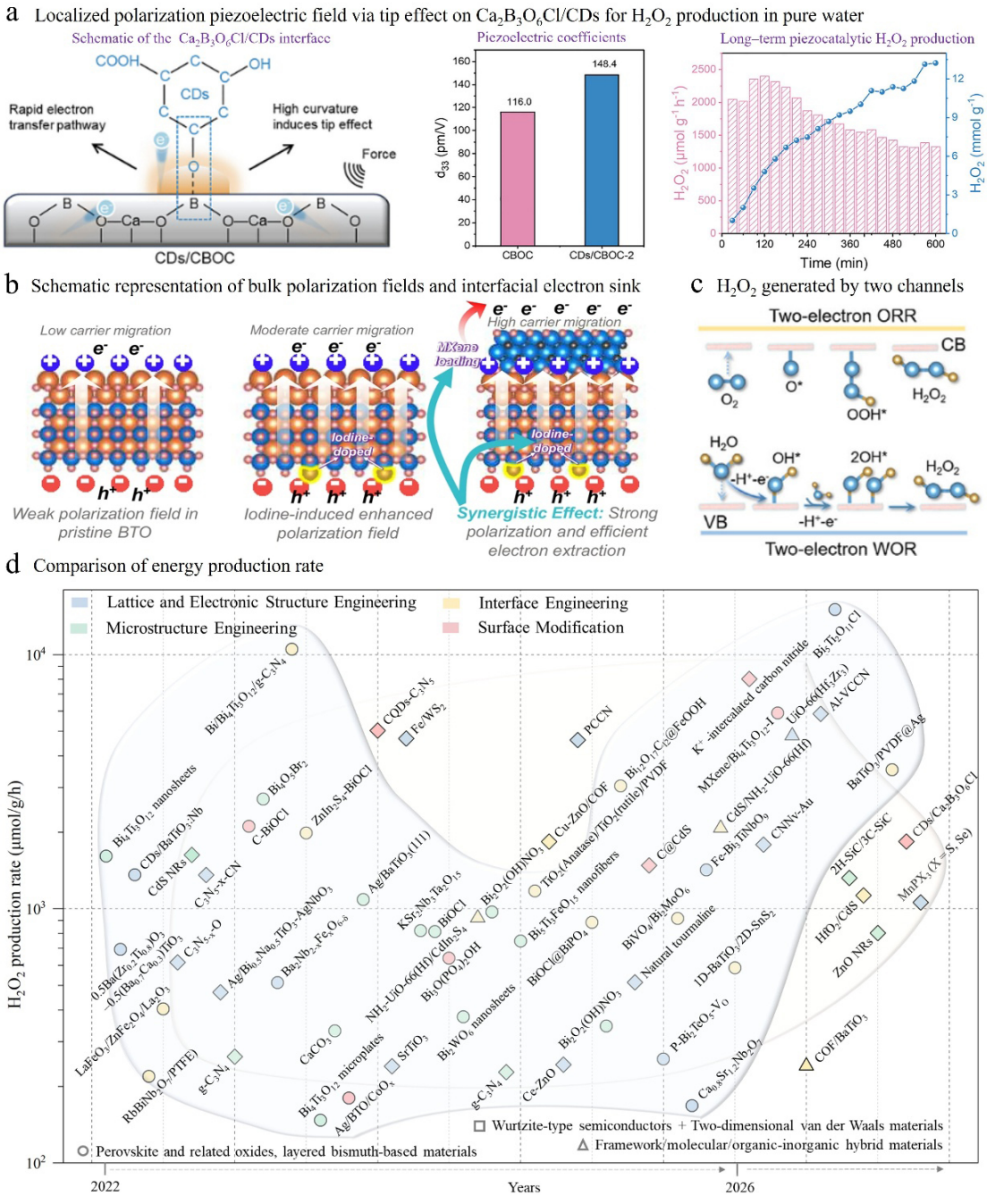


Figure 9 a, Localized polarization piezoelectric field via tip effect on $Ca_2B_3O_6Cl$/CDs for H_2O_2 production in pure water. Reproduced with permission.[205] Copyright 2026, Wiley-VCH GmbH. b, Interfacial electron sink and bulk polarization fields in MXene-modified iodine-doped $Bi_4Ti_3O_{12}$. Reproduced with permission.[140] Copyright 2026, Springer Nature. c, H_2O_2 generated by two C@CdS channels. Reproduced with permission.[212] Copyright 2025, Wiley-VCH GmbH. d, Comparison of H_2O_2 production rates over representative piezocatalysts. Detailed data are provided in Table S4 of the Supporting Information.

charge shielding, thereby allowing for the efficient separation and migration of photogenerated carriers and delivering better multifield-coupled catalytic performance compared with single-component catalysts.[207] Iodine-doped $Bi_4Ti_3O_{12}$ coupled with MXene co-catalysts strengthens the internal polarization fields through bulk doping, while the interfacial MXene component serves as a high-efficiency electron capture center. The resulting synergistic effect optimizes interfacial charge transport and the oxygen reduction kinetics, thus providing excellent H_2O_2 yields and high environmental remediation capability (Figure 9b).[140]

COF-mediated *in situ* confinement of $BaTiO_3$ leads to the formation of a dual-functional micro-reaction interface. The tailored interface is well matched to the two major production pathways—water oxidation and oxygen reduction—and spatially restrains the four-electron side reaction.[208] Defect engineering breaks the central symmetry of the crystal structure in UiO-66 and makes this inert MOF material intrinsically piezoelectric. The modified MOF drives dual-pathway piezocatalytic synthesis via water and oxygen activation, providing a universal guideline for the rational design of framework-based piezocata-

DOI: 10.68642/ftms.202600008

lysts.[93] As an example of fine surface regulation, the nitrogen vacancies on carbon nitride anchored with gold nanoparticles precisely modulate the electronic structure of the $Au^{\delta+}$ active sites, thus effectively enhancing the O_2 adsorption and activation capability.[209] Carbon quantum dot modification optimizes the intermolecular hydrogen-bond network of C_3N_5 and accelerates synergistic proton-electron transfer to boost the piezocatalytic reaction rates.[210] Cyano-group and potassium ion co-modified carbon nitride facilitates in-depth coupling between piezoelectric polarization effects and molecular framework engineering. The modification strategy synchronously optimizes the separation efficiency and the thermodynamics of the *OOH intermediate.[211] Carbon shell-modified CdS enables precise regulation of the d-band center and spatial separation of the oxidation and reduction active sites. The modified material shows enhanced piezoelectric responses, thus leading to stable and continuous generation of the desired product through a dual-channel mechanism (Figure 9c).[212]

In summary, high-efficiency piezocatalytic H_2O_2 production is governed by the coordinated optimization of the entire energy-to-chemical conversion process rather than the optimization of a single material parameter. To systematically compare the effects of different modification strategies, the relevant studies were reviewed and classified by publication year. The results are summarized in Figure 9d and Table S4 (Supporting Information). At the atomic scale, ion substitution, defect engineering, and coordination-environment reconstruction lead to enhanced polarization and regulate the adsorption and conversion of key intermediates, particularly *OOH. At the mesoscale, crystal-facet exposure, dimensional regulation, heterojunction construction, and cocatalyst modification promote directional charge separation and interfacial transport while suppressing the four-electron oxygen reduction and oxygen evolution side reactions. At the macroscopic scale, appropriate matching between the piezoelectric response, mechanical deformation behavior, and external energy input determines the effective utilization of ultrasound, vibrations, or fluid flow. Collectively, these multi-scale strategies enable simultaneous control over the two-electron oxygen reduction and water oxidation pathways, improving H_2O_2 selectivity, productivity, and operational stability. A clear transition from the isolated enhancement of piezoelectric coefficients toward the integrated regulation of mechanical energy harvesting, polarization-field generation, charge dynamics, stabilization of intermediates, and product desorption establishes a systematic design framework for sustainable H_2O_2 synthesis under mild conditions.

4.5 ROS-mediated degradation of small organic pollutants

Besides promoting the selective synthesis of fuels and platform chemicals, piezocatalysis can serve as a mechanically driven advanced oxidation process for removing small organic pollutants, particularly aquatic micropollutants. Under periodic mechanical deformation, incompletely screened polarization charges on piezoelectric materials can drive interfacial redox reactions involving O_2, $HO_2\cdot$, and OH^-, thereby generating ROS. Specifically, piezo-induced electrons can reduce the adsorbed O_2 to $\cdot O_2^-$, which can subsequently be protonated to $HO_2\cdot$ and converted into H_2O_2 via further electron transfer or disproportionation.[213] When the oxidation potential of piezo-induced holes is sufficiently positive, H_2O or OH^- can be oxidized to ·OH, while two-electron water oxidation can provide an additional pathway for H_2O_2 formation.[214] The *in situ* generated H_2O_2 can then be activated at transition-metal centers or defect-associated sites to produce additional ·OH. These ROS attack aromatic and heterocyclic structures via hydroxylation, dealkylation, bond cleavage, and ring opening to produce low-molecular-weight intermediates and, under sufficiently oxidative conditions, yield mineralized products.

Recent studies have increased the efficiency of ROS-mediated pollutant conversion through defect engineering, phase/interface regulation, and spatial coupling between H_2O_2 generation and activation. In P-doped BiOCl, the local structural asymmetry strengthens piezoelectric polarization, while the P sites and oxygen vacancies promote O_2 and H_2O activation, thereby accelerating bisphenol B degradation.[215] Similarly, the isolated Co atoms in mixed-phase 1T/2H MoS_2 induce local lattice distortion and reinforce charge separation across Schottky interfaces, thereby promoting O_2 activation and $\cdot O_2^-$ generation during ciprofloxacin removal.[4] Beyond these direct ROS-generation pathways, the $BiOIO_3$/γ-FeOOH system couples two-electron oxygen reduction with two-electron water oxidation to generate H_2O_2.[216] Meanwhile, proton enrichment on the electron-rich γ-FeOOH surface creates a localized acidic environment that facilitates the conversion of H_2O_2 into ·OH over a broad pH range. Similarly, Fe-doped SnS_2 combines an enhanced piezoelectric response with a self-Fenton process driven by Fe redox cycling, thereby promoting H_2O_2 activation and decreasing the toxicity of the treated solution.[217] These studies demonstrate that efficient remediation requires both rapid ROS generation and spatial proximity between the pollutant adsorption, H_2O_2 formation, and H_2O_2 activation sites. However, disappearance of the parent pollutant alone is insufficient evidence of remediation. In ultrasound-driven systems, piezocatalysis is entangled with other phenomena such as sonolysis, cavitation, adsorption, local heating, and mechanically enhanced mass transfer. Therefore, appropriate blank experiments, radical-quenching tests, isotope or probe studies, total organic carbon analysis, toxicity evaluation, and complete reporting of ultrasonic or mechanical parameters are required. Real water matrices introduce additional challenges because natural organic matter and inorganic ions can quench ROS or alter surface adsorption, while partially oxidized intermediates may remain toxic. Future catalyst and reactor design should integrate efficient strain-to-charge conversion, directional transport of charges to O_2^- and H_2O activation sites, controlled ROS generation near adsorbed pollutants, and verification of detoxification and mineralization rather than relying solely on the apparent degradation percentage.

4.6 Oxidative conversion of methane

Beyond the established conversion systems involving H_2O, O_2, CO_2, and nitrogen-containing species, as well as ROS-mediated environmental oxidation, piezocatalysis further expands the activation scope of inert substrates via chemical-bond perturbation

DOI: 10.68642/ftms.202600008

induced by strong and dynamically varying interfacial electric fields. Selective oxidation of methane plays a pivotal role in C1 clean energy chemistry and hence has emerged as a novel research direction in piezoelectric catalysis. The C–H bond of methane has a high dissociation energy of 439 kJ mol^{-1}, whereas primary oxidation products such as methanol and formaldehyde possess low thermodynamic stability and are susceptible to successive oxidative degradation.[218,219] Activation of methane under mild conditions while preventing consecutive oxidation of the desired oxygenates thus remains a central challenge. Alternating mechanical stress generates dynamic polarization fields that regulate methane adsorption, charge transfer, and stability of intermediates. Piezo-generated charges can also activate O_2 and H_2O to form species such as ·OH and $\cdot O_2^-$. These reactive species abstract H atoms from CH_4 to produce $\cdot CH_3$ intermediates, which can subsequently form methanol, formaldehyde, or other oxygenated products. Structural engineering and multifield coupling are key strategies for balancing C–H activation and product selectivity. Functionalized piezoelectric MOFs facilitate the synergistic optimization of piezoelectric responses and catalytic selectivity by virtue of their tunable structures and exposed metal active sites. The Cu-UiO-66-NH_2 material delivers prominent piezoelectric polarization under ultrasonic excitation, which facilitates the *in situ* generation of H_2O_2 and ·OH dissociation to substantially accelerate the activation of C–H bonds in methane.[220] Surface Cu(II)-O· species further regulate the oxidation pathway and suppress the excessive oxidation of methanol. These distinctive structural features support the highly selective synthesis of methanol in continuous-flow reaction systems and fully validate the structural regulation advantages inherent to framework-based piezoelectric materials.

Building on the above progress, piezo-photo-coupled heterostructures serve as a valid means to overcome the inherent performance limitations of single piezoelectric catalysis. The $BaTiO_3$/g-C_3N_4 composite realizes a strong interfacial built-in electric field via ultrasonic-triggered polarization, and this strengthened electric field substantially enhances the separation and migration of photogenerated charge carriers while reducing the energy barrier for the rate-determining step involved in methane oxidation.[221] Through cooperative radical pathways, the composite enables the conversion of dilute methane to formaldehyde at ambient temperature and pressure. Tandem reaction design can further suppress overoxidation while upgrading C_1 intermediates to higher-value products. In the hydroxyapatite (HAp) system, the piezoelectric catalytic effect drives a tandem process integrating methane oxidation with methanol coupling to convert methane into lower alcohols.[222] Probe molecule adsorption and Au^{3+} reduction reactions under ultrasonic agitation corroborate that the HAp-mediated process proceeds via piezoelectric catalysis and not via sonocatalysis. Under ultrasonic agitation, the surface-induced charges on HAp act as surface cathodes and anodes to trigger electrochemical reactions, enabling the activation of methane, O_2 and H_2O molecules. The hydroxyl radicals generated from the activation of O_2 and H_2O subsequently attack the C–H bonds of methane, converting it into lower alcohols. This HAp-based piezoelectric catalytic system yields methanol, ethanol and isopropanol with production rates of 84.4, 43.2 and 9.6 μmol g^{-1} h^{-1}, respectively, without any detectable CO or CO_2 formation. By extending methane conversion beyond a single C_1 product and incorporating C–C coupling, this strategy provides a possible route to alleviate methanol overoxidation while upgrading methane to higher-value liquid oxygenates. Nevertheless, piezocatalytic methane conversion remains at an early proof-of-concept stage. Current limitations include low methane conversion, incomplete carbon balances, insufficient operando evidence for proposed radical and surface-intermediate pathways, inadequate separation of piezocatalytic effects from cavitation-enhanced mass transfer, and limited long-term stability data. Future studies should quantify the mechanical-energy input and utilization efficiency, monitor both gas- and liquid-phase products, establish complete carbon and electron balances, and determine the manner in which time-dependent polarization fields alter C–H activation and C–C coupling. These requirements are essential for shifting the field from isolated demonstrations toward reproducible reaction engineering.

This chapter systematically reviews the research progress in piezocatalysis for the directional conversion of various core small molecules and summarizes the common understandings inherent in this field. Looking across the various reaction systems, one can find that the piezoelectric polarization effect provides a common thermodynamic driving force for the activation of diverse small molecules. Meanwhile, different reactions are associated with distinctive regulation strategies because of the differences in the chemical bond energies and the number of transferred electrons. For water splitting, the piezoelectric polarization effect provides the thermodynamic driving force; further, heterointerface engineering together with multifield coupling strategies effectively alleviates the sluggish kinetics of the oxygen evolution reaction and resolves the carrier recombination issue, thereby greatly improving the catalytic efficiency. The CO_2RR system utilizes the polarization electric field to regulate the adsorption configuration of intermediates and achieves directional control of the reaction pathway. In addition, preliminary breakthroughs have been made in the selective synthesis of multi carbon products and the analysis of microscopic mechanisms. Ambient nitrogen fixation has confirmed that the polarization electric field can activate the N≡N triple bond, and the product yield has been significantly improved through atomic-scale design of active sites and optimization of the reaction microenvironment. H_2O_2 production fully exploits the advantage of precise regulation of the electron transfer number, and the dual-channel synergy of oxygen reduction and water oxidation effectively enhances the production yield. Moreover, ROS-mediated degradation of small organic pollutants provides a direct connection between piezocatalytic H_2O_2 generation and environmental remediation, because mechanically generated ·OH, $\cdot O_2^-$, $^1O_2$, and reactive holes can initiate dehalogenation, aromatic-ring opening, and eventual mineralization. Emerging directions such as methane C–H bond activation and biomass conversion further expand the application landscape of piezocatalysis. At present, this field still faces common bottlenecks such as low energy conversion efficiency, difficulty in controlling the selectivity of multi electron reac-

DOI: 10.68642/ftms.202600008

tions, and non-uniform performance evaluation standards. Therefore, future research must elucidate the three-phase interfacial interaction mechanisms at the atomic scale and establish a full-chain optimization scheme covering catalyst design, reaction system regulation, and reactor integration.

5 Conclusions and Outlook

Piezocatalysis has emerged as a promising platform for green chemical conversion because it transforms mechanical deformation into localized electrochemical driving forces, thereby enabling small-molecule activation under mild conditions. Instead of being governed solely by a high piezoelectric coefficient, the piezocatalytic performance is influenced by the dynamic coupling of lattice polarization, charge generation and transport, interfacial screening, and surface reaction kinetics. This review presents a multiscale picture of this process, extending from the crystallographic origin of piezoelectricity, including symmetry breaking, spontaneous polarization, and piezoelectric tensor anisotropy, to ferroelectric domain evolution, strain-induced surface potentials, and interfacial redox chemistry. Within this framework, pure piezocatalysis can be understood as a sequential process involving stress-induced polarization, carrier separation and migration, dynamic screening and descreening at the solid–liquid interface, and matching between the achievable surface potential and the thermodynamic requirements of the target reaction. Coupling of piezoelectricity with optical, electrical, or thermal fields further expands the available energy-input modes and may enhance carrier generation, spatial charge separation, and reaction-pathway regulation. The material landscape of piezocatalysis now encompasses perovskite and related oxides, layered bismuth-based compounds, ferroelectric polymers, wurtzite semiconductors, two-dimensional van der Waals materials, and other inorganic piezoresponsive materials, as well as framework, molecular, and organic–inorganic hybrid systems. Across these material classes, structural and morphological regulation, band-structure engineering via doping and defect control, and interfacial optimization through polarization engineering, heterojunction construction, and cocatalyst integration constitute the principal design strategies. Importantly, these approaches should not be applied as generic performance-enhancement tools. Instead, material design should begin with the rate-determining step and key intermediates of the target reaction and then work backward to optimize the polarization field, charge lifetime, active-site configuration, and local reaction environment. Piezocatalytic materials have demonstrated potential for application to water splitting, CO_2RR, N_2 fixation, nitrate reduction, O_2 reduction for H_2O_2 production, ROS-mediated degradation of small organic pollutants, and oxidative conversion of methane. A distinctive feature of these systems is that alternating mechanical stress can dynamically redistribute interfacial charges and modulate the adsorption energies and activation barriers of the reaction intermediates. The time-dependent interfacial regulation introduces an additional degree of freedom for controlling multistep and multielectron reactions. However, this also makes the catalytic behavior strongly dependent on the stress waveform, excitation frequency, ionic environment, and characteristic timescales of charge transfer and surface chemistry (Figure 10).

Despite substantial progress in mechanistic understanding and materials development, the transition of piezocatalysis from laboratory proof-of-concept studies to practically relevant technologies remains limited by six interconnected challenges. First, it is difficult to isolate the intrinsic piezoelectric contribution

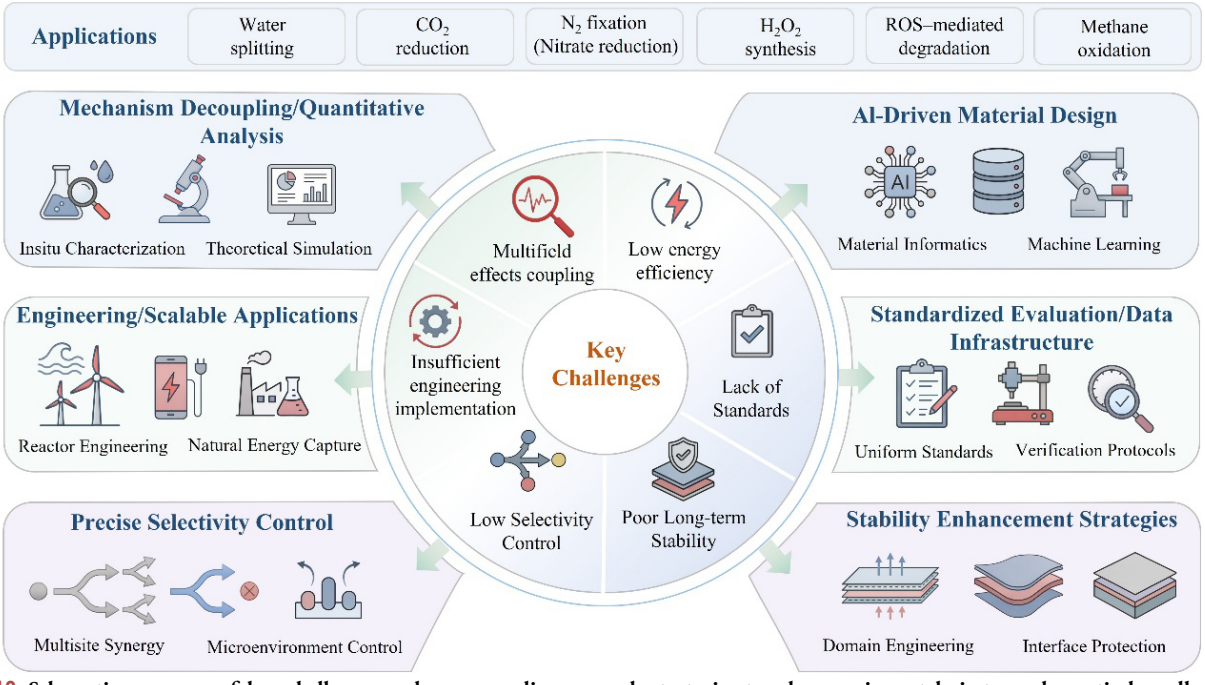


Figure 10 **Schematic summary of key challenges and corresponding research strategies to advance piezocatalysis toward practical small-molecule conversion.**

DOI: 10.68642/ftms.202600008

because cavitation, flexoelectricity, triboelectricity, local heating, and sonochemical processes may coexist under mechanical excitation. Second, mechanical-to-chemical energy conversion efficiencies remain low because of inefficient stress transfer, mechanical dissipation, ionic screening, and bulk or interfacial charge recombination. Third, the absence of standardized testing and reporting protocols prevents a reliable comparison among studies with different excitation conditions, reactor geometries, catalyst loadings, and product-quantification procedures. Fourth, cyclic stress and chemically reactive environments can induce domain-wall fatigue, lattice damage, particle fracture, interfacial delamination, dissolution, and surface reconstruction. Fifth, the transient nature of the piezopotential complicates the selective control of multielectron and proton-coupled electron-transfer reactions, particularly when several intermediates and competing pathways have similar energetics. Sixth, most studies still rely on powder suspensions in small batch reactors, whereas catalyst immobilization, continuous operation, natural mechanical-energy harvesting, mass-transfer management, and product separation remain underdeveloped. Because these limitations reinforce one another, further progress will require coordinated advances in mechanistic analysis, data infrastructure, materials design, reaction engineering, and device integration.

I. Mechanistic Decoupling through Operando Characterization and Multiscale Modeling. Quantitative separation of piezoelectricity from cavitation, flexoelectricity, triboelectricity, and thermal effects is essential for establishing a reliable mechanistic framework. Operando techniques, including piezoresponse force microscopy, Kelvin probe measurements, vibrational spectroscopy, electron paramagnetic resonance, and synchrotron-based spectroscopy, should be combined to track polarization, charge redistribution, reactive species, and intermediates under mechanical loading. Coupling these measurements with finite-element analysis, density functional theory calculations, and microkinetic modeling will enable quantitative correlations among applied stress, polarization dynamics, charge transfer, and catalytic performance.

II. Data-driven and Artificial-intelligence-assisted Materials Discovery. Artificial intelligence and high-throughput computation can accelerate the discovery of piezocatalysts beyond empirical trial-and-error. Therefore, standardized databases integrating crystal symmetry, piezoelectric tensors, electronic structures, mechanical properties, defect configurations, adsorption energies, and catalytic performance are urgently needed. Graph neural networks, generative models, active learning, and machine-learning potentials may facilitate the identification of non-centrosymmetric compounds, lead-free ferroelectrics, low-dimensional materials, and stable heterostructures. Their integration with automated synthesis and characterization could establish a closed-loop workflow of prediction, fabrication, testing, and feedback.

III. Standardized Evaluation Protocols and Open Data Infrastructure. Unified evaluation protocols are required for enabling a meaningful comparison across different materials and reactor systems. Key parameters should include mechanical input power, excitation frequency and amplitude, stress distribution, reactor geometry, catalyst loading, temperature, electrolyte composition, and product-analysis methods. The catalytic performance should be normalized against the effective mechanical energy delivered to the catalyst rather than the catalyst mass alone. Implementing isotope labeling, blank controls, mass balances, and error analysis as standard practices is necessary, particularly for N_2 fixation, CO_2 conversion, and water splitting.

IV. Durability Enhancement through Domain Engineering and Interfacial Protection. Long-term stability requires simultaneous protection of polarization, crystal structures, interfaces, and active sites. Domain orientation, defect-dipole pinning, grain-boundary regulation, and polarization pretreatment may suppress ferroelectric fatigue, whereas ultrathin protective layers, robust heterointerfaces, and selective cocatalysts can mitigate corrosion and surface reconstruction. Immobilized films, flexible composites, porous supports, and monolithic catalysts may further improve mechanical integrity and mitigate catalyst loss. Stability should ultimately be evaluated under prolonged and application-relevant operating conditions.

V. Selectivity Control through Multifunctional Sites and Engineered Microenvironments. Complex multielectron reactions require multifunctional sites that separately regulate reactant adsorption, electron transfer, proton delivery, stabilization of intermediates, and product desorption. Such spatially differentiated architectures may suppress competing pathways and improve the formation of target products in CO_2RR, N_2 fixation, H_2O_2 synthesis, and CH_4 conversion. Hydrophobic interfaces, confined pores, ionomer layers, and tailored solvent environments can further regulate the local reactant concentration and proton transport. The mechanical excitation frequency and waveforms should also be matched to the characteristic timescales of charge relaxation and surface reactions.

VI. Reactor Engineering and Integration with Ambient Mechanical-energy Sources. Practical implementation requires a shift from ultrasonic batch suspensions toward continuous-flow systems driven by water flow, waves, wind-induced vibration, machinery motion, or acoustic energy. Flexible membranes, aligned piezoelectric fibers, porous monoliths, structured packed beds, and microfluidic reactors may improve stress transfer, mass transport, and catalyst recovery. Reactor assessment should consider the complete energy pathway from mechanical-energy harvesting to product separation. Long-term operation, scale-up, techno-economic analysis, and life-cycle assessment will be essential for identifying the applications in which piezocatalysis offers genuine advantages over established catalytic technologies.

In summary, the future of piezocatalysis depends on coordinated progress in mechanistic quantification, data-driven material discovery, standardized benchmarking, durability enhancement, selectivity control, and reactor engineering. Such advances may enable the transition of piezocatalysis from laboratory demonstrations to a viable platform for sustainable small-molecule conversion.

DOI: 10.68642/ftms.202600008

Supporting Information

Supplementary data associated with this article can be found, in the online version, at https://doi.org/10.68642/ftms.202600008.

Competing Interests

The authors declare no competing financial or non-financial interests.

Acknowledgements

This work was jointly supported by the National Key Research and Development Program of China (Grant No. 2022YFB3803600), the National Natural Science Foundation of China (Grant Nos. 52272244 and 51972288), and the Fundamental Research Funds for the Central Universities (Grant No. 2652022202).

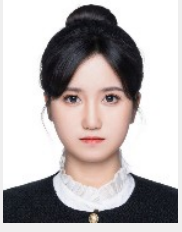
This is an open access article under the terms of the Creative Commons Attribution 4.0 International License (CC BY 4.0, https://creativecommons.org/licenses/by/4.0/).
© The Author(s) 2026.



Haiyan Xie is currently a Ph.D. degree candidate in Prof. Huang's group in the School of Materials Science and Engineering, China University of Geosciences (Beijing). She obtained her master's degree from North Minzu University in 2024. Her research focuses on the synthesis of multifunctional materials for polarization-driven photocatalysis.



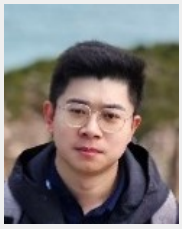
Jing Zhang is currently a graduate student of Professor Huang's team at the School of Materials Science and Engineering, China University of Geosciences, Beijing. He received a bachelor's degree from China University of Geosciences (Beijing) in 2024. His research focuses on functional photocatalysis for pollutant degradation and carbon dioxide reduction.



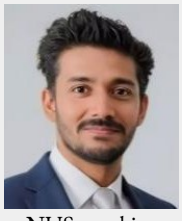
Yifan Pan is currently an undergraduate student in Professor Huang's team at the School of Materials Science and Engineering, China University of Geosciences (Beijing). Her research focuses on the synthesis of photocatalytic materials.



Pengwei Jia received his master's degree in 2023 from North China University of Science and Technology. He is currently a Ph.D. candidate at Prof. Huang's group in School of Materials Science and Technology, China University of Geosciences (Beijing). His research interests mainly focus on the piezocatalysis and photocatalysis.



Xiaowen Ruan received his Ph.D. degree in materials physics and chemistry from Jilin University in 2023 under the supervision of Prof. Xiaoqiang Cui. In 2023, he took up a postdoctoral position at City University of Hong Kong under the supervision of Prof. Sai Kishore RAVI. His research interests focus on the design and synthesis of nanomaterials for catalytic applications.



Sai Kishore Ravi is an assistant professor at the School of Energy and Environment, City University of Hong Kong (CityU). He earned his Ph.D. in 2018 from the Department of Materials Science & Engineering at the National University of Singapore (NUS) and continued his postdoctoral fellowship at NUS working on biohybrid photoelectrochemical cells integrating photosynthetic pigment-protein complexes. His research interests include studying hybrid materials for artificial and semi-artificial photosynthesis, solar desalination, and atmospheric water harvesting. Before joining CityU in 2022, he was an associate editor at Wiley-VCH GmbH, Germany, and now serves as the editor-in-chief of the journal *Energy Technology*.



Hongwei Huang is a Professor at Beijing Key Laboratory of Materials Utilization of Nonmetallic Minerals and Solid Wastes, School of Materials Science and Technology, China University of Geosciences (Beijing). He received his Ph.D. in 2012 from the Technical Institute of Physics and Chemistry, Chinese Academy of Sciences, and worked as a visiting scholar in the labs of Prof. Thomas Mallouk at The Pennsylvania State University (2016–2017). His current research mainly focuses on polar nanocrystals and their applications in photocatalysis and piezocatalysis

References and Notes

1. Hong, P., Xu, C., Zhao, H. & Lei, Y. Atomic Size Misfit for Electrocatalytic Small Molecule Activation. *Adv. Funct. Mater.* **2026**, 36, 2502833. DOI: 10.1002/adfm.202502833
2. Li, C., Zhang, T., Qiu, Z., Ye, B., Liang, X., Liu, X., Chen, M., Xia, X., Wang, C., Wan, W., *et al*. Plasma -assisted Fabrication of Multiscale Materials for Electrochemical Energy Conversion and Storage. *Carbon Energy* **2025**, 7, e641. DOI: 10.1002/cey2.641
3. Landaeta, V. R., Horsley Downie, T. M. & Wolf, R. Low-Valent Transition Metalate Anions in Synthesis, Small Molecule Activation, and Catalysis. *Chem. Rev.* **2024**, 124, 1323–1463. DOI: 10.1021/acs.chemrev.3c00121
4. Shen, X., Pan, C., Wei, X., Liu, J., Liu, M., Liu, G. & Pan, M. Single-Atom Engineering and Phase-Transition Optimization in MoS_2 for Enhanced Schottky Junction Piezocatalysis. *ACS Nano* **2025**, 19, 28257–28267. DOI: 10.1021/acsnano.5c05239
5. Yasin, G., Tabish, M., Ajmal, S., Zhuo, Q., Mushtaq, M. A., Saad, A., Alam, M. M. & Song, H. Single Atom Horizons for Shaping the Future of Catalysis and Sustainability: the Next Frontiers in Energy Conversion and Storage. *Prog. Mater. Sci.* **2026**, 155, 101525. DOI: 10.1016/j.pmatsci.2025.101525
6. Chung, H. Y., Wong, R. J., Wu, H., Gunawan, D., Amal, R. & Ng, Y. H. Scalable and Integrated Photocatalytic Reactor Systems for Solar-to-Fuel Production: Photoredo$_x$ and Photoreforming Processes. *Adv. Energy Mater.* **2025**, 15, 2404956. DOI: 10.1002/aenm.202404956
7. Li, J., Wang, Y., Ji, X., Zhao, H., Yu, W., Huang, Y., Chang, B., Chen, L., Liu, H., Tan, H., *et al*. Unraveling Tandem Catalytic Sites for Elec-

trocatalytic Nitrate Reduction to Ammonia. *Adv. Energy Mater.* **2026**, 16, e03822. DOI: 10.1002/aenm.202503822
8. Zhang, N., Gong, W. & Xiong, Y. Modern Organic Transformations: Heterogeneous Thermocatalysis or Photocatalysis? *Chem. Soc. Rev.* **2025**, 54, 5189–5223. DOI: 10.1039/d2cs00097k
9. Xu, L., Zhang, X., Yu, D., Zhang, Y., Yun, J. & Wang, S. Multi-Energy-Driven Photocatalysis: Mechanism, Progress, and Perspective. *Exploration* **2026**, 6, 20240195. DOI: 10.1002/exp.20240195
10. Xie, C., Chen, W., Wang, Y., Yang, Y. & Wang, S. Dynamic Evolution Processes in Electrocatalysis: Structure Evolution, Characterization and Regulation. *Chem. Soc. Rev.* **2024**, 53, 10852–10877. DOI: 10.1039/d3cs00756a
11. Zhang, Q., Jia, Y., Wu, W., Pei, C., Zhu, G., Wu, Z., Zhang, L., Fan, W. & Wu, Z. Review on Strategies toward Efficient Piezocatalysis of $BaTiO_3$ Nanomaterials for Wastewater Treatment through Harvesting Vibration Energy. *Nano Energy* **2023**, 113, 108507. DOI: 10.1016/j.nanoen.2023.108507
12. Shi, K. -Q., Jin, C. -C., Liu, D. -M., Cai, Y. -X., Gui, Z. -Y., Sun, J. -H., Li, L., Chen, Z. & Wu, Q. Strain Engineering in Piezocatalysis: From Microscopic Atomic Modulation to Macroscopic Applications. *Mater. Today* **2026**, 93, 103222. DOI: 10.1016/j.mattod.2026.103222
13. Liu, J., Qi, W., Xu, M., Thomas, T., Liu, S. & Yang, M. Piezocatalytic Techniques in Environmental Remediation. *Angew. Chem. Int. Ed.* **2023**, 62, e202213927. DOI: 10.1002/anie.202213927
14. Jia, P., Yu, Y., Chen, T. & Huang, H. "Electricity"-Assisted Catalytic Solar-to-Fuel Processes. *Angew. Chem. Int. Ed.* **2025**, 64, e202508809. DOI: 10.1002/anie.202508809
15. Wang, C., Hu, C., Chen, F., Ma, T., Zhang, Y. & Huang, H. Design Strategies and Effect Comparisons toward Efficient Piezocatalytic System. *Nano Energy* **2023**, 107, 108093. DOI: 10.1016/j.nanoen.2022.108093
16. Zhang, B., Zhao, M., Cheng, K., Wu, J., Kubuki, S., Zhang, L. & Yong, Y. -C. Piezoelectric Effect Coupled Advanced Oxidation Processes for Environmental Catalysis Application. *Coord. Chem. Rev.* **2025**, 523, 216234. DOI: 10.1016/j.ccr.2024.216234
17. Amaechi, I. C., Hadj Youssef, A., Dörfler, A., González, Y., Katoch, R. & Ruediger, A. Catalytic Applications of Non-Centrosymmetric Oxide Nanomaterials. *Angew. Chem. Int. Ed.* **2022**, 61, e202207975. DOI: 10.1002/anie.202207975
18. Sabu, S., Mondal, S., Rahman, A. & Thomas, S. P. From Flexible Crystals to Piezoelectrics: The Advent of a New Class of Flexible Functional Molecular Materials. *Small* **2025**, 21, 2412561. DOI: 10.1002/smll.202412561
19. Meng, N., Liu, W., Jiang, R., Zhang, Y., Dunn, S., Wu, J. & Yan, H. Fundamentals, Advances and Perspectives of Piezocatalysis: A Marriage of Solid-state Physics and Catalytic Chemistry. *Prog. Mater. Sci.* **2023**, 138, 101161. DOI: 10.1016/j.pmatsci.2023.101161
20. Jia, P., Li, J. & Huang, H. Piezocatalysts and Piezo-Photocatalysts: From Material Design to Diverse Applications. *Adv. Funct. Mater.* **2024**, 34, 2407309. DOI: 10.1002/adfm.202407309
21. Zhong, T., Gao, Y., Ren, Y. & Wu, M. Theoretical Designs of Low-barrier Ferroelectricity. *WIREs Comput. Mol. Sci.* **2023**, 13, e1682. DOI: 10.1002/wcms.1682
22. Wang, K., Han, C., Li, J., Qiu, J., Sunarso, J. & Liu, S. The Mechanism of Piezocatalysis: Energy Band Theory or Screening Charge Effect? *Angew. Chem. Int. Ed.* **2022**, 61, e202110429. DOI: 10.1002/anie.202110429
23. Wang, L., Liu, S., Feng, X., Zhang, C., Zhu, L., Zhai, J., Qin, Y. & Wang, Z. L. Flexoelectronics of Centrosymmetric Semiconductors. *Nat. Nanotechnol.* **2020**, 15, 661–667. DOI: 10.1038/s41565-020-0700-y
24. Xu, S., Zhang, L., He, L., Bo, C., Chen, K., Yan, Y., Zhang, C., Wang, H., Aziz, A., Deng, J., *et al*. Ultrahigh Piezo-Photocatalysis Efficiency and Speed in Lead-Free Ferroelectric Nanoparticles by Employing Rare-Earth Tailored Band/Polar Structures. *Adv. Funct. Mater.* **2026**, 36, e19351. DOI: 10.1002/adfm.202519351
25. Schroeder, U., Park, M. H., Mikolajick, T. & Hwang, C. S. The Fundamentals and Applications of Ferroelectric HfO_2. *Nat. Rev. Mater.* **2022**, 7, 653–669. DOI: 10.1038/s41578-022-00431-2
26. Liu, Z., Wang, H., Li, M., Tao, L., Paudel, T. R., Yu, H., Wang, Y., Hong, S., Zhang, M., Ren, Z., *et al*. In-plane Charged Domain Walls with Memristive Behaviour in a Ferroelectric Film. *Nature* **2023**, 613, 656–661. DOI: 10.1038/s41586-022-05503-5
27. Hershkovitz, A., Hemaprabha, E., Khorshid, D., Ma, L., Liu, S., Cohen, S. & Ivry, Y. Oxygen-vacancy Mediated Deterministic Domain Distribution at the Onset of Ferroelectricity. *Acta Mater.* **2025**, 286, 120738. DOI: 10.1016/j.actamat.2025.120738
28. Zuo, T., Dewanjee, S., Zhang, C., Chakraborty, P., Lu, W., Jha, N. K., Bhattacharya, H., Gangopadhyay, M., Fleishman, J., Jha, S. K., *et al*. Biopiezoelectric-based Nanomaterials; a Promising Strategy in Cancer Therapy. *J. Exp. Clin. Cancer Res.* **2025**, 44, 171. DOI: 10.1186/s13046-025-03427-2
29. Qian, W., Yang, W., Zhang, Y., Bowen, C. R. & Yang, Y. Piezoelectric Materials for Controlling Electro-Chemical Processes. *Nano-Micro Lett.* **2020**, 12, 149. DOI: 10.1007/s40820-020-00489-z
30. Rogée, L., Wang, L., Zhang, Y., Cai, S., Wang, P., Chhowalla, M., Ji, W. & Lau, S. P. Ferroelectricity in Untwisted Heterobilayers of Transition Metal Dichalcogenides. *Science* **2022**, 376, 973–978. DOI: 10.1126/science.abm5734
31. Yuan, S., Zhang, Y., Dai, M., Chen, Y., Yu, H., Ma, Z., Io, W. F., Luo, X., Hou, P. & Hao, J. A Giant Tunable Piezoelectric Performance in Two-dimensional In_2Se_3 via Interface Engineering. *Adv. Electron. Mater.* **2024**, 10, 2300741. DOI: 10.1002/aelm.202300741
32. Li, Y., Wang, L., Ning, Y., Yuan, Y., Fu, X., Cui, J. & Jiang, Y. Oxygen Doping Enhances Piezo-photocatalytic Degradation of Carbamazepine by Molybdenum Disulfide. *Environ. Sci. Ecotechnol.* **2025**, 28, 100639. DOI: 10.1016/j.ese.2025.100639
33. Xie, J., Li, D., Li, H., Peng, B., Bao, Q., Jiang, J., Li, B. & Liu, W. Surface and Bulk Defect Passivation in $MAPbI_3$ Perovskites with Daminozide: Effects on Carrier Dynamics and Mobility. *Adv. Sci.* **2025**, 12, 2500530. DOI: 10.1002/advs.202500530
34. Wu, T., Liu, K., Liu, S., Feng, X., Wang, X., Wang, L., Qin, Y. & Wang, Z. L. Highly Efficient Flexocatalysis of Two-Dimensional Semiconductors. *Adv. Mater.* **2023**, 35, 2208121. DOI: 10.1002/adma.202208121
35. Ren, Z., Chen, F., Zhao, Q., Zhao, G., Li, H., Sun, W., Huang, H. & Ma, T. Efficient CO_2 Reduction to Reveal the Piezocatalytic Mechanism: From Displacement Current to Active Sites. *Appl. Catal. B Environ.* **2023**, 320, 122007. DOI: 10.1016/j.apcatb.2022.122007
36. Jiang, T., Wang, Y., Cai, C., Nie, C., Peng, H. & Ao, Z. Piezocatalysis for Water Treatment: Mechanisms, Recent Advances, and Future Prospects. *Environ. Sci. Ecotechnol.* **2025**, 23, 100495. DOI: 10.1016/j.ese.2024.100495
37. Feng, W., Yuan, J., Gao, F., Weng, B., Hu, W., Lei, Y., Huang, X., Yang, L., Shen, J., Xu, D., *et al*. Piezopotential-driven Simulated Electrocatalytic Nanosystem of Ultrasmall MoC Quantum Dots Encapsulated in Ultrathin N-doped Graphene Vesicles for Superhigh H_2 Production from Pure Water. *Nano Energy* **2020**, 75, 104990. DOI: 10.1016/j.nanoen.2020.104990
38. Chen, J. -P., Xie, L. -F., Huang, W. -H., Niu, L., Ni, Q. -L., Huang, T. -H., Gui, L. -C. & Wang, X. -J. Piezocatalytic Performances of Conjugated Microporous Polymers with Donor–Acceptor Structures for Overall Water Splitting. *ACS Catal.* **2024**, 14, 7853–7866. DOI: 10.1021/acscatal.4c00918
39. Tu, S., Guo, Y., Zhang, Y., Hu, C., Zhang, T., Ma, T. & Huang, H. Piezocatalysis and Piezo -Photocatalysis: Catalysts Classification and Modification Strategy, Reaction Mechanism, and Practical Application. *Adv. Funct. Mater.* **2020**, 30, 2005158. DOI: 10.1002/adfm.202005158
40. Zhou, X., Shen, B., Lyubartsev, A., Zhai, J. & Hedin, N. Semiconducting Piezoelectric Heterostructures for Piezo- and Piezophotocatalysis. *Nano Energy* **2022**, 96, 107141. DOI: 10.1016/j.nanoen.2022.107141
41. Jiang, S., Mai, Q., Xu, H., Ma, Y., Jia, B. & Ma, T. Piezocatalysis and Piezo-assisted Catalysis in Environmental Remediation and Energy Conversion. *Chem. Commun.* **2026**, 62, 3745–3760. DOI: 10.1039/d5cc06489a
42. Zhu, X., Zhan, C. & Kan, E. Understanding Piezocatalysis of Barium Titanate in Solution from Quantum-continuum-electrochemical Theory. *npj Comput. Mater.* **2025**, 11, 252. DOI: 10.1038/s41524-025-01746-8
43. Su, R., Wang, Z., Zhu, L., Pan, Y., Zhang, D., Wen, H., Luo, Z., Li, L., Li, F., Wu, M., *et al*. Strain-Engineered Nano-Ferroelectrics for High-Efficiency Piezocatalytic Overall Water Splitting. *Angew. Chem. Int. Ed.* **2021**, 60, 16019–16026. DOI: 10.1002/anie.202103112
44. Saravanakumar, B., Thiyagarajan, K., Balasingam, S. K., Siva, T., Pai, R. K. & Ramadoss, A. Recent Advances and Innovations in the Piezoelectrochemical Process for Energy and the Environment: A Review. *J. Energy Storage* **2024**, 83, 110576. DOI: 10.1016/j.est.2024.110576
45. Yan, X., Zhu, J., Xu, J., Yang, S., Liu, Y., He, H., Liu, S. & Wang, K. Hybrid Piezo-photocatalysts: Harnessing Dual Functionalities for Advanced Charge Dynamics and Catalytic Performance. *Chem. Eng. J.* **2024**, 500, 157440. DOI: 10.1016/j.cej.2024.157440
46. Jing, L., Xu, Y., Xie, M., Li, Z., Wu, C., Zhao, H., Wang, J., Wang, H., Yan, Y., Zhong, N., *et al*. Piezo-photocatalysts in the Field of Energy and Environment: Designs, Applications, and Prospects. *Nano Energy* **2023**, 112, 108508. DOI: 10.1016/j.nanoen.2023.108508
47. Davari, N., Pasikhani, J. V., Bianchi, C. L., Yargeau, V. & Boffito, D. C. Recent Progress on Ti-based Piezo-photocatalysts for Wastewater Treatment. *Curr. Opin. Chem. Eng.* **2025**, 47, 101090. DOI: 10.1016/j.coche.2025.101090
48. Sood, A., Desseigne, M., Dev, A., Maurizi, L., Kumar, A., Millot, N. & Han, S. S. A Comprehensive Review on Barium Titanate Nanoparticles as a Persuasive Piezoelectric Material for Biomedical Applications:

Prospects and Challenges. *Small* **2023**, 19, 2206401. DOI: 10.1002/smll.202206401
49. Liu, Y., Wang, Y., Ma, J., Li, S., Pan, H., Nan, C. -W. & Lin, Y. -H. Controllable Electrical, Magnetoelectric and Optical Properties of $BiFeO_3$ via Domain Engineering. *Prog. Mater. Sci.* **2022**, 127, 100943. DOI: 10.1016/j.pmatsci.2022.100943
50. Huang, X., Lei, R., Yuan, J., Gao, F., Jiang, C., Feng, W., Zhuang, J. & Liu, P. Insight into the Piezo-photo Coupling Effect of $PbTiO_3$/CdS Composites for Piezo-photocatalytic Hydrogen Production. *Appl. Catal. B Environ.* **2021**, 282, 119586. DOI: 10.1016/j.apcatb.2020.119586
51. Wang, X., Jiang, J., Yang, L., An, Q., Xu, Q., Yang, Y. & Guo, H. Enhanced Piezoelectric Polarization by Subtle Structure Distortion to Trigger Efficient Photocatalytic CO_2RR. *Appl. Catal. B Environ.* **2024**, 340, 123177. DOI: 10.1016/j.apcatb.2023.123177
52. Zhao, Y., Zhang, Y., Xu, Q., Gong, H., Yan, M., Feng, K., Zhou, X., Zhou, X. & Zhang, D. Enhanced Piezoelectricity and Spectral Absorption in Nd-doped Bismuth Titanate Hierarchical Microspheres for Efficient Piezo-photocatalytic H_2 Production and Pollutant Degradation. *J. Mater. Chem. A* **2024**, 12, 1753–1763. DOI: 10.1039/d3ta06341k
53. Liu, Q., Zhan, F., Luo, H., Luo, X., Yi, Q., Sun, Q., Xiao, Z., Zhang, Y., Zhang, D. & Bowen, C. R. Na -Sm Bimetallic Regulation and Band Structure Engineering in $CaBi_2Nb_2O_9$ to Enhance Piezo-photo-catalytic Performance. *Adv. Funct. Mater.* **2023**, 33, 2303736. DOI: 10.1002/adfm.202303736
54. Zhao, Q., Xiao, H., Huangfu, G., Zheng, Z., Wang, J., Wang, F. & Guo, Y. Highly-efficient Piezocatalytic Performance of Nanocrystalline $BaTi_{0.89}Sn_{0.11}O_3$ Catalyst with T_c Near Room Temperature. *Nano Energy* **2021**, 85, 106028. DOI: 10.1016/j.nanoen.2021.106028
55. Xu, M., Lu, M., Qin, G., Wu, X., Yu, T., Zhang, L., Li, K., Cheng, X. & Lan, Y. Piezo -Photocatalytic Synergy in $BiFeO_3$@COF Z -Scheme Heterostructures for High -Efficiency Overall Water Splitting. *Angew. Chem. Int. Ed.* **2022**, 61, e202210700. DOI: 10.1002/anie.202210700
56. Xu, X., Xiao, L., Wu, Z., Jia, Y., Ye, X., Wang, F., Yuan, B., Yu, Y., Huang, H. & Zou, G. Harvesting Vibration Energy to Piezo-catalytically Generate Hydrogen through Bi_2WO_6 Layered-perovskite. *Nano Energy* **2020**, 78, 105351. DOI: 10.1016/j.nanoen.2020.105351
57. Wang, C., Chen, F., Hu, C., Ma, T., Zhang, Y. & Huang, H. Efficient Piezocatalytic H_2O_2 Production of Atomic-level Thickness $Bi_4Ti_3O_{12}$ Nanosheets with Surface Oxygen Vacancy. *Chem. Eng. J.* **2022**, 431, 133930. DOI: 10.1016/j.cej.2021.133930
58. Chen, T., Chen, F., Wang, C., Hu, C., Tian, N., Li, J. & Huang, H. Identifying Polar and Non-polar Octahedron Units in Isomorphic Layered Perovskites towards Efficient Piezocatalytic H_2 Evolution. *Nano Energy* **2024**, 131, 110334. DOI: 10.1016/j.nanoen.2024.110334
59. Zhou, Y., Dong, H., Xu, Z., Zha, Q., Zhu, M. & Meng, Y. Carbon Modification Facilitates Piezocatalytic H_2O_2 Production Over BiOCl Nanosheets: Correlation between Piezoresponse and Surface Reaction. *Appl. Catal. B Environ.* **2024**, 343, 123504. DOI: 10.1016/j.apcatb.2023.123504
60. Li, C., He, J., Cai, T., Chen, X., Tao, H., Zhou, Y. & Zhu, M. Surface Oxygen Vacancies of BiOBr Regulating Piezoelectricity for Enhancing Efficiency and Selectivity of Photocatalytic CO_2 Reduction. *Chin. J. Catal.* **2025**, 74, 130–143. DOI: 10.1016/s1872-2067(25)64649-3
61. Yuan, C., Tian, N., Huang, H. & Zhang, Y. Polarization Synergizes Defective Interface Heterojunctions Boosting Piezocatalytic Hydrogen Production and Simultaneous Pollutant Degradation. *J. Mater. Chem. A* **2025**, 13, 15713–15724. DOI: 10.1039/d5ta02029h
62. Sha, Z., Chen, F., Hu, C. & Huang, H. Piezocatalytic Reforming of Plastics into High-value Chemicals. *Nat. Commun.* **2026**, 17, 5244. DOI: 10.1038/s41467-026-71948-1
63. Xu, Z., Chen, F., Gao, H., Chen, E., Wang, Y. & Huang, H. π-Conjugated Aligned Polar [CO_3] Triangulars Synergizing Hydroxylation Enables Stress -Enhanced Geometric–Electronic Asymmetries for Hydrogen Piezoevolution. *Adv. Mater.* **2026**, 38, e74229. DOI: 10.1002/adma.74229
64. Cai, H., Lin, L., Yu, Y., Li, T., Zhu, Z., Chen, T. & Huang, H. Piezoelectric Field Driven Proton-Coupled Electron Transfer Reaction and p-Band Center Shift for H_2O_2 Synthesis in Pure Water and Air. *Adv. Funct. Mater.* **2026**, 36, e24126. DOI: 10.1002/adfm.202524126
65. Qiu, J., Yu, T., Chen, J., Li, W., Zhang, X., Li, J., Guo, R., Huang, Z. & Liu, X. Modulate Surface Potential Well Depth of $Bi_{12}O_{17}Cl_2$ by FeOOH in $Bi_{12}O_{17}Cl_2$@FeOOH Heterojunction to Boost Piezoelectric Charge Transfer and Piezo-self-fenton Catalysis. *Acta Phys. -Chim. Sin.* **2026**, 42, 100157. DOI: 10.1016/j.actphy.2025.100157
66. Wu, Y., Wang, P., Che, H., Liu, W., Tang, C. & Ao, Y. Triggering Dual Two-electron Pathway for H_2O_2 Generation by Multiple $[Bi–O]_n$ Interlayers in Ultrathin $Bi_{12}O_{17}Cl_2$ towards Efficient Piezo-self-Fenton Catalysis. *Angew. Chem. Int. Ed.* **2024**, 63, e202316410. DOI: 10.1002/anie.202316410
67. Sun, F., Xu, Q., Wang, X., Luo, C., Zhao, M., Ma, Q., Yu, H., Yu, W. & Dong, X. Multi -Electric Field -Enhanced $CuInS_2$-Modified TiO_2(Anatase)/TiO_2(Rutile)/PVDF Nanofiber Membrane for Multifunctional Piezo-Photocatalysis. *Adv. Funct. Mater.* **2025**, 35, e05795. DOI: 10.1002/adfm.202505795
68. Wei, H., Liu, B., Cao, F., Li, B., Kou, J., Chen, Y., Lu, C. & Xu, Z. Spontaneous Chirality Transition-Mediated Piezo-Pyroelectric Synergy for Photocatalytic Hydrogen Production from Saturated Vapor of VOC Aqueous Solutions. *Adv. Funct. Mater.* **2026**, 36, e18394. DOI: 10.1002/adfm.202518394
69. Alam, M. M. & Crispin, X. The Past, Present, and Future of Piezoelectric Fluoropolymers: Towards Efficient and Robust Wearable Nanogenerators. *Nano Res. Energy* **2023**, 2, e9120076. DOI: 10.26599/nre.2023.9120076
70. Parija, A., Das, K. K., Mohanty, U. A. & Parida, K. Multifunctional PVDF Based Composite for Sustainable Catalysis: Insights into Piezo-photocatalytic Environmental and Energy Application. *Chem. Eng. J.* **2025**, 522, 167260. DOI: 10.1016/j.cej.2025.167260
71. Lee, G. -C., Lyu, L. -M., Hsiao, K. -Y., Huang, Y. -S., Perng, T. -P., Lu, M. -Y. & Chen, L. -J. Induction of a Piezo-potential Improves Photocatalytic Hydrogen Production Over ZnO/ZnS/MoS_2 Heterostructures. *Nano Energy* **2022**, 93, 106867. DOI: 10.1016/j.nanoen.2021.106867
72. Wang, J., Hu, C., Zhang, Y. & Huang, H. Engineering Piezoelectricity and Strain Sensitivity in CdS to Promote Piezocatalytic Hydrogen Evolution. *Chin. J. Catal.* **2022**, 43, 1277–1285. DOI: 10.1016/s1872-2067(21)63976-1
73. Lin, S., Li, S., Huang, H., Yu, H. & Zhang, Y. Synergetic Piezo-Photocatalytic Hydrogen Evolution on $Cd_xZn_{1-x}S$ Solid-Solution 1D Nanorods. *Small* **2022**, 18, 2106420. DOI: 10.1002/smll.202106420
74. Abdollahifar, M., Greve, E., Lumma, J. & Adelung, R. Functional Tetrapodal Zinc Oxide: from Synthesis and Multiphysics to Advanced Applications. *Chem. Soc. Rev.* **2026**, 55, 3834–3930. DOI: 10.1039/d5cs00594a
75. Consonni, V. & Lord, A. M. Polarity in ZnO Nanowires: A Critical Issue for Piezotronic and Piezoelectric Devices. *Nano Energy* **2021**, 83, 105789. DOI: 10.1016/j.nanoen.2021.105789
76. Ma, J., Xiong, X., Wu, D., Wang, Y., Ban, C., Feng, Y., Meng, J., Gao, X., Dai, J., Han, G., *et al*. Band Position -Independent Piezo -Electrocatalysis for Ultrahigh CO_2 Conversion. *Adv. Mater.* **2023**, 35, 2300027. DOI: 10.1002/adma.202300027
77. Meng, F., Guo, C., Cui, T., Wang, Y., Julian, R. A., Chen, X., Yu, B., Pan, D., DuBois, D. B., Tressel, J., *et al*. Rapid Synthesis of Single-layer Iron-doped 2H Tungsten Sulfide via Magnetic Induction Heating for Piezocatalytic Reduction of Oxygen to Hydrogen Peroxide. *Appl. Catal. B Environ.* **2025**, 371, 125224. DOI: 10.1016/j.apcatb.2025.125224
78. Han, Q., Han, Z., Wang, Y., Zhang, S., Fang, J., Li, H. & Fang, P. Enhanced Photocatalytic Hydrogen Evolution by Piezoelectric Effects Based on $MoSe_2$/Se-decorated CdS Nanowire Edge-on Heterostructure. *J. Colloid Interface Sci.* **2023**, 630, 460–472. DOI: 10.1016/j.jcis.2022.10.120
79. Li, S., Zhou, H., Hu, W., Sofer, Z., Zhang, J. & Li, J. Se-induced Coordination Engineering in $MnPX_3$ for Efficient Piezo-photocatalytic H_2O_2 Evolution and Uranium Recovery. *Appl. Catal. B Environ.* **2027**, 401, 127292. DOI: 10.1016/j.apcatb.2026.127292
80. Guo, Z., Sun, K., Zou, S., Xiong, B., Wang, L., Shi, W., Sun, Y. & Guo, F. Construction of Surface Pit-structured G-C_3N_4 by Induced SiO_2 Hard Template for Boosted Piezoelectric-assisted Photocatalytic H_2O_2 Production. *J. Colloid Interface Sci.* **2025**, 699, 138118. DOI: 10.1016/j.jcis.2025.138118
81. Mishra, H. K., Ankush, Barman, N., Mondal, B., Jha, M., Thapa, R. & Mandal, D. Beyond Conventional Catalysts: Monoelemental Tellurium as a Game Changer for Piezo-Driven Hydrogen Evolution. *Small* **2024**, 20, 2402421. DOI: 10.1002/smll.202402421
82. Ren, T., Tian, W., Shen, Q., Yuan, Z., Chen, D., Li, N. & Lu, J. Enhanced Piezocatalysis of Polymorphic Few-layered MoS_2 Nanosheets by Phase Engineering. *Nano Energy* **2021**, 90, 106527. DOI: 10.1016/j.nanoen.2021.106527
83. Nie, C., Wang, J., Cai, B., Lai, B., Wang, S. & Ao, Z. Multifunctional Roles of MoS_2 in Persulfate-based Advanced Oxidation Processes for Eliminating Aqueous Organic Pollutants: A Review. *Appl. Catal. B Environ.* **2024**, 340, 123173. DOI: 10.1016/j.apcatb.2023.123173
84. He, Y., Tian, N., An, Y., Sun, R., Zhang, Y. & Huang, H. Morphology Regulation and Oxygen Vacancy Construction Synergistically Boosting the Piezocatalytic Degradation and Pure Water Splitting of $SrTiO_3$. *Small* **2024**, 20, 2407624. DOI: 10.1002/smll.202407624
85. Zhao, X., Lu, X., Chen, W. -J., Yang, M. -Q., Pan, X. & Bian, Z. Exceptional Piezocatalytic H_2 Production of Nitrogen-doped TiO_2@carbon Nanosheets Induced by Engineered Piezoelectricity. *J. Colloid Interface Sci.* **2024**, 659, 11–20. DOI: 10.1016/j.jcis.2023.12.101
86. Wang, H., Cao, J., Wu, H., Yao, W. & Li, H. Mild Acid Etching

Promotes Near-surface Polar/structural Modification in Centrosymmetric $SrZrO_3$ for Enhanced Piezocatalytic H_2 Evolution. *Appl. Catal. B Environ.* **2026**, 393, 126774. DOI: 10.1016/j.apcatb.2026.126774
87. Gong, Y., Qiu, D., He, X., Shao, J., Li, N., Chen, D., Li, H., Xu, Q. & Lu, J. Polyoxometalate Cluster-metal Oxide Hybrid Subnanobelts on Hf-O-Mo Interfacial Electron Coupling for Piezocatalytic Reduction of Dilute CO_2. *Appl. Catal. B Environ.* **2027**, 401, 127332. DOI: 10.1016/j.apcatb.2026.127332
88. Chen, H., Li, Z., Yang, J., Gong, L. & Zhu, M. Unveiling the Role of Fe in Natural Tourmaline to Tune the Polarization Field for Hydrogen Peroxide Synthesis Under Ambient Conditions. *Chin. Chem. Lett.* **2026**, 37, 111743. DOI: 10.1016/j.cclet.2025.111743
89. Xu, Y., Zhou, Z., Lin, Z., Liu, X., Zhou, Y., Mutailipu, M. & Fan, X. Π–Conjugated B_3O_6 Units Drive Directional O_2 Adsorption and Charges Separation for Efficient Piezoelectric H_2O_2 Production. *Appl. Catal. B Environ.* **2026**, 386, 126378. DOI: 10.1016/j.apcatb.2025.126378
90. Guo, Z., Zhao, C., Meng, L., Fu, H., Wang, C., Chen, Z., Zheng, Y., Li, Y. -H., Wang, J. -F. & Wang, C. -C. Unraveling Synergistic Effect of In–O–Hf Bond and Piezo-photocatalysis in Simultaneous H_2O_2 Production and Diclofenac Sodium Degradation. *Appl. Catal. B Environ.* **2025**, 377, 125507. DOI: 10.1016/j.apcatb.2025.125507
91. Jalili, H., Aghdasinia, H., Ebrahimi Farshchi, M. & Ahadzadeh, I. Construction of a Synergistic Z-scheme Heterojunction for Efficient Piezo-photocatalytic Hydrogen Production via Water Splitting Using NH_2-MIL-101(Fe/Cr)@ZnO Nanocomposite. *Int. J. Hydrogen Energy* **2025**, 196, 152629. DOI: 10.1016/j.ijhydene.2025.152629
92. Huang, J., Dong, H., An, L., Zhu, M. & Qin, J. Al-based Metal-organic Framework for Piezocatalytic Hydrogen Peroxide Production: Efficiency, Pathway, and Mechanism. *Chem. Eng. J.* **2025**, 504, 158555. DOI: 10.1016/j.cej.2024.158555
93. Liu, T., Liu, Z., Lv, G., Guo, L., Liu, M., Guo, J., Wang, G., Zhang, Z., Liu, Y., Wang, L., *et al*. Efficient Dual-Path Piezosynthesis of Hydrogen Peroxide by Breaking Symmetry of UiO-66. *Adv. Funct. Mater.* **2026**, 36, e74769. DOI: 10.1002/adfm.74769
94. Du, X., Fu, Y., Arandiyan, H., Li, P., Fan, H., Zhu, L., Li, H., Zhang, L. & Ma, T. Emerging Piezocatalysts: Metal–Organic Frameworks and Their Derivatives. *Nano Today* **2025**, 65, 102841. DOI: 10.1016/j.nantod.2025.102841
95. Liang, Z. -Z., Wang, Y., Li, X. -A., Peng, X. -B., Gong, L., Xiao, L. -M., Yang, X., Zou, B., Zhou, Y. & Liu, J. -M. Enhanced Piezo-photocatalytic Water Splitting Activity via Engineering Robust Dipole Moments in Covalent Organic Frameworks. *Nat. Commun.* **2025**, 17, 729. DOI: 10.1038/s41467-025-67467-0
96. Huang, B., Wu, Z., Xu, M., Chen, Z., Wu, Y., Li, T., Weng, W., Xiao, W., Lu, L., Ge, P., *et al*. Unraveling Synergistic Effect of Ferroelectric Polarization and Z-scheme Heterostructure for Exceptional Piezo-photocatalytic Water Splitting. *Nano Mater. Sci*. **2026**, in press. DOI: 10.1016/j.nanoms.2026.02.005
97. Li, Z., Dong, Z., Zhang, Z., Wei, B., Meng, C., Zhai, W., Wang, Y., Cao, X., Han, B. & Liu, Y. Covalent Organic Frameworks for Boosting H_2O_2 Photosynthesis via the Synergy of Multiple Charge Transfer Channels and Polarized Field. *Angew. Chem. Int. Ed.* **2025**, 64, e202420218. DOI: 10.1002/anie.202420218
98. Guan, L., Li, Z., Wang, K., Gong, L., Fang, Y., Yu, G., Zhu, M. & Jin, S. Bottom-up Synthesis of Piezoelectric Covalent Triazine-based Nanotube for Hydrogen Peroxide Production from Water and Air. *Angew. Chem. Int. Ed.* **2025**, 64, e202419867. DOI: 10.1002/anie.202419867
99. Wang, X., Li, X., Li, M., Li, Z., Lei, Z., Huang, S., Yi, J., Yuan, Z. -Y., Ye, L., Cui, W. -G., *et al*. Polarisation Engineering in Covalent Organic Frameworks for Catalysis. *Nano-Micro Lett.* **2026**, 18, 347. DOI: 10.1007/s40820-026-02183-y
100. Liu, F., Wang, M., Liu, J., Gao, F., Lin, J., He, J., Zhu, F., Liu, C. & Lin, Z. Recovery of Lead-Zinc Slags to Methyl-Ammonium Lead Tri-Iodide With Single-Atom Fe–N_4 Sites for Piezocatalytic Hydrogen Evolution. *Carbon Energy* **2025**, 7, e70055. DOI: 10.1002/cey2.70055
101. Sun, X., Cheng, Y., Li, R., Zhang, B., Guan, J., Xu, H., Liu, Q. & Chen, X. Discovery of Piezoelectricity in Inorganic-organic Hybrid ZnS(en)0.5 Nanosheets for Ultrahigh, Selective CO_2-to-CO Conversion. *Appl. Catal. B Environ.* **2026**, 383, 126053. DOI: 10.1016/j.apcatb.2025.126053
102. Zhu, M., Su, H., Yang, F., Qin, Y., Hui, F. C. -H., Zhang, R., Geng, J., Wang, K., Fan, X., Wong, W. -Y., *et al*. Piezoelectrically Enhanced Charge Carriers Transfer in a Highly Conjugated Nickel(II)-Acetylide Framework for Photocatalytic CO_2 Reduction. *J. Am. Chem. Soc.* **2025**, 147, 29192–29204. DOI: 10.1021/jacs.5c08037
103. Li, C., Chen, P., Zhang, Y., Ye, Y. -X., Zou, G., Ouyang, G. & Guo, L. Pyridine Nitrogen-strengthened Structural Polarization in Donor-acceptor Polymers for Enhanced Photo/piezo-catalytic H_2 and H_2O_2 Co-generation in Pure Water. *Appl. Catal. B Environ.* **2026**, 396, 126916. DOI: 10.1016/j.apcatb.2026.126916
104. Zhang, K., Sun, X., Hu, H., Yan, G., Qin, A., Ma, Y., Huang, H. & Ma, T. Defect Engineered Microcrystalline Cellulose for Enhanced Cocatalyst -Free Piezo -Catalytic H_2 Production. *Small* **2023**, 19, 2304674. DOI: 10.1002/smll.202304674
105. Cui, Y., Zhou, W., Yang, H., Li, D., Han, H., Zhang, Y. & Dunn, S. Lattice Distortion and Morphology Modulation Enhanced Piezocatalytic Activity of Ca-doped $Sr_2Nb_2O_7$ towards H_2O_2 Production and Piezo-self-fenton Degradation. *Nano Energy* **2025**, 146, 111540. DOI: 10.1016/j.nanoen.2025.111540
106. Yang, Z., Li, Y., Wang, B., Pan, J., Kleppe, A. K. & Hall, D. A. Acceptor Doping and Actuation Mechanisms in Sr-doped $BiFeO_3BaTiO_3$ Ceramics. *J. Mater.* **2024**, 10, 57–69. DOI: 10.1016/j.jmat.2023.04.007
107. Amdouni, W., Otoničar, M., Alamarguy, D., Erdem, E., Gemeiner, P., Mazaleyrat, F., Maghraoui-Meherzi, H., Kreisel, J., Glinsek, S. & Dkhil, B. Enhancement of the Piezocatalytic Response of La -Doped $BiFeO_3$ Nanoparticles by Defects Synergy. *Small* **2024**, 20, 2406425. DOI: 10.1002/smll.202406425
108. Han, W., Zhang, X., Li, H., Fu, Y., Shen, B., Guo, S. -Q. & Ma, T. Band Tilt with Enhanced Charge Separation Induced by Nb-doped Piezoelectric to Boost Photocatalysis. *Nano Energy* **2025**, 139, 110929. DOI: 10.1016/j.nanoen.2025.110929
109. Peng, W. -B., Jiang, B. -D., Guan, S. -H. & Li, H. Wind-driven Piezocatalytic HCHO Degradation by N-doped ZnO: A Combined Experimental and Theoretical Study. *Nano Energy* **2025**, 145, 111453. DOI: 10.1016/j.nanoen.2025.111453
110. Lei, J., Wang, C., Feng, X., Ma, L., Liu, X., Luo, Y., Tan, L., Wu, S. & Yang, C. Sulfur-regulated Defect Engineering for Enhanced Ultrasonic Piezocatalytic Therapy of Bacteria-infected Bone Defects. *Chem. Eng. J.* **2022**, 435, 134624. DOI: 10.1016/j.cej.2022.134624
111. Hao, A., Ning, X., Liu, X., Zhan, L. & Qiu, X. Phosphorus Heteroatom Doped BiOCl as Efficient Catalyst for Photo-piezocatalytic Degradation of Organic Pollutant and Unveiling the Mechanism: Experiment and DFT Calculation. *Chem. Eng. J.* **2024**, 499, 155823. DOI: 10.1016/j.cej.2024.155823
112. Zhou, F., Dong, Z., Dong, Y., Chen, J., Wang, Y., Wang, Y., Lin, Z., Zhang, Z., Liu, Y. & Han, B. Regulation of Piezoelectric Polarization for Uranium Extraction Dynamics by Spatially Gradient Manipulation of Oxygen Vacancies. *Appl. Catal. B Environ.* **2026**, 390, 126603. DOI: 10.1016/j.apcatb.2026.126603
113. Hsu, F. -R., Chen, Y. -C., Yeh, C. -H., Lin, H. -Y., Chen, H. -Y. T. & Wu, J. M. Boosting Piezoelectric Catalytic Ammonia Synthesis: A Synergistic Approach with Sulfur Vacancy Engineered CdS Pyramid-surface Nanospheres. *Nano Energy* **2025**, 142, 111270. DOI: 10.1016/j.nanoen.2025.111270
114. Peng, X., Xu, E., Zhang, X., Qin, X., Hou, S. & Wang, H. Design of $MnIn_2S_4$ Piezoelectric Photocatalyst with Synergistic Regulation by Double Cation Vacancies and Its Efficient Uranium Removal Performance. *J. Colloid Interface Sci.* **2026**, 721, 140722. DOI: 10.1016/j.jcis.2026.140722
115. Sha, Z., Hu, C., Tu, S., Li, T., Chen, F. & Huang, H. Piezo-activating Oxygen Vacancy Regulates Quantum Well Effect and P-band Center for Exceptional Photocatalysis. *Nano Energy* **2025**, 139, 110919. DOI: 10.1016/j.nanoen.2025.110919
116. Li, Z., Zhou, X., Pei, H., Lv, Q., Pan, Z., Chen, Y., Ivanov, E., Lavorgna, M., Cardon, L. & Edeleva, M. Achieving Intelligent Sensing through a Novel Mesoscopic Dipole Orientation Strategy in Sandwich Piezoelectric Composites. *Chem. Eng. J.* **2026**, 527, 171574. DOI: 10.1016/j.cej.2025.171574
117. Wang, Y., Gao, C., Yu, H., Li, S., Wang, S., Dou, X., Zhang, L., Yu, J. & Cheng, X. The Synergy of Atomic-level Charge Transfer Bridges and Extra Piezoelectric Electric Field Endow Efficient Pure Water Splitting into H_2O_2 and H_2. *Nano Energy* **2025**, 140, 111067. DOI: 10.1016/j.nanoen.2025.111067
118. Zheng, S., Zhang, N., Zhao, X., Chen, D. & Wang, H. Size-dependent Mechanical Analysis of Porous Functionally Graded Piezoelectric Micro/nanoscale Structures: a Literature Review. *Smart Mater. Struct.* **2024**, 33, 093002. DOI: 10.1088/1361-665x/ad5809
119. Moradi, A., Ansari, R., Hassanzadeh-Aghdam, M. K., Sahmani, S. & Jang, S. -H. Modeling-based Mechanistic Insights into the Role of Barium Titanate Shape and Microstructural Defects in Coupled-field Responses of Piezoelectric Nanocomposites. *Compos. Part B Eng.* **2025**, 305, 112755. DOI: 10.1016/j.compositesb.2025.112755
120. He, Y., Tian, N., An, Y., Chen, F., Zhang, Y. & Huang, H. Synergistic Piezocatalysis in Hydrogen Production on Ordered-disordered Core-

shell $BaTi_2O_5$ Nanorods. *Appl. Catal. B Environ.* **2026**, 391, 126684. DOI: 10.1016/j.apcatb.2026.126684
121. Kim, J. Y., Hwang, W., Han, S. Y., Jung, Y. S., Pang, F., Shen, W., Park, C., Kim, S., Soon, A. & Cho, Y. S. Oxygen -Doped 2D In_2Se_3 Nanosheets with Extended In -Plane Lattice Strain for Highly Efficient Piezoelectric Energy Harvesting. *Adv. Sci.* **2025**, 12, 2410851. DOI: 10.1002/advs.202410851
122. Ye, Y. -Z., Liu, H. -Y., Gong, Y. -J., Xu, Z. -Z., Zhao, Y., Yu, N., Wang, Q. -S., Wen, W., Yang, T. -Y., Li, W., *et al*. Design of Piezoelectric Organic Cage Salts for Energy Harvesting. *Chem* **2024**, 10, 1118–1131. DOI: 10.1016/j.chempr.2023.12.006
123. Zhao, Y., Xu, Z., Bian, C., Huang, L., Xu, T., Chen, M., Sun, T., Deng, X., Yu, X., Song, L., *et al*. $Comple_x$ II Inhibitor-loaded Hollow Piezoelectric Nanocarriers Potentiate Respiration-driven Piezocatalytic Therapy for Malignant Pleural Effusion. *J. Control. Release* **2026**, 397, 115180. DOI: 10.1016/j.jconrel.2026.115180
124. Yu, Z., Tian, A., Xu, Z., Sui, Z., Hu, T., Zhao, X., Tan, F., Fu, J., Xie, A. & Zuo, R. Hierarchical Domain Engineered BF-PT Based Piezoelectric Ceramics with Large Piezoelectricity Over Broad Temperature Range. *Acta Mater.* **2026**, 314, 122311. DOI: 10.1016/j.actamat.2026.122311
125. Li, J., Tian, S., Cheng, J., Zeng, X., Cao, F., Shi, J., Tan, C. & Liu, H. Engineering ZnO/CuO Heterojunctions via Supramolecular Mediation Leading to Morphology -Dependent High -Performance Piezoelectric Catalyst. *Small* **2025**, 21, e07661. DOI: 10.1002/smll.202507661
126. Gao, W., Xie, B., Ma, C., Gao, X., Liu, Z., Lu, Q., Luo, H., Wang, Q. & Bowen, C. Ultrahigh Piezocatalytic Performance Based on the Micron-scale $BaTiO_3$ Single Crystal Sheets with {111} Highly Exposed Polar Facets. *Chem. Eng. J.* **2025**, 506, 160084. DOI: 10.1016/j.cej.2025.160084
127. Wang, B., Zhang, Q., He, J., Huang, F., Li, C. & Wang, M. Co-catalyst-free Large ZnO Single Crystal for High-efficiency Piezocatalytic Hydrogen Evolution from Pure Water. *J. Energy Chem.* **2022**, 65, 304–311. DOI: 10.1016/j.jechem.2021.06.004
128. Wang, F., Zhang, J., Jin, C. -C., Ke, X., Wang, F. & Liu, D. Unveiling the Effect of Crystal Facets on Piezo-photocatalytic Activity of $BiVO_4$. *Nano Energy* **2022**, 101, 107573. DOI: 10.1016/j.nanoen.2022.107573
129. Meng, L., Zhao, C., Zhang, X., Guo, R., Zheng, Y., Chu, H., Fu, H., Wang, P. & Wang, C. -C. Piezo-photocatalytic Synergetic for H_2O_2 Generation via Dual-pathway Over Z-scheme ZIF-l/g-C_3N_4 Heterojunction. *Nano Energy* **2024**, 128, 109795. DOI: 10.1016/j.nanoen.2024.109795
130. Niu, Q., Chen, J., Fan, S., Yao, X., Gu, Y., Hsiao, B. S., Wei, H. & Zhang, Y. Silk Nanoribbon Films with Enriched Silk II Structure and Enhanced Piezoelectricity for Self-powered Implantable and Wearable Devices. *Nano Today* **2024**, 56, 102228. DOI: 10.1016/j.nantod.2024.102228
131. Lu, H., Bao, S., Lei, B., Sun, S., Wu, L., Zhou, J. & Zhang, L. Spin-splitting Above Room-temperature in Janus Mn_2ClSeH Antiferromagnetic Semiconductor with a Large Out-of-plane Piezoelectricity. *npj Comput. Mater.* **2025**, 11, 71. DOI: 10.1038/s41524-025-01566-w
132. Ma, J., Yuan, M., Yang, Z., Ma, Z., Zhang, J., Li, Z., Ma, P., Cheng, Z. & Lin, J. Surface Oxygen Vacancies and Corona Polarization of $Bi_4Ti_3O_{12}$ Nanosheets for Synergistically Enhanced Sonopiezoelectric Therapy. *J. Am. Chem. Soc.* **2024**, 146, 22348–22359. DOI: 10.1021/jacs.4c05103
133. Xi, K., Wang, H., Huang, S., Zheng, M., Shi, X., Zhu, M. & Hou, Y. Thermally Stable Piezoelectric Properties of Lead-free Ceramics Featuring Polar Topological Domains. *Acta Mater.* **2025**, 294, 121152. DOI: 10.1016/j.actamat.2025.121152
134. Ni, Z., Zhao, S., Guo, L., Yang, J., Zhang, Y., Zhang, Y., Zhang, Y. & Yang, J. Multiphysics-driven Coupled Opto-electro-thermo-mechanical Model for Nonlinear Mechanics of Perovskite Plates. *Int. J. Mech. Sci.* **2026**, 325, 111820. DOI: 10.1016/j.ijmecsci.2026.111820
135. Qi, J. -X., Gong, J. -W., Zhang, C. -R., Peng, Z. -H., Cai, Y. -J., Liu, X., Liu, J. -L., Chen, X. -J., Liang, R. -P. & Qiu, J. -D. Ocean Wave-driven Covalent Organic framework/ZnO Heterostructure Composites for Piezocatalytic Uranium Extraction from Seawater. *Nat. Commun.* **2025**, 16, 1078. DOI: 10.1038/s41467-025-56471-z
136. Zhou, M., Wu, C., Thiruppathiraja, T., Liu, X., Wu, W., Lv, X., Jiang, Z., Ou, H. & Ho, W. -K. Piezo-driven Cation-exchange Induced Regulation of Single Pt Sites on Poly(heptazine Imide) Triggers Photocatalytic NO Oxidation. *Appl. Catal. B Environ.* **2026**, 384, 126193. DOI: 10.1016/j.apcatb.2025.126193
137. Hamza, M., Kanwal, Q., Hussain, M. I., Peng, W., Wang, B., Liu, Z., Liu, C. & Chen, Z. 3D Printing of High-performance Ag/$BaTiO_3$ Ceramic-polymer Piezoelectric Sensors for Biomedical Applications. *Chem. Eng. J.* **2025**, 523, 168848. DOI: 10.1016/j.cej.2025.168848
138. Xia, H., Zhang, Y., Jiang, Z. & Wen, G. A New Trifunctional MoS_2@Au Piezoelectric Nanocatalytic Probe for Selective Detection of Ultratrace 2-mercaptobenzothiazole Based on the RRS Effect of AuNPs. *Chem. Eng. J.* **2026**, 529, 172755. DOI: 10.1016/j.cej.2026.172755
139. Ma, X., Yang, X., Li, K., Ning, P., Sun, X., Tang, Y., Bao, S. & Wang, C. Piezoelectric-enhanced Rapid Degradation of Sulfamethoxazole Using the Co_3O_4/$Bi_{0.5}Na_{0.5}TiO_3$/Peroxymonosulfate Process. *Chem. Eng. J.* **2025**, 512, 161955. DOI: 10.1016/j.cej.2025.161955
140. Ruan, X., Ding, C., Cai, H., Jiang, R., Xu, M., Meng, D., Fang, G., Zhang, D., Wang, L., Cui, X., *et al*. Bulk Polarization Fields and Interfacial Electron Sink in MXene-modified Iodine-doped Bi_4Ti3O_{12} Enhance Piezocatalytic H_2O_2 Generation. *Nat. Commun.* **2026**, 17, 3915. DOI: 10.1038/s41467-026-70169-w
141. Zhao, Q., Yang, Y., Xiong, G., Chen, J., Xu, T., Xu, Q., Zhang, R., Yao, W., Li, H. & Lee, C. -S. Calcium Single Atom Confined in Nitrogen-Doped Carbon-Coupled Polyvinylidene Fluoride Membrane for High-Performance Piezocatalysis. *J. Am. Chem. Soc.* **2024**, 146, 16648–16658. DOI: 10.1021/jacs.4c03851
142. Zhang, S., Chen, D., Guo, Y., Zhang, R., Zhao, Y., Huang, Z., Fan, J., Ho, J. C. & Zhi, C. Piezoelectricity Regulated Ohmic Contact in M/$BaTiO_3$ (M = Ru, Pd, Pt) for Charge Collision and Hydrogen Free Radical Production in Ammonia Electrosynthesis. *Mater. Today* **2023**, 66, 17–25. DOI: 10.1016/j.mattod.2023.03.011
143. Lan, Y., Gao, L., Qian, J., Liu, J., Shen, B., Yang, M., Tu, W., Zhai, J. & Liu, G. Accelerated Confined Mass Transfer in Piezoelectric Semiconducting Metal–Organic Frameworks for H_2O_2 Piezo-photosynthesis. *Chem. Sci.* **2026**, 17, 394–405. DOI: 10.1039/d5sc07619f
144. Zhang, X., Chen, Y., Guo, R., Zhang, Z., Sun, Z., Zhang, Y. & Yan, F. Three Birds with One Stone: A Piezo-photocatalytic System for Synergistic Environmental Remediation through Simultaneous Ionic Liquids Degradation, H_2 Production, and Uranium Reduction. *Appl. Catal. B Environ.* **2025**, 372, 125314. DOI: 10.1016/j.apcatb.2025.125314
145. Zhao, Y., Zhang, Y., Zhou, X., Feng, K., Xu, Q., Gong, H., Zhai, D., Yan, M., Zhang, D. & Bowen, C. {110} Surface-Exposed $Bi_{3.15}$ $Nd_{0.85}$ Ti3 O_{12} Ferroelectric Nanosheet Arrays on Porous Ceramics as Efficient and Recyclable Piezo -Photocatalysts. *Small* **2025**, 21, 2410145. DOI: 10.1002/smll.202410145
146. Ma, W., Suo, S., Du, S., Li, Y., Wang, Y., Fang, J., Zhang, Z., Han, Z., Chen, C., Xu, H., *et al*. The Synergy Electron Mediator and Sulfur Vacancies Regulating Charge Transfer for Piezo-photocatalytic H_2O_2 and H_2 Generation. *Renewable Energy* **2025**, 247, 123027. DOI: 10.1016/j.renene.2025.123027
147. Tang, Q., Wu, J., Kim, D., Franco, C., Terzopoulou, A., Veciana, A., Puigmartí-Luis, J., Chen, X., Nelson, B. J. & Pané, S. Enhanced Piezocatalytic Performance of $BaTiO_3$ Nanosheets with Highly Exposed {001} Facets. *Adv. Funct. Mater.* **2022**, 32, 2202180. DOI: 10.1002/adfm.202202180
148. Zhang, P., Li, Q., Su, R., Wang, H., Shi, X., Deng, S., Bai, Y., Zeng, H., Yu, X., Li, Z., *et al*. Polarization Rearrangement Induced High-Efficiency Piezocatalytic Overall Pure Water Splitting in Ultrathin (001)-Confined $PbTiO_3$. *J. Am. Chem. Soc.* **2025**, 147, 12012–12023. DOI: 10.1021/jacs.4c18542
149. Wang, C., Chen, F., Chen, E., Chen, T., Ma, T. & Huang, H. Unveiling Strong Electric Fields of Ultrafine Hollow Nanotubes Axially Orienting Asymmetric Polar [Bi_5O_7] Units for Efficient Piezocatalytic Water Splitting. *ACS Nano* **2025**, 19, 22387–22401. DOI: 10.1021/acsnano.5c06046
150. Wang, C., Tu, S., Chen, F., Ma, T. & Huang, H. Asymmetric Single-Unit-Cell Layer Enriching Polar Inherent Hydroxyls Eliminates Interlayer Electric Field Shielding Effect and In Situ Self-Polarize for Piezocatalytic Water Splitting. *Adv. Mater.* **2025**, 37, 2505592. DOI: 10.1002/adma.202505592
151. Mondal, S., Dilly Rajan, K., Patra, L., Rathinam, M. & Ganesh, V. Sulfur Vacancy-Induced Enhancement of Piezocatalytic H_2 Production in MoS_2. *Small* **2025**, 21, 2411828. DOI: 10.1002/smll.202411828
152. Feng, W., Yuan, J., Li, S., Tang, X., Xu, D., Meng, S., Wang, K. & Weng, B. Strain-induced Local Polarization Field Modulation and Spin State Alternation in Atomic Ni-anchored Carbon Nitride for Boosting Piezo-photocatalysis. *Appl. Catal. B Environ.* **2026**, 399, 127127. DOI: 10.1016/j.apcatb.2026.127127
153. Weirang, X., Wenying, L., Jiasheng, G., Wangying, X., Qiubao, L., Xiaowei, C., Weicheng, H. & Danqing, L. Interfacial Engineering of Palladium Quantum Dots Decorated Pd-$BaTiO_3$ Heterojunction for High-efficiency Piezocatalytic Hydrogen Evolution. *Chem. Eng. J.* **2026**, 538, 176726. DOI: 10.1016/j.cej.2026.176726
154. Zhang, D., Ruan, X., Wang, L., Cheng, B., Xu, M., Ding, C., Huang, H.

& Ravi, S. K. Enhanced Lattice Polarization and Directed Charge Transport Toward Pt Surface Sites Accelerate the Volmer Step in Piezocatalytic H_2 Evolution on Co-Doped $BiFeO_3$. *Adv. Energy Mater.* **2026**, 16, e70895. DOI: 10.1002/aenm.70895

155. Lin, H. & Wu, J. M. Revolutionary Energy Harvesting: Gravity-Driven Piezocatalysts for Sustainable Hydrogen Production in MoS_2@Mo_2CT_x Systems. *Adv. Energy Mater.* **2024**, 14, 2402164. DOI: 10.1002/aenm.202402164
156. Feng, H., Li, Y., Gu, Y., Liu, X., Zhang, L., Wang, Z. & Li, Z. Piezoelectric Polarization Field Modulated Dual-channel Charges Transfer of SV-CdS/$W_{18}O_{49}$ for Enhanced Photocatalytic H_2 Production. *Appl. Catal. B Environ.* **2025**, 365, 124862. DOI: 10.1016/j.apcatb.2024.124862
157. Pan, Y., Liao, L., Qiao, D., Bermejo, I. L., Liu, Y., Su, R. & López-Salas, N. Tin Chloride Metal Salt Modified Carbon Nitride for Efficient Hydrogen and Hydrogen Peroxide Production from Pure Water via Piezocatalysis. *J. Mater. Chem. A* **2026**, 14, 8575–8583. DOI: 10.1039/d5ta07919e
158. Gao, L., Yuan, C., Yu, W., Guo, S., Tian, N., Zhang, X., Zhang, Y. & Huang, H. Piezoelectric Polarization Optimized Photocharge Separation and Surface Proton Cycling for Efficient Pure Water Splitting. *Angew. Chem. Int. Ed.* **2026**, 65, e25592. DOI: 10.1002/anie.202525592
159. Li, X., Wang, Y., Liang, Z., Peng, X., Xiao, L., Gong, L., Yang, X., Zou, B., Zhou, Y. & Liu, J. A Dual-Piezoelectric Metal–Organic Cage/COF Z -Scheme Heterojunction for Solar-Mechanical Water Splitting. *Adv. Sci.* **2026**, 13, e23030. DOI: 10.1002/advs.202523030
160. Ghosh, A., Surendran, D., Barman, S., Jena, R., Bhakar, M., Nath, S., Sheet, G., Zaręba, J. K. & Maji, T. K. Photo-Piezocatalytic Water Splitting by Post-Synthetic Charge-Transfer Complexation Driven Cluster Modification in Ce-based MOF-808. *Adv. Mater.* **2026**, 38, e11679. DOI: 10.1002/adma.202511679
161. Hu, H., Li, X., Zhang, K., Yan, G., Kong, W., Qin, A., Ma, Y., Li, A., Wang, K., Huang, H., *et al*. Dual Modification of Metal–Organic Frameworks for Exceptional High Piezo -Photocatalytic Hydrogen Production. *Adv. Mater.* **2025**, 37, 2419023. DOI: 10.1002/adma.202419023
162. Wang, Y., Li, X., Chen, Y., Li, Y., Liu, Z., Fang, C., Wu, T., Niu, H., Li, Y., Sun, W., *et al*. Pulsed-Laser-Triggered Piezoelectric Photocatalytic CO_2 Reduction over Tetragonal $BaTiO_3$ Nanocubes. *Adv. Mater.* **2023**, 35, 2305257. DOI: 10.1002/adma.202305257
163. Zhong, Q., Sun, Y., Yang, S. -G., Dai, Y. -H., He, H. & Liu, Z. -Q. Lattice Strain-mediated $MoSe_2$ Enable Superior Piezocatalysis Activity for Upcycling of Organic Pollutants. *Nat. Commun.* **2026**, 17, 4659. DOI: 10.1038/s41467-026-71183-8
164. Bi, C., Xu, H., Zhou, G., Song, H., Xu, J., Li, Q., Wang, B., Ding, P., Li, L., Chu, P. K., *et al*. Lattice Energy Transfer from Homo-crystalline Substitution for Enhanced Piezo-photocatalytic CO_2 Conversion. *Chem. Eng. J.* **2024**, 501, 157345. DOI: 10.1016/j.cej.2024.157345
165. Lu, S., Zhang, S., Li, L., Liu, C., Li, Z. & Luo, D. Piezoelectric Effect-assisted Z-scheme Heterojunction $ZnIn_2S_4$/$BaTiO_3$ for Improved Photocatalytic Reduction of CO_2 to CO. *Chem. Eng. J.* **2024**, 483, 149058. DOI: 10.1016/j.cej.2024.149058
166. Han, Z., Wei, J., Zhang, Z., Fu, Z., Wang, Y., Ma, W., Li, Y., Suo, S. & Fang, P. Selective CO_2 to C_2H_4 Conversion and One-electron Water Oxidation to H_2O_2 via Sulfur-vacancy-rich Z-scheme Piezo-catalyst $BaTiO_3$/SnS_2 Heterojunction. *J. Colloid Interface Sci.* **2026**, 708, 139872. DOI: 10.1016/j.jcis.2026.139872
167. Liu, L., An, Q., Zou, X., Zha, Y., Zhao, G., Liu, Q., Duan, L. & Guo, H. Piezo-photocatalytic Coupling Field Driven Efficient C_2H_4 Synthesis: Proton-coupled Electron Transfer Path Optimization. *Appl. Catal. B Environ.* **2026**, 382, 125915. DOI: 10.1016/j.apcatb.2025.125915
168. Luo, Y., Wang, J., Li, H., Sun, Y., Zhao, Q. & Ma, T. Dual Piezoelectric Catalytic System for Efficient CO_2 Reduction. *Green Carbon* **2025**, 3, 260–269. DOI: 10.1016/j.greenca.2025.01.005
169. Xia, W., Liu, X., Huang, H., Zhangkai, L. & Zeng, X. Piezocatalytic Activity in Highly Oriented Hexagonal SnS_2 Nanosheets for Efficient Photocatalytic CO_2 Reduction. *J. Environ. Chem. Eng.* **2025**, 13, 116850. DOI: 10.1016/j.jece.2025.116850
170. Lu, L., Zhu, X., Liang, Y., Wang, J., Zhang, H., Xue, J., Shen, Q., Shang, J. K. & Li, Q. Superior CO_2 Conversion Performance by Er-Doped BiOCl Nanosheets Through Synergistic Photocatalytic Memory Effect and Er-Doping. *Carbon Energy* **2026**, 8, e70204. DOI: 10.1002/cey2.70204
171. He, X., Shao, J., Li, N., Chen, D., Li, H., Xu, Q., Wang, H. & Lu, J. Metal-free Fluorinated Carbon Nitride with Piezo-boosted Hydrogen-bonding Networks Enable 100% CO Selectivity in CO_2 Reduction. *Chin. J. Catal.* **2026**, 85, 130–142. DOI: 10.1016/s1872-2067(26)65035-8
172. Dong, X., Dai, W., Yang, C., Li, X., Tang, R. & Shi, X. Lattice Distortion Engineering of (GaFeCoAlNi)O_x High Entropy Oxides for Boosting Piezocatalytic CO_2 Reduction. *Mater. Today Energy* **2025**, 53, 101993. DOI: 10.1016/j.mtener.2025.101993
173. He, J., Wang, X., Feng, P., Zhou, Y., Wang, K., Zou, B. & Zhu, M. Isostructural Phase Transition-induced Piezoelectricity in All-inorganic Perovskite $CsPbBr_3$ for Catalytic CO_2 Reduction. *Appl. Catal. B Environ.* **2024**, 355, 124186. DOI: 10.1016/j.apcatb.2024.124186
174. Cui, H., Zhang, M., Zhang, W., Luo, C., Zhang, X., Li, Y. & Zhang, L. Nanosphere ZnO Modified $Cs_3Bi_2Br_9$ Lead-free Perovskite for Boosting Piezo-photocatalytic CO_2 Reduction and Selective Oxidation of Toluene. *Mater. Today Chem.* **2026**, 54, 103747. DOI: 10.1016/j.mtchem.2026.103747
175. Farshchi, M. E., Asgharizadeh, K., Jalili, H., Nejatbakhsh, S., Azimi, B., Aghdasinia, H. & Mohammadpourfard, M. Bimetallic MOF@CdS Nanorod Composite for Highly Efficient Piezo-photocatalytic CO_2 Methanation Under Visible Light. *J. Environ. Chem. Eng.* **2024**, 12, 113909. DOI: 10.1016/j.jece.2024.113909
176. Xu, Q., Wang, L., Sheng, X., Yang, Y., Zhang, C., Duan, L. & Guo, H. Understanding the Synergistic Mechanism of Single Atom Co-modified Perovskite Oxide for Piezo-photocatalytic CO_2 Reduction. *Appl. Catal. B Environ.* **2023**, 338, 123058. DOI: 10.1016/j.apcatb.2023.123058
177. Hu, J., Zhao, R., Ni, J., Luo, W., Yu, H., Huang, H., Wu, B., Wang, Y., Han, J. & Guo, R. Enhanced Ferroelectric Polarization in Au@$BaTiO_3$ Yolk-in-Shell Nanostructure for Synergistic Boosting Visible-Light-Piezocatalytic CO_2 Reduction. *Adv. Sci.* **2024**, 11, 2410357. DOI: 10.1002/advs.202410357
178. Zhu, X., Xu, H., Bi, C., Song, H., Zhou, G., Zhong, K., Yang, J., Yi, J., Xu, H. & Wang, X. Piezo-photocatalysis for Efficient Charge Separation to Promote CO_2 Photoreduction in Nanoclusters. *Ultrason. Sonochem.* **2023**, 101, 106653. DOI: 10.1016/j.ultsonch.2023.106653
179. Wei, Z., Ji, T., Zhou, X., Guo, J., Yu, X., Liu, H. & Wang, J. Synergistic Enhancement of Photocatalytic CO_2 Reduction by Built-in Electric Field/Piezoelectric Effect and Surface Plasmon Resonance via PVDF/CdS/Ag Heterostructure. *Small* **2023**, 19, 2304202. DOI: 10.1002/smll.202304202
180. Wang, S., Li, Z., Yang, G., Xu, Y., Zheng, Y., Zhong, S., Zhao, Y. & Bai, S. Embedding Nano-Piezoelectrics into Heterointerfaces of S-Scheme Heterojunctions for Boosting Photocatalysis and Piezophotocatalysis. *Small* **2023**, 19, 2302717. DOI: 10.1002/smll.202302717
181. Yang, G., Wang, S., Wu, Y., Zhou, H., Zhao, W., Zhong, S., Liu, L. & Bai, S. Spatially Separated $Redo_x$ Cocatalysts on Ferroelectric Nanoplates for Improved Piezophotocatalytic CO_2 Reduction and H_2O Oxidation. *ACS Appl. Mater. Interfaces* **2023**, 15, 14228–14239. DOI: 10.1021/acsami.2c20685
182. Chang, G., Chen, X., Lv, J. -J., Kong, Z. & Wang, Z. -J. Cobalt-Based Electrocatalysts for Sustainable Nitrate Conversion: Structural Design and Mechanistic Advancements. *Nano-Micro Lett.* **2026**, 18, 73. DOI: 10.1007/s40820-025-01877-z
183. Collado, L., Pizarro, A. H., Barawi, M., García-Tecedor, M., Liras, M. & de la Peña O'Shea, V. A. Light-driven Nitrogen Fixation Routes for Green Ammonia Production. *Chem. Soc. Rev.* **2024**, 53, 11334–11389. DOI: 10.1039/d3cs01075a
184. Wang, J. -X., Lin, H. -Y., Tu, K. Y. & Wu, J. -M. Defect-tailored ZnO Nanoflowers Enable Efficient, Metal-free Ammonia Synthesis through Coupled Piezoelectric and Photocatalytic Activation. *J. Mater. Chem. A* **2026**, 14, 10633–10645. DOI: 10.1039/d5ta08002a
185. Chen, Y. -C., Liao, Y. -S., Chen, P. -H., Chou, J. -P., Tsai, C. -K., Lin, Y. -D., Lin, Y. -G., Peng, Y. -R. & Wu, J. M. Direct and Sustainable Ammonia Synthesis from Air and Water with Sulfur-Deficient MoS_2 Piezocatalysts. *ACS Nano* **2025**, 19, 36602–36613. DOI: 10.1021/acsnano.5c11903
186. Zhan, X., Zhou, H., Yin, Z., Wang, P., Wu, Q., Lv, Y. & Wang, Z. Coulomb Repulsion Induced Symmetry-breaking in $BaZrO_3$ Perovskites for Triggering Piezo-photocatalytic Nitrogen Fixation Reaction. *Appl. Catal. B Environ.* **2026**, 387, 126471. DOI: 10.1016/j.apcatb.2026.126471
187. Xia, M., Gong, X., Teng, W., Xiao, H., Li, H., Ou, H. & Yang, G. Nanopit-mediated Electron Pooling Effect for Efficient Piezo-photocatalytic N_2 Fixation in Pure Water. *Appl. Catal. B Environ.* **2026**, 380, 125756. DOI: 10.1016/j.apcatb.2025.125756
188. Ma, K. -C., Lin, H. -Y., Chen, Y. -C., Tsai, C. -H., Zheng, K. -H. & Wu, J. M. Enhanced Ammonia Production via Synergistic Piezo-photocatalysis Using TiO_2 @Layered Silicate Magadiite Nanosheets. *J. Mater. Chem. A* **2024**, 12, 26866–26876. DOI: 10.1039/d4ta04298k

189. Mardaniafzal, A., Khosroshahi, N. & Safarifard, V. Partial MOF-derived $BiFeO_3$ from Fe/Bi-BDC Framework for Efficient Piezo-photocatalytic Reduction of Cr(VI) and N_2 Fixation Under Visible Light. *J. Environ. Chem. Eng.* **2024**, 12, 113164. DOI: 10.1016/j.jece.2024.113164
190. Song, M., Yang, S., Peng, H., Zhao, T., Liu, F., Chen, P. & Yin, S. -F. Linkage Engineered the Donor–Acceptor Motifs of Poly(heptazine Imide) for Enhancing the Piezo-photocatalytic Nitrogen Fixation. *Nano Energy* **2023**, 116, 108784. DOI: 10.1016/j.nanoen.2023.108784
191. Yuan, J., Chen, F., Feng, W., Xiao, J., Wang, L., Luo, S., Zhang, Z., Long, J., Dai, W. & Huang, H. Dynamic Switching Spin State of Fe Single Atoms for Piezoelectric -Mediated Overall Nitrogen Fixation Photosynthesis. *Adv. Mater.* **2025**, 37, 2504015. DOI: 10.1002/adma.202504015
192. Wang, C., Lai, G., Yang, X., Ruan, D., Zhu, D., Guo, Y. & Zhi, C. Mechanoluminescence-Enhanced Ammonia Synthesis via Mechanochemical Nitrate Reduction. *ACS Nano* **2026**, 20, 17695–17704. DOI: 10.1021/acsnano.6c05545
193. Yang, H., Wang, Y., Wei, Z., Wang, F., Ning, P., Wang, C., Sun, X., Bao, S., Li, M. & Li, K. Electric Field Reconstruction Enables Piezoelectric Ammonia Synthesis From Low -Concentration Nitrates. *Adv. Energy Mater.* **2026**, 16, e71118. DOI: 10.1002/aenm.71118
194. Liu, S., Li, J., Liu, Z., Song, J., Lv, H., Xiao, D., Wang, Q., Zhang, Y. & Xue, Q. Lattice Strain and Piezoelectric Field Modulated Piezo - Photocatalytic Nitrate -to -Ammonia Conversion in Chemically Bonded S - Scheme Heterojunction. *Adv. Sci.* **2026**, 13, e18794. DOI: 10.1002/advs.202518794
195. Liu, J., Jin, L., Dai, Z., Ji, Y., Qian, J., Lu, Y., Wang, J., Shen, B., Li, Y., Xu, R., *et al*. Single Atom Embedding Enhanced Macroscopic Polarization in Carbon Nitride Nanosheets for pH-Universal Piezo-Photocatalytic Nitrate Reduction over a Wide Concentration Range. *ACS Catal.* **2025**, 15, 4025–4038. DOI: 10.1021/acscatal.4c06247
196. Tian, N., Zhou, T., He, Y., Huang, H. & Zhang, Y. Piezoelectric Polarization Enhanced Photocatalytic H_2O_2 Production: Recent Advances and Future Perspectives. *Int. J. Hydrogen Energy* **2026**, 200, 152871. DOI: 10.1016/j.ijhydene.2025.152871
197. Xie, B., Gao, W., Liu, Z., Guo, K., Wang, Q., Jiang, S., Bowen, C., Luo, H. & Li, T. Superior Piezocatalytic Activity and Environmental Adaptability in Micro -Nano -Engineered $BaTiO_3$/PVDF@Ag Composite Structure. *Adv. Funct. Mater.* **2026**, 36, e77213. DOI: 10.1002/adfm.77213
198. Chen, Z., Yan, D., Wang, X., Ding, G., Wang, Z., Xiao, Y., Liu, X., Wang, P., Chen, L., Shuai, L., *et al*. Biochar-Tailored Carbon Nitride Enables Piezo-Photocatalytic H_2O_2 Production via Boosted Charge Transport. *ACS Catal.* **2025**, 15, 13568–13580. DOI: 10.1021/acscatal.5c02889
199. Jin, Z., Lu, M., Jiang, C., Wu, S., Tang, L., Hu, C., Liu, L., Fang, L. & Cheng, Z. Mechanocatalytic H_2O_2 Production Using Ferroelectric $KSr_2Nb_3Ta2O_{15}$ Nanorods. *Nano Energy* **2025**, 138, 110892. DOI: 10.1016/j.nanoen.2025.110892
200. Sun, X., Lv, K., Liu, F., Wang, P., Zhang, K., Zhang, J. & Chen, P. Insight into Interfacial Engineering for Enhancing the Synergistic Effect of Piezo-photocatalytic Hydrogen Peroxide Production. *Chem. Eng. J.* **2024**, 497, 154504. DOI: 10.1016/j.cej.2024.154504
201. Zhang, Y., Xu, S., Chen, J., Zhang, J., Mu, Z., Zhou, C., Abdelsalam, H. & Zhang, Q. Strategic B-site Cation Engineering in Sillén–Aurivillius Perovskite Oxyhalides for Ultra-high Efficiency Piezocatalytic H_2O_2 Production. *Mater. Horiz.* **2026**, 13, 4111–4122. DOI: 10.1039/d6mh00204h
202. Foo, J. J., Chiah, Z. -J., Khoo, V., Ng, S. -F., Yuan, S., Zeng, X. & Ong, W. -J. Modulating Lattice Polarization in Crystalline Carbon Nitride via Vacancy-anchored Aluminum for Simultaneous Piezo-photocatalytic H_2O_2 and Acetaldehyde Synthesis. *Appl. Catal. B Environ.* **2026**, 391, 126685. DOI: 10.1016/j.apcatb.2026.126685
203. Xiong, R., Liu, F., Huang, J., Xiao, Y., Cheng, B. & Lei, S. Spin Polarization-coupled Piezocatalysis in Fe-doped Bi_3TiNbO_9: Synchronous Kinetic and Thermodynamic Optimization for Superior H_2O_2 Production. *Chem. Eng. J.* **2025**, 525, 170344. DOI: 10.1016/j.cej.2025.170344
204. Li, Y., Zhang, X., Li, T., Hu, C., Chen, F., Cai, H. & Huang, H. Few-layer Oxygen Vacant $Bi_2O_2(OH)NO_3$ for Dual-channel Piezocatalytic H_2O_2 Production from H_2O and Air. *Chin. J. Catal.* **2025**, 75, 105–114. DOI: 10.1016/s1872-2067(25)64750-4
205. Xu, Y., Zhou, Z., Li, Y., Lin, Z., Liu, X., Zhou, Y., Zhou, Z. & Fan, X. Intensifying Localized Polarization Piezoelectric Field via Tip Effect on Carbon Quantum Dots Modified $Ca_2B_3O_6Cl$ for H_2O_2 Production in Pure Water. *Adv. Funct. Mater.* **2026**, 36, e76955. DOI: 10.1002/adfm.76955
206. Jiang, Y., Song, H., Li, J., Xing, Y., Wang, L., Chen, C., Liu, Y., Liao, X., Xu, S., Liu, S., *et al*. Unlocking the "Piezocatalytic Sweet Spot": A Synergistic Match of System-Wide Energy Capture and Unit-Level Piezoelectricity for Efficient H_2O_2 Production. *Adv. Funct. Mater.* **2026**, 36, e76451. DOI: 10.1002/adfm.76451
207. Wang, B., Wu, C., Tan, M., Sun, Y., Lv, X., Yang, Y., Zhang, Z. & Hou, Y. Achieving the Gain Effects of Excitation Field Coupling via Rationally Designed Piezo-photo Heterojunction for Enhanced H_2O_2 Production. *Chem. Eng. J.* **2026**, 541, 177471. DOI: 10.1016/j.cej.2026.177471
208. Li, X., Yang, X., Chen, Q., Yuan, Q., Huang, H., Tu, S., Zhang, Q., Chen, F. & Fu, M. Dual-Microsite Covalent Organic Framework-Functionalized Barium Titanate for Promoting Piezo -Catalytic Dual - Pathway H_2O_2 Production. *Small* **2026**, 22, e00067. DOI: 10.1002/smll.202600067
209. Tian, N., Yuan, C., Zhou, T., Yu, W., Wang, Y., Zhang, N., Zhang, Y. & Huang, H. Defect-coordinated Au Nanoparticles in Carbon Nitride for Efficient Piezo-photocatalytic Hydrogen Peroxide Production. *Chin. J. Catal.* **2026**, 81, 272–283. DOI: 10.1016/s1872-2067(25)64901-1
210. Li, Z., Tong, K., Dong, H., Li, Y., Wang, K., Ding, T., Yun, Y., Zhou, Y. & Zhu, M. H-Bonds in Carbon Quantum Dot-anchored C_3N_5 to Boost Proton -Coupled Electron Transfer for Piezoelectric -Driven Hydrogen Peroxide Synthesis under Ambient Conditions. *Angew. Chem. Int. Ed.* **2025**, 64, e202502390. DOI: 10.1002/anie.202502390
211. Zhang, X., An, Y., Yu, W., Zhang, Y., Tian, N., Li, J. & Huang, H. Beyond Charge Separation: Unraveling the Synergy of Piezoelectric Polarization and Structure Engineering in Carbon Nitride for Thermodynamically Boosted H_2O_2 Production. *Nano Energy* **2026**, 149, 111711. DOI: 10.1016/j.nanoen.2026.111711
212. Che, H., Wang, X., Yue, H., Chen, C., Xie, D., Yang, S., Liu, B. & Ao, Y. Precise Regulation of D -Band Centers Inducing to High -Efficiency Dual -Channel Piezocatalytic H_2O_2 Production. *Adv. Funct. Mater.* **2026**, 36, e16979. DOI: 10.1002/adfm.202516979
213. Hamza, M., Yamin, M. H., Kanwal, Q., Najeeb, J., Ahmed, I., Yasir, M., Ahmed, M., Abu Elella, M. H. & Deshmukh, K. Advances in Piezoelectric Catalysts for Environmental Remediation and Sustainable Energy Conversion: A Comprehensive Review. *Coord. Chem. Rev.* **2026**, 569, 218469. DOI: 10.1016/j.ccr.2026.218469
214. Guan, Y., Wei, H., Hu, Z., Li, Y., Sun, J., Yao, K., Chen, X., Ke, Y., Yang, Y., Liu, H., *et al*. Piezoelectric Catalysis in Water Treatment: Mechanism, Material Design and Application Progress. *Chin. J. Struct. Chem*. **2026**, *in press*, 101075. DOI: 10.1016/j.cjsc.2026.101075
215. Lian, W., Zhang, P., Che, H., Liu, B. & Ao, Y. Efficiently Piezo-catalytic Generation of Reactive Oxygen Species on Phosphorus -Doped BiOCl Enhancing Micropollutants Degradation. *Small* **2025**, 21, 2504949. DOI: 10.1002/smll.202504949
216. Xu, J., Gu, K., Wang, P., Cheng, P., Che, H., Tang, C., Zhang, K. & Ao, Y. Piezo-catalytic in-site H_2O_2 Generation and Activation across Wide pH Range to Drive Hydroxyl Radical-mediated Pollutant Degradation. *Nat. Commun.* **2025**, 16, 7908. DOI: 10.1038/s41467-025-63337-x
217. Jiang, R., Lu, G., Wang, M., Chen, Y., Liu, J., Yan, Z. & Xie, H. Lattice Distortion SnS_2 Piezoelectric Self-fenton System for Efficient Degradation and Detoxification of Pollutants. *npj Clean Water* **2023**, 6, 79. DOI: 10.1038/s41545-023-00293-3
218. Andrade, L. S., Lima, H. H., Silva, C. T., Amorim, W. L., Poço, J. G., López-Castillo, A., Kirillova, M. V., Carvalho, W. A., Kirillov, A. M. & Mandelli, D. Metal–Organic Frameworks as Catalysts and Biocatalysts for Methane Oxidation: The Current State of the Art. *Coord. Chem. Rev.* **2023**, 481, 215042. DOI: 10.1016/j.ccr.2023.215042
219. Zhang, M., He, J., Zhang, J., Sun, H., Wang, S. & Duan, X. Decoupling Activation and Preservation: Architectural Design Principles of Organic Frameworks for Selective Photocatalytic Methane Oxidation. *Adv. Mater.* **2026**, 38, e74071. DOI: 10.1002/adma.74071
220. Che, C., Li, R., Jia, T., Wang, W., Zeng, D., Qin, X., Xu, S., Jiang, B., Wang, W., Yang, H., *et al*. Selective Oxidation of Methane by Piezoelectric Catalysis Under Mild Conditions. *ChemCatChem* **2025**, 17, e202402105. DOI: 10.1002/cctc.202402105
221. Zhang, Q., Rong, L., Jiang, Y., Zhu, Z., Lin, X., Ding, Y., Dong, H. & Liu, D. Direct Oxidation of Trace Methane to Formaldehyde Under Ambient Conditions by Piezo-photocatalytic Synergy. *Chem. Eng. J.* **2025**, 524, 168689. DOI: 10.1016/j.cej.2025.168689
222. Zhou, Y., Wang, H., Liu, X., Qiao, S., Shao, D., Zhou, J., Zhang, L. & Wang, W. Direct Piezocatalytic Conversion of Methane into Alcohols Over Hydroxyapatite. *Nano Energy* **2021**, 79, 105449. DOI: 10.1016/j.nanoen.2020.105449